

Reservoir and Completion Parametric Study on a Shale Gas Reservoir

By
Ahmed Saleh Mohammed Aleid

May, 2018

**RESEEROVR AND COMPLETION PARAMETRIC
STUDY ON A SHALE GAS RESERIVOR**

BY

AHMED SALEH MOHAMMED ALEID

A Thesis Presented to the
DEANSHIP OF GRADUATE STUDIES

KING FAHD UNIVERSITY OF PETROLEUM & MINERALS

DHAHRAN, SAUDI ARABIA

In Partial Fulfillment of the
Requirements for the Degree of

MASTER OF SCIENCE

In

PETROLEUM ENGINEERING

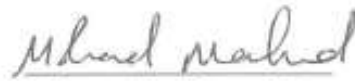
May, 2018

KING FAHD UNIVERSITY OF PETROLEUM & MINERALS

DHAHRAN- 31261, SAUDI ARABIA

DEANSHIP OF GRADUATE STUDIES

This thesis, written by AHMED SALEH MOHAMMED ALEID under the direction of his thesis advisor and approved by his thesis committee, has been presented to and accepted by the Dean of Graduate Studies, in partial fulfilment of the requirements for the degree of **MASTER OF SCIENCE IN PETROLEUM ENGINEERING**.



Dr. Mohamed A. Mahmoud
(Thesis Advisor)



Dr. Hasan Y. Al-Yousef
(Co-Advisor)



Dr. Dhafer A. Al-Shehri
Department Chairman



Dr. Salam A. Zummo
Dean of Graduate Studies

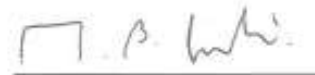
15/13
Date



Dr. Dhafer A. Al-Shehri
(Member)



Dr. Salaheldin M. Elkatatny
(Member)



Dr. Mohammed B. Issaka
(Member)

@AHMED SALEH MOHAMMED ALEID

2018

بِسْمِ اللَّهِ الرَّحْمَنِ الرَّحِيمِ

رَبَّنَا تَقَبَّلْ مِنَّا إِنَّكَ أَنْتَ السَّمِيعُ الْعَلِيمُ

ACKNOWLEDGMENT

The author would like to thank the Department of Petroleum Engineering at King Fahad University of Petroleum & Minerals for all their support and the opportunity to gain more knowledge and experience and fulfill my master degree in petroleum engineering.

I would like to thank Dr. Mohamed A. Mahmoud, my thesis advisor, and Dr. Hasan Y. Al-Yousef, Dr. Dhafer A. Al-Shehri, Dr. Salaheldin ElKatatny, and Dr. Mohammed Issak, my thesis commit, for their support, guidance, and assistance throughout my work.

TABLE OF CONTENTS

ACKNOWLEDGMENT	I
TABLE OF CONTENTS	II
LIST OF TABLES	V
LIST OF FIGURES.....	VI
ABSTRACT	XI
ملخص الرسالة	XIII
CHAPTER 1	1
INTRODUCTION.....	1
CHAPTER 2.....	4
LITERATURE REVIEW	4
2.1 Overview	4
2.1.1 Gas Shale Definition.....	4
2.1.2 Geological Settings.....	5
2.2 Reservoir Characterization	6
2.2.1 Mineralogy.....	6
2.2.2 Organic Material.....	7
2.2.3 Petrophysics.....	8
2.3 Stimulation Treatment.....	10
2.3.1 Horizontal Drilling.....	10

2.3.2 Multistage Hydraulic Fracturing.....	11
2.3.3 Other Stimulation Techniques	12
2.3.4 Pumping Schedule	15
2.3.5 Fracture Geometry.....	17
2.4 Production Analysis.....	19
2.4.1 Background.....	19
2.4.2 Flow Regimes	21
2.4.3 Analysis Methods	27
2.4.4 Horizontal Multifrac Composite Model	29
2.4.5 Proposed Production Analysis Workflow	30
2.4.6 Probabilistic Evaluation.....	31
CHAPTER 3.....	32
RESEARCH OBJECTIVES AND METHODOLOGY	32
3.1 Problem Statement.....	32
3.2 Research Objectives	33
3.3 Research Methodology	33
3.3.1 Initial Production Analysis	34
3.3.2 Probabilistic Evaluation.....	34
3.3.3 Sensitivity analysis	36
CHAPTER 4.....	38
RESULTS AND DISSCUSSION	38
4.1 Uncertainties Constrain	38
4.1.1 Fracture Height	39
4.1.2 Fracture Half-length	39

4.1.3 Number of Fractures	40
4.1.4 Permeability	40
4.1.5 Initial Pressure	40
4.1.6 Fluid Properties.....	41
4.2 Case Studies.....	41
4.2.1 Well A.....	41
4.2.2 Well B.....	63
4.2.3 Well C.....	87
CHAPTER 5	109
CONCLUSIONS	109
NOMENCLATURE	112
REFERENCES	114
VITA.....	118

LIST OF TABLES

Table 1: Summary of The Reported Parametes From The Literature	34
Table 2: Main Reservoir and Completion Parameters Examined	35
Table 3: Reservoir Model for Analysis	35
Table 4: Fixed Well Parameter for Well A	42
Table 5: Initial and Final Distribution for Uncertain Well A Parameters	47
Table 6: Fixed Well Parameter for Well B.....	64
Table 7: Initial and Final Distribution for Uncertain Well B Parameters	68
Table 8: Fixed Well Parameter for Well C.....	87
Table 9: Initial and Final Distribution for Uncertain Well C Parameters	92

LIST OF FIGURES

Figure 1: Hydrocarbon Resource Triangle.....	1
Figure 2: Location of Assessed Basins in EIA Report.....	2
Figure 3: Jafurah Basin of Saudi Arabia	5
Figure 4: Mineralogy Composition of Productive Shale Gas	6
Figure 5: Comparison of TOC of Shale Plays Around the World	8
Figure 6: Flow Regimes as per Knudsen in Microscopic Porous Medium.....	9
Figure 7: Porosity-Permeability Cross of Two Prominent Shale Formations	9
Figure 8: Plug-And-Perf Versus Ball-And-Sleeve Multistage Fracturing Completion	13
Figure 9: Proppant Concentration Along the Induced Hydraulic Fracture	16
Figure 10: Different Classification of Fracture Half-Length	16
Figure 11: Possible Fracture Geometries	18
Figure 12: Typical Flow Sequence Adapted in Shale Wells Production.	20
Figure 13: Normalized Rate Over Time in Five Shale Plays in North America.....	20
Figure 14: Flow Regime Sequence as Describe by Song & Ehlig-Economides.....	22
Figure. 15: Flow Regimes Observed in Typical Stimulated Shale Reservoir.....	23
Figure 16: Comparison of Analysis Methods for Gas Shale Production	28
Figure 17: Schematic of Trilinear Flow Within the Composite Model.....	30
Figure 18: Suggested Production Data Analysis for Unconventional Gas Wells	31

Figure 19: Used Methodology Workflow	37
Figure 20: Well A Normalized Rate Versus Material Balance Time (Log-Log Scale)	43
Figure 21: Well A Square Root Time Plot	44
Figure 22: Well A Flowing Material Balance Plot.....	44
Figure 23: Well A Production History Match	46
Figure 24: Well A Forecasted Normalized Gas Rate Versus Normalized Time.....	47
Figure 25: Well A Fracture Half-Length Sensitivity.....	49
Figure 26: Well A Fracture Half-Length Sensitivity (Log-Log Plot)	49
Figure 27: Well A Fracture Number Sensitivity	50
Figure 28: Well A Fracture Number Sensitivity (Log-Log Plot).....	50
Figure 29: Well A Well Length Sensitivity.....	51
Figure 30: Well A Well Length Sensitivity (Log-Log Plot)	52
Figure 31: Well A fracture conductivity sensitivity	53
Figure 32: Well A Fracture Conductivity Sensitivity (Log-Log Plot)	53
Figure 33: Well A Well Spacing Sensitivity	54
Figure 34: Well A Well Spacing Sensitivity (Log-Log Plot).....	55
Figure 35: Well A Fracture Height Sensitivity.....	56
Figure 36: Well A Fracture Height Sensitivity (Log-Log Plot)	56
Figure 37: Well A Inner Permeability Sensitivity.....	57
Figure 38: Well A Inner Permeability Sensitivity (Log-Log Plot).....	58
Figure 39: Well A Outer Permeability Sensitivity	59
Figure 40: Well A Outer Permeability Sensitivity (Log-Log Plot).....	59

Figure 41: Well A porosity sensitivity	60
Figure 42: Well A Porosity Sensitivity (Log-Log Plot)	61
Figure 43: Well A Adsorption Sensitivity.....	62
Figure 44: Well A Adsorption Sensitivity (Log-Log Plot)	62
Figure 45: Well B Normalized Rate Versus Material Balance Time (Log-Log Scale)	65
Figure 46: Well B Normalized Rate Versus Square Root Material Balance Time	66
Figure 47: Well B Flowing Material Balance Plot.....	66
Figure 48: Well B Production History Match	67
Figure 49: Well B Probabilistic Production Forecast.....	69
Figure 50: Well B Fracture Half-Length Sensitivity	70
Figure 51: Well B Fracture Half-Length Sensitivity (Log-Log Plot).....	71
Figure 52: Well B Fracture Number Sensitivity.....	72
Figure 53: Well B Fracture Number Sensitivity (Log-Log Plot)	72
Figure 54: Well B well length sensitivity.....	73
Figure 55: Well B well length sensitivity (log-log plot)	74
Figure 56: Well B Fracture Conductivity Sensitivity.....	75
Figure 57: Well B Fracture Conductivity Sensitivity (Log-Log Plot)	75
Figure 58: Well B well spacing sensitivity.....	76
Figure 59: Well B Well Spacing Sensitivity (Log-Log Plot).....	77
Figure 60: Well B Fracture Height Sensitivity.....	78
Figure 61: Well B Fracture Height Sensitivity (Log-Log Plot)	78
Figure 62: Well B Inner Permeability Sensitivity	79

Figure 63: Well B Inner Permeability Sensitivity (Log-Log Plot).....	80
Figure 64: Well B Outer Permeability Sensitivity	81
Figure 65: Well B Outer Permeability Sensitivity (Log-Log Plot)	81
Figure 66: Well B Porosity Sensitivity.....	82
Figure 67: Well B Porosity Sensitivity (Log-Log Plot)	83
Figure 68: Well B Adsorption Sensitivity.....	84
Figure 69: Well B Adsorption Sensitivity (Log-Log Plot).....	84
Figure 70: Well B Initial Pressure Sensitivity.....	85
Figure 71: Well B Initial Pressure Sensitivity (Log-Log Plot).....	86
Figure 72: Well C Normalized Rate Versus Material Balance Time (Log-Log Scale)	88
Figure 73: Well C Square Root Time Plot	89
Figure 74: Well C flowing material balance plot	90
Figure 75: Well C production history match.....	91
Figure 76: Well C Probabilistic Forecast (Semi-Log Scale).....	92
Figure 77: Well C Fracture Half-Length Sensitivity	94
Figure 78: Well C Fracture Half-Length Sensitivity (Log-Log Plot).....	94
Figure 79: Well C Well Length Sensitivity.....	95
Figure 80: Well C Well Length Sensitivity (Log-Log Plot).....	96
Figure 81: Well C Fracture Conductivity Sensitivity.....	97
Figure 82: Well C Fracture Conductivity Sensitivity (Log-Log Plot)	97
Figure 83: Well C Well Spacing Sensitivity	98
Figure 84: Well C Well Spacing Sensitivity (Log-Log Plot).....	99

Figure 85: Well C Fracture Height Sensitivity.....	100
Figure 86: Well C fracture height sensitivity (log-log plot).....	100
Figure 87: Well C inner permeability sensitivity	101
Figure 88: Well C inner permeability sensitivity (log-log plot).....	102
Figure 89: Well C Outer Permeability Sensitivity	103
Figure 90: Well C Outer Permeability Sensitivity (Log-Log Plot).....	103
Figure 91: Well C Porosity Sensitivity.....	104
Figure 92: Well C Porosity Sensitivity (Log-Log Plot)	105
Figure 93: Well C Adsorption Sensitivity.....	106
Figure 94: Well C Adsorption Sensitivity (Log-Log Plot).....	106
Figure 95: Well C Initial Pressure Sensitivity.....	107

ABSTRACT

Full Name : Ahmed Saleh Mohammed Aleid

Thesis Title : Reservoir and Completion Parametric Study on a Shale Gas Reservoir

Major Field : Petroleum Engineering

Date of Degree: May 2018

Gas shale belongs to reservoirs that are often characterized by low permeability rock formations that produce mainly gas. The quantities of the gas held in shale gas sources exceed that of conventional reservoirs by several folds. Until recently, the commercial production of natural gas from unconventional resources was made difficult due to many technical challenges. The advancements made in commingled wells drilling, and hydraulic fracture treatment, all helped in improving recovery by exposing more of the reservoir to the wellbore. However, there are high uncertainty in forecasting shale gas and determining parameters affecting its production. The previous lead to utilizing probabilistic approach to solve this problem.

The objective of this work is to evaluate the reservoir and completion key parameters that affect short-term shale gas production in single, multi-fractured, horizontal well. Current approaches rely mainly on decline curve analysis or analogs from a similar shale play to forecast production. These approaches are problematic because they calibrate their forecast

on short production history and do not assist the impact of uncertainty in reservoir and completion data.

To accomplish the objectives, reservoir and completion parameters are collected from different available resources and probability distributions of gathered uncertain data are defined. The probability distributions were then fed to analytical model supported by stochastic simulation such as Monte Carlo to create a probabilistic forecast for the selected wells, and to refine the probability distribution of reservoir and completion parameters. A sensitivity is then performed to define the impact of parameters on gas production.

Probabilistic approach has been previously tried to analyze uncertainties on conventional and unconventional resources. However, they studied basins in North America, and the examined parameters are different in this study. In this study, the uncertainties of the targeted shale basins are evaluated and probable production is presented. After that, sensitivities are conducted on several completion and reservoir parameters to assist their impact on the production.

The outcome of this work is anticipated to be applicable in the target shale play. It quantifies the parameters affecting production, and define the prominent one(s). In the three wells cases, fracture dimension was found to be significantly restricted, and the reservoirs quality of Well B to be below average. This would help in guiding accomplishing more effective stimulation treatments and define the potentiality of the basin.

ملخص الرسالة

الإسم الكامل: أحمد صالح محمد العبد

عنوان الرسالة: دراسة معيارية على مكامن وإستكمال الغاز الصخري

التخصص: هندسة النفط

تاريخ الدرجة العلمية: مايو ٢٠١٨

الغاز الصخري ينتمي إلى تكوينات الصخور منخفضة النفاذية التي تنتج غالبا غاز. كميات الغاز الكامنه في الغاز الصخري تفوق المكامن التقليدية بأضعاف عديدة. إلى زمن قريب كان الإنتاج التجاري من المصادر غير التقليدية صعبا لعدة لعوامل تقنية. التقدم الحاصل في الحفر الجمعي والتكسير الهيدروليكي للأبار ساعد في تحسن الإستخلاص وذلك عن طريق تعريض قدر أكبر من المكن للبنر. لكن هنالك شك كبير في توقع إنتاج الغاز الصخري وتحديد العوامل المؤثرة في إنتاجه. ماسبق يؤدي إلى إستخدامنا النهج الإحتمالي لحل هذه المشكلة.

هدف هذا العمل هو تقييم المعايير الأساسية للمكن والإستكمال الذي تؤثر في إنتاج الغاز الصخري قصير المدى في البئر الأفقي المكسر هدرولكية. النهج الحالي لتوقع الإنتاج يعتمد أساسا في تحليل منحنى الإنخفاض أو النظير من غاز صخري مماثل. هذه النهج إشكالية لأنها تعابر توقعاتها على إنتاج قصير التاريخ ولا تقيم أثر المجاهيل في معلومات المكن و الإستكمال. لإنجاز أهدافنا ، معايير المكن والإستكمال تجمع من مصادر متوفرة والتوزيع الإحتمالي للمجاهيل محدد . التوزيع الإحتمالي تدخل الى نموذج تحليلي مدعوم بمحاكاة عشوائية لأجل خلق توقع إحتمالي للأبار المحددة ولأجل تحديد التوزيع الإحتمالي لمعايير المكن والإستكمال. تحليل الحساسية ينفذ بعد ذلك لتحديد وقع المعايير على إنتاج الغاز.

النهج الإحتمالي قد جرب سابقا لتحليل المجاهيل في المصادر التقليدية وغير التقليدية . ولكن ما تم دراسته كان في أحواض رسوبية في أمريكا الشمالية ، والمعايير المدروسة كانت مختلفة عن هذه الدراسة. في هذه الدراسة تقيم المجاهيل من أحواض الغاز الصخري المستهدفة والإنتاج المحتمل لها سيعرض . بعد ذلك ، ستقام دراسة حساسية على عدة معايير استكمال ومكن لتقييم أثرها على الإنتاج.

حصيلة هذا العمل يتوقع لها أن تكون قابلة لتطبيق في الغاز الصخري المستهدف و تساعد في تحديد المعايير المؤثرة بالإنتاج وتحديد الأبرز منها . في الأبار الثلاثة المدروسة وجد أن أبعاد التكسير الهيدروليكي محدودة بشكل كبير وجودة المكن في البئر (ب) أقل من المعدل . هذا سوف يساعد في إرشاد إنجاز تكسير صخري أكثر فعالية لعمليات التكسير الهيدروليكي وتحديد إمكانية الحقل الرسوبي.

CHAPTER 1

INTRODUCTION

Shale gas belongs to reservoirs that are often characterized by low permeability rock formations that produce mainly gas. The quantities of the reserve held in shale gas sources exceed that of conventional reservoirs by several folds (**Figure1**). The U.S. Energy Information Administration (EIA) estimates the global conventional gas reserves to be about eight thousand trillion cubic feet. In contrast, EIA approximates the global shale gas at thirty-five thousand trillion cubic feet, which is about five times the amount of conventional reserves. (U.S. Energy Information Administration, 2010)

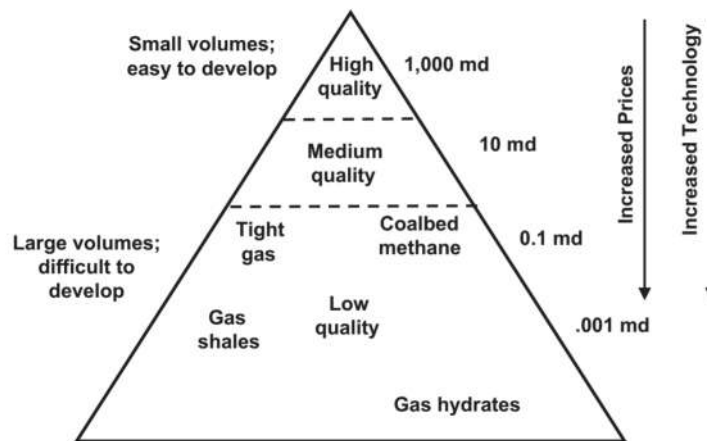


Figure 1: Hydrocarbon Resource Triangle (Holditch & Ma , 2016)

The energy will soon drive the need for exploration and production of these huge unexploited resource (**Figure 2**). For example, Saudi Arabia is facing shortage in natural gas resource. In order to substitute the shortage, Saudi Arabia is consuming thirteen percent of its oil production as feedstock for power generation. Furthermore, oil consumption is growing five percent yearly. Exploiting the Kingdome’s vast unconventional resources seems lucrative option considering the current conditions. (Casey, 2015)

Until recently, the commercial production of natural gas from unconventional resources was made difficult due to many technical challenges. The advancements made in horizontal drilling, and hydraulic fracture treatment, all helped in improving recovery by exposing more of the reservoir to the wellbore.

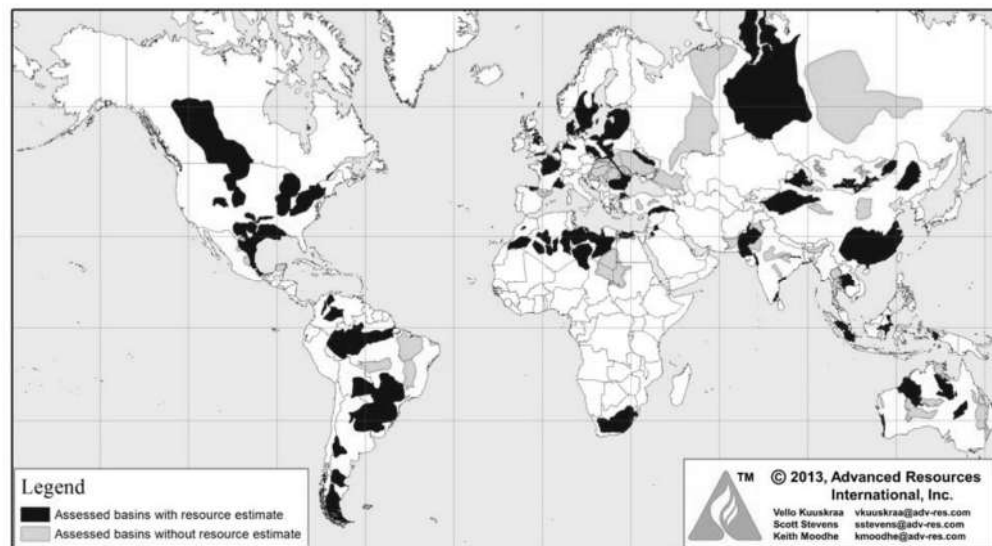


Figure 2: Location of Assessed Basins in EIA Report

The objective of this work is to evaluate the reservoir and completion key parameters affecting short-term shale gas production in single, multi-fractured, horizontal well. Current approaches rely mainly on decline curve analysis or analogs from a similar shale play to forecast production. These approaches are problematic because they calibrate their forecast on short production history and do not assist the impact of uncertainty in reservoir and completion data.

CHAPTER 2

LITERATURE REVIEW

In the literature review, an introduction of what gas shale is, and geological settings of the typical shale basin. Then, key reservoir and completion parameters that affect shale gas production are discussed. After that, flow regimes observed in shale gas wells, and the most suitable method to analyze production data are illustrated. Finally, a summary of probabilistic approach will be introduced highlighting the difference between previous work and the proposed one.

2.1 OVERVIEW

2.1.1 Gas Shale Definition

Gas shale can be defined as any tight, fine-grained, organic rich, gas self-sourced, sedimentary formation. Gas shale contains all elements of petroleum system. Gas shale is a source rock of its hydrocarbon. Gas is generated within the shale through maturation of the organic material that reaches up to fifty percent of its weight. The generated gas is stored adsorbed in the organic/clay material or free in pores. While maturing in relatively impermeable shale, the rate of hydrocarbon generation far exceeds the rate of migration

resulting in accumulation of hydrocarbon within the shale formation. Therefore, many maturing gas shale plays tend to be overpressure, and the fraction hydrocarbon that migrated to conventional resource is far less than what left within the maturing shale.

2.1.2 Geological Settings

Shale Gas shale formed in low-energy, oxygen deficit part of basin. Low-energy environment results in fine grain of the shale while oxygen deficiency preserves the organic material from oxidizing and decomposing. An example of local source is Tuwaiq Mountain in Jafurah Basin of Saudi Arabia (**Figure 3**). Tuwaiq Mountain is mostly composed of carbonate layers and its formation dates back to Jurassic period. The basin hosts some of biggest oil fields in the world such as Ghawar, Dukhan and Abqaiq field.

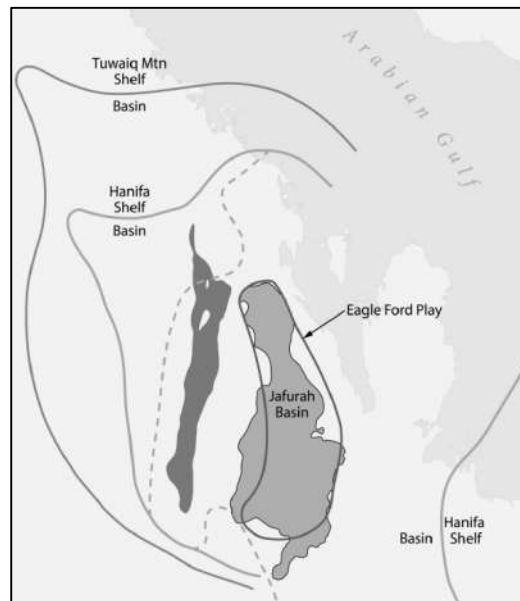


Figure 3: Jafurah Basin of Saudi Arabia (Al-Momin, 2015)

2.2 Reservoir Characterization

2.2.1 Mineralogy

In terms of mineralogy, shale is classified into three types: siliceous, calcareous, and clastic shale. The more clay rich the shale is, the more ductile, and stressful it is, and the harder to hydraulic fracture. Ductility usually results in creep and proppants impediment. Stressful rocks are harder to confine the hydraulic fracture within. Shale is considered to be of commercial potential if it contains fifty percent or less clay. **Figure 4** shows comparison of five global shale plays, and it can be observed that clay content is minimal in comparison to conventional shale.

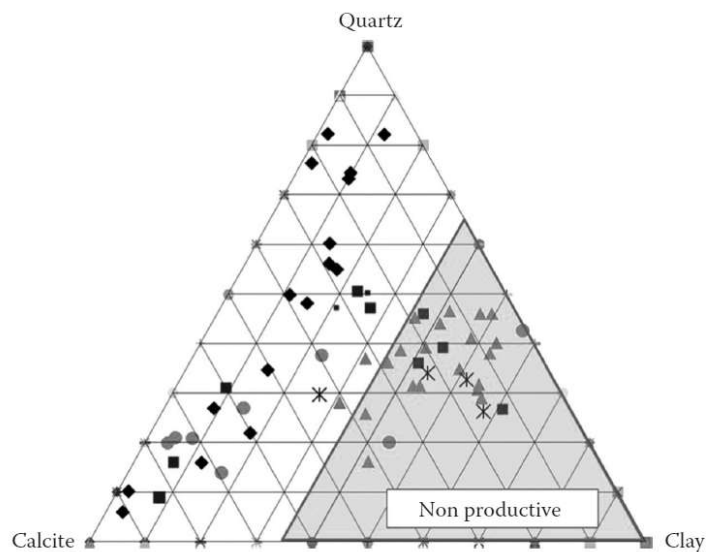


Figure 4: Mineralogy Composition of Productive Shale Gas (Al-Momin, 2015)

2.2.2 Organic Material

Organic material plays roles in generating and storing hydrocarbon. Hydrocarbon is created through organic material, kerogen, and maturation by heat and pressure over long geological time. The Generated hydrocarbon is also stored by adsorption in the organic material. High organic concentration implies high hydrocarbon concentration. Total organic content, TOC, is a measure of how much organic material a shale contains. Shale plays are considered economically worthy if the TOC is over 2%. For example, Tuwaiq Mountain is well suited above many well-known North American shale plays with TOC 4% as shown in **Figure 5**. (Al-Momin, 2015; Lindsay, et al., 2015)

The maturity of shale is measure by Vitrinite Reflectance, VR_o , which is a test to measure light reflection from vitrinite particles associated with kerogen thermal maturity. Immature kerogen will not produce hydrocarbon, and over-mature kerogen means that all hydrocarbon has been burned out. Tuwaiq Mountain shale is within liquid-rich gas generation window as shown in **Figure 6**. (Lindsay, et al., 2015) As result of high hydrocarbon generation potential and low matrix permeability, the shale formation is overpressure with a pressure gradient over 0.6 psi/ft.

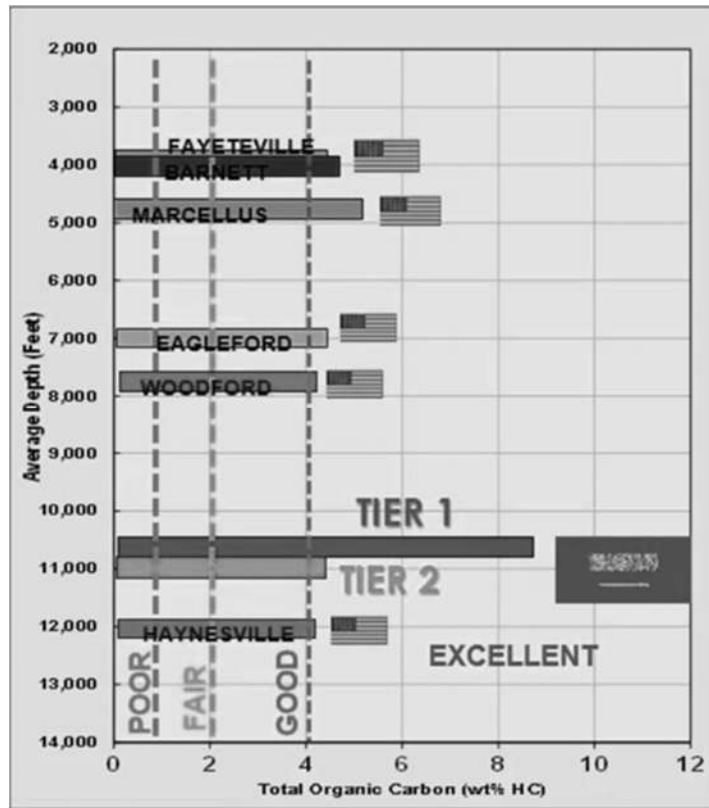


Figure 5: Comparison of TOC of Shale Plays Around the World (Al-Momin, 2015)

2.2.3 Petrophysics

Shale pores are in nano-scale, ranging from several nanometers to few micrometers. Nano pores define the flow regime allowed in shale matrix to be confined between slip flow and transition flow (**Figure 6**). This implies Darcy flow model is theoretically no longer valid within rock matrix, and the expected shale permeability to be in order of nano-Darcy. (Blasingame T. , 2013) However, Darcy flow occurs in the open natural fractures and fissures on the shale formation and also in the induced fractures. In the study case, it is

estimated that the permeability be ~150 nano-Darcy, and the porosity to be ~6.5% (Figure 7). The gross thickness is between 110-160 feet. (Al-Momin, 2015)

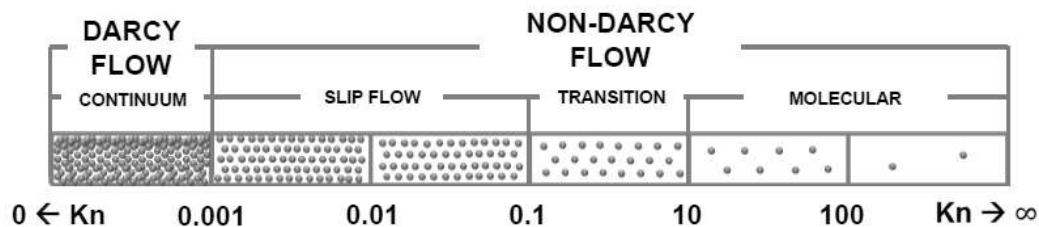


Figure 6: Flow Regimes as per Knudsen in Microscopic Porous Medium (Blasingame T. , 2013)

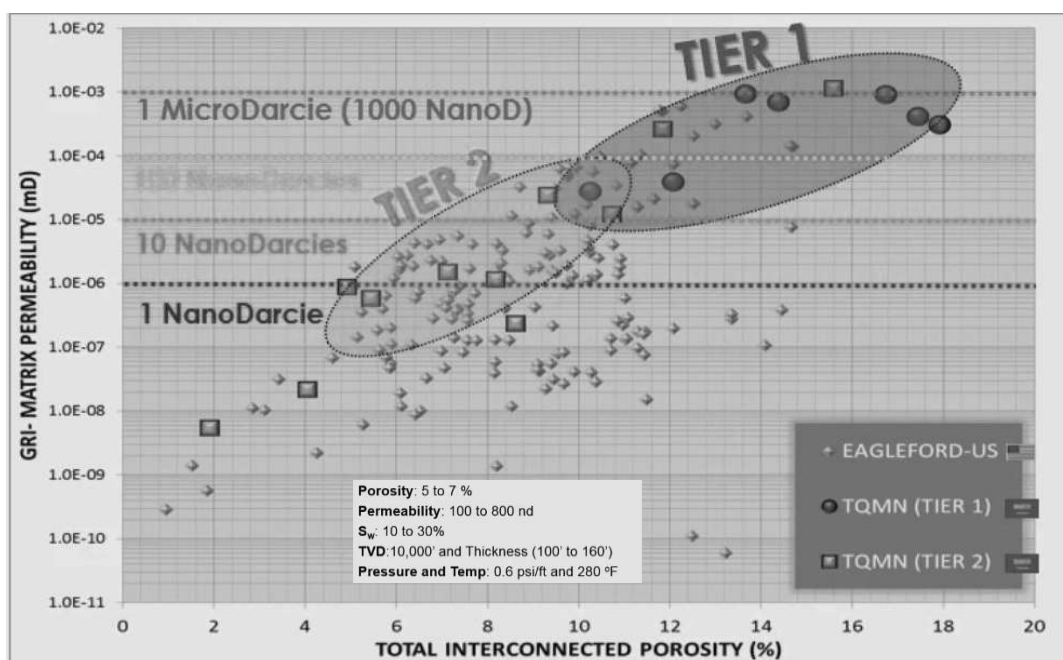


Figure 7: Porosity-Permeability Cross of Two Prominent Shale Formations (Al-Momin, 2015)

2.3 Stimulation Treatment

It is important to understand how hydraulic fractures are created in order to understand the performance of hydraulically fractured reservoir. During production analysis, fracture and reservoir signals are inseparable.

2.3.1 Horizontal Drilling

The first step in extracting shale gas, is through drilling. The drilling operations start vertically to a certain depth called the kickoff point. After the kickoff point, a downhole motor with measurements while drilling (MWD) instruments is used to make the angle or curve building process. In this step, a curvature is made to change the well orientation from vertical to horizontal. Horizontal section is oriented in the direction of the minimum stress to assist the creation of planned hydraulic fractures and to take advantage of natural open fractures. Once the curve is completed, the drilling starts in horizontal section of the well called the lateral. Lateral length has increased from several hundreds of feet in early 2000s to more than six thousand feet nowadays. Once the horizontal section is completed, the drilling pipe is removed for the last time. (Doung , Holditch , & McVay, 2013)

Production casing is inserted to the full length of the horizontal well and cement is pumped to occupy the annulus between the casing and the wellbore. Casing is placed to prevent the wellbore from collapsing and to prevent the formation fluids from overflowing the

wellbore. After the well has been cemented and cased, the unassembled drilling rig is mobilized few yards within the same drilling pad to drill another adjacent horizontal well. Several horizontal wells are drilled in the same drilling pad in order to increase the efficiency of drilling, and to exploit formation volume with minimum cost and drilling footprint. (Energy Information Administration, 2012) The distance between two parallel horizontal wells is called spacing, and it is controlled mainly by wells drainage area. Once the drilling rig is not any more needed, a temporary wellhead is installed. The location is prepared for service crew to start the well stimulation operation.

2.3.2 Multistage Hydraulic Fracturing

The first step in the well stimulation is perforation. The wellbore is isolated from the formation rocks by the casing and the cement. Perforations create communication tunnels between the wellbore and the reservoir rock through the casing and the cement. The perforations are usually made by perforating guns equipped with cone shaped explosive charges. A perforation gun is lowered through the well by a wire line to predefined perforation intervals of the horizontal leg. Each interval is called a cluster, and up to six clusters are usually perforated in each fracturing stage. An electrical current is then sent down the wire line in order to set off the charges that create small perforations through the casing, cement, and out to a short distance to the formation. The shot gun is then pulled out the hole to prepare the well to the second step of the well stimulation which is hydraulic fracture. (Gillis & Varhaug, 2010)

Because shale gas bearing formations are tight and compacted, the well needs to be fractured. Hydraulic fracturing is a process where a mixture of water, proppants, and chemicals are pumped down the well and then into the formation under extremely high pressure exceeding formation minimum stress. As the mixture is forced into the formation rock, and down to surrounding rocks, the pressure causes the formation to fracture. These fractures grow perpendicular to the formation minimum stress, form a larger surface area connecting the reservoir to the well, and allow the release of gas into the well. As the pumping pressure is lowered down at the end of each stage, the fractures are kept barely open by the pumped proppants. The shape of the created fracture(s) is a function of many variables such as pad volume, fluid viscosity, proppant concentration, in-situ stress and geomechanic of the rock. Once the far end of the horizontal well is fractured, a plug is inserted to isolate the fractured section of the well. Then, another stage of perforations, fracturing and then plugging is repeated several times to the heel of the horizontal section. Currently over sixteen fracture stages are completed in each well. Once all the stages are completed, the plugs are drilled out, preparing for the well flowback. (Hydraulic Fracturing, 2010)

2.3.3 Other Stimulation Techniques

The pervious stimulation method is called ‘plug and perf’ stimulation and it is by far one of the most commonly used method. It requires a cemented cased hole, and interrupts hydraulic fracturing operation by repeated interventions of perforation gun, and coiled tubing. ‘Ball and sleeve’ is an open hole, multistage stimulation method, requires downhole

installed sleeves activated by progressively smaller size balls (**Figure 8**). The advantage of ‘balls and sleeve’ method is that it enables of seamless pumping operation, and it connects the wellbore directly to the natural fracture. (Ayers, Holditch, & alt, 2007) However, the location and the number of initiated hydraulic fractures are not well controlled as in ‘plug and perf’ method. The initiated fractures are usually concentrated around the installed packers used to isolate stages. Packers exercise some compression stress on the wellbore necessary for stage isolation and thus change the wellbore hoop stress which eases the initiation of hydraulic fractures around the packers. (Li, Allison, & Soliman, 2011)

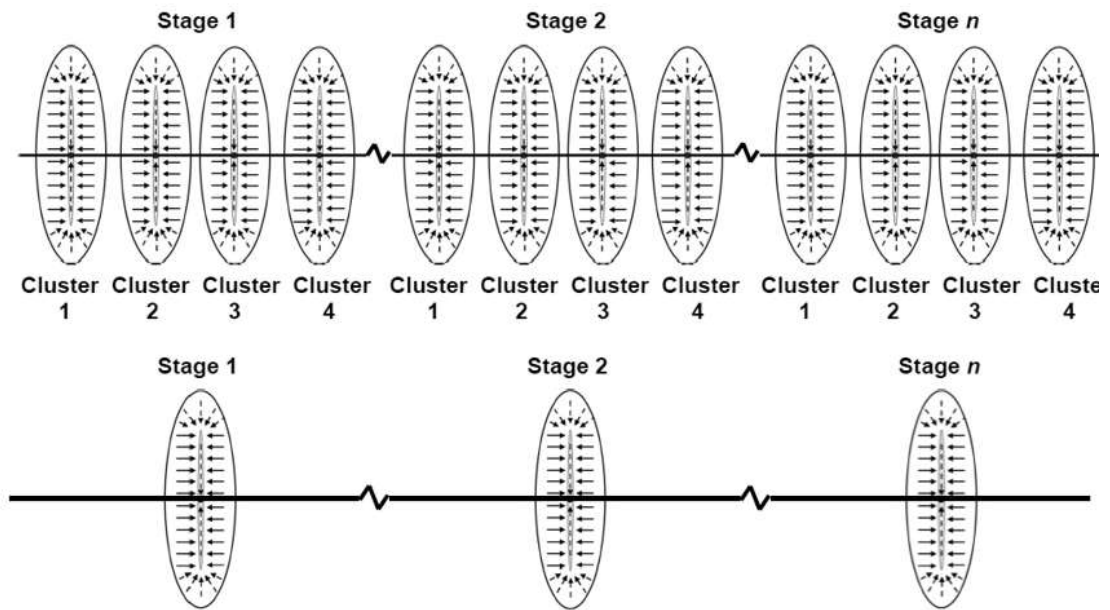


Figure 8: Plug-And-Perf (Above) Versus Ball-And-Sleeve (Below) Multistage Fracturing Completion (Blasingame T. , 2013)

‘Plug and perf’ has more control over the location and number of initiated fractures. Fractures are expected to grow from each perforated cluster intervals; however, this not the

common case. In general, around fifty percent of cluster contribute to the production while eighty percent of the production comes only from twenty percent of the clusters in each stage. (Soliman, Daal, & East, 2012) In another detailed study where over a hundred production logs from six main shale plays in North America were analyzed, it has been found that on average twenty percent of the cluster does not contribute in four cluster per stage. The number of not contributing cluster increases as the cluster concentration increases. For example, in six cluster per stage only half the cluster contributes to the production. (Wigger, et al., 2014) The factors for no or low contribution could be attributed to several variables such as interaction between fractures through stress shadow (Roussel & Sharma, 2011), near wellbore tortuosity (Smith & Montgomery, 2015), wellbore fluid dynamic during pumping (Daneshy, 2011), proppants over displacement (Soliman, Daal, & East, 2012), wellbore deviation, etc. In short, high uncertainty exists in defining the cluster contribution. Cluster production contribution could be assisted through production logs, radioactive tracers to determine entry point, or distributed fiber-optic sensors. However, these methods are rarely used due to expense or practicality.

Another stimulation technique gaining popularity is ‘pinpoint’ during which only on a cluster per stage is pumped. The main advantage of this method is to ensure that no zone left unstimulated. Also, it requires less horsepower and personnel to treat each stage. However, ‘pinpoint’ method requires more time and cost for stimulation of a well. Stage spacing is shorter than ‘plug and perf’ and ‘ball and sleeve’, and therefore more stages are required to be stimulated. Moreover, service companies usually charge more for stages

rather than pumped volume which, consequently, adding cost to stimulation treatment. (Soliman, Daal, & East, 2012)

2.3.4 Pumping Schedule

It is important to understand how fracture is created in order to understand the performance of hydraulic fractured reservoir. Induced fracture and reservoir signals are inseparable during production analysis. As mentioned, fractures are initiated once the wellbore fluid pressure exceeds the minimum stress acting on the wellbore plus the rock tensile strength. Fracture grows where they face minimum resistance which is in normal fault regime perpendicular to the minimum horizontal stress. Once the fracture is initiated, an extra pressure has to be maintained in order to propagate fractures, to transport fluid to tip of fracture, and to overcome near wellbore pressure friction loss (or tortuosity). This is usually achieved in stages. The first stage is called pad and it mainly consists of clear fluid. The pad objective is to create the fracture with the pre-designed dimension. Following stages are called slurry, and they consist of an ever-increasing proppant mixed in transporting fluids. The objective of the slurry is to transport proppants that will keep the fracture open when the pumping stops. The last stage consists of clear fluid with objective to displace slurry from the wellbore into the fractures. Once the pumping stops, the fluid leaks into the formation, and flow is permitted through proppants left in the fractures. (Smith & Montgomery, 2015) Error! Reference source not found. shows the final distribution of the proppant in the hydraulic fracture where the concentration of the proppants decreases rapidly away from the wellbore. Decreasing proppant concentration implies decreasing

fracture conductivity. As result, only portion of the propped fractures effectively contributes to the production. Based on production, fracture half-length could be subdivided to effective half-length, propped half-length, and hydraulic half-length (**Figure 10**). Effective half-length is related more to production and could be verified through production analysis.

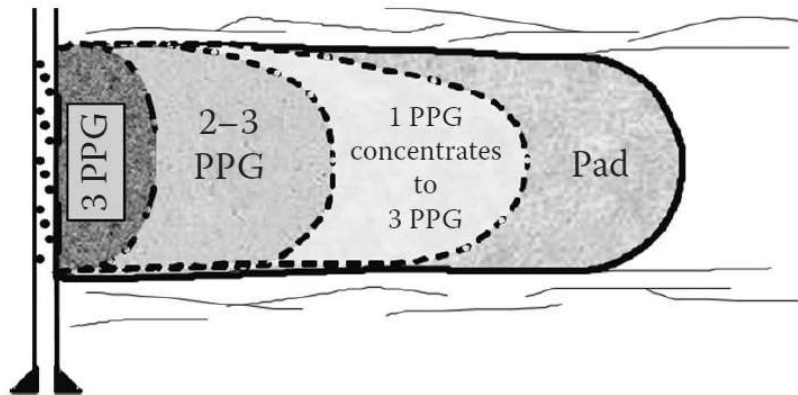


Figure 9: Proppant Concentration Along the Induced Hydraulic Fracture (Smith & Montgomery, 2015)

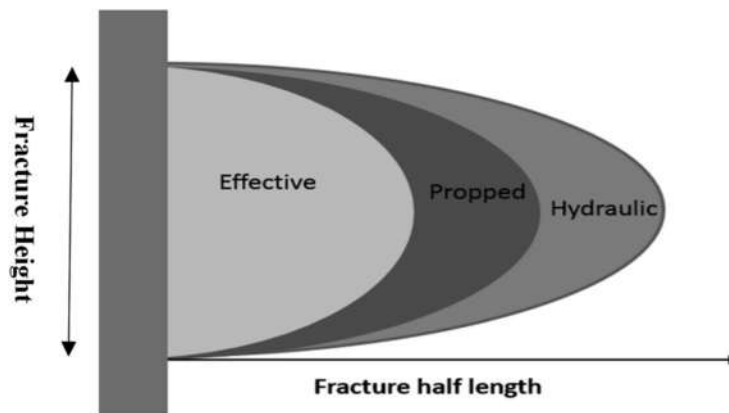


Figure 10: Different Classification of Fracture Half-Length (Holditch & Ma , 2016)

2.3.5 Fracture Geometry

The geometry of the created fracture(s) is a function of many variables such as pumping rate and pressure, pad volume, fluid viscosity, proppant concentration, in-situ stress and rock fabric. Idealistically, fracture grows as plane in both length and height until it reaches other formations with higher in-situ (stress barriers). After that, the fracture continues growing in length until the end of the pumping treatment. The resulted fracture is planer and extended as biwing away from the wellbore; therefore, it is usually called bi-wing fracture, planer fracture, or simple fracture. (Smith & Montgomery, 2015) Other fracture geometries might occur due to many reasons such as the existence of natural fractures, and low stress anisotropy (Sayers & Le Calvez, 2011). Warpinski et al demonstrated four possible fracture geometry that are expected for hydraulically fractured reservoirs through observing microseismic activities (**Figure 11**). In shale, understanding the fractures complexity is essential because well performance is greatly influenced by the created fractures geometry and because hydraulic fracture signal is inseparable from the reservoir signal. Moreover, fracture complexity is pursued in stimulation treatment because it does not only connect more rock surface area to the wellbore, but also it enhances reservoir effective permeability by activating more natural fractures and fissures. When such complex fracture geometry is created, it is called stimulated reservoir volume (SRV). The effect might be minor on conventional reservoir but significant in shale gas. (Smith & Montgomery, 2015) Gomaa, Qu, Nelson, & Maharidge (2014) showed in experimental studies an increase of complex fracture complexity with a decrease of fluid viscosity. Baihly et al. (2007) attributes microseismic activities that extend far beyond induced fracture to the existence of SRV. Ehlig-Economides & Economides (2011) explained how SRV is

created when fracturing water is imbibed in the high capillary shale, blocking fractures from closing and acting as conduit to hydrocarbon to flow to the induced fracture. Fracture fluid role in production was examined in other studies. Following shale stimulation operation, only quarter to half of pumped fluid is recovered, and the remaining is trapped in the reservoir. From actual practice, it is generally considered a bad sign to recover more stimulation treatment fluid. (Erdle, et al., 2016)

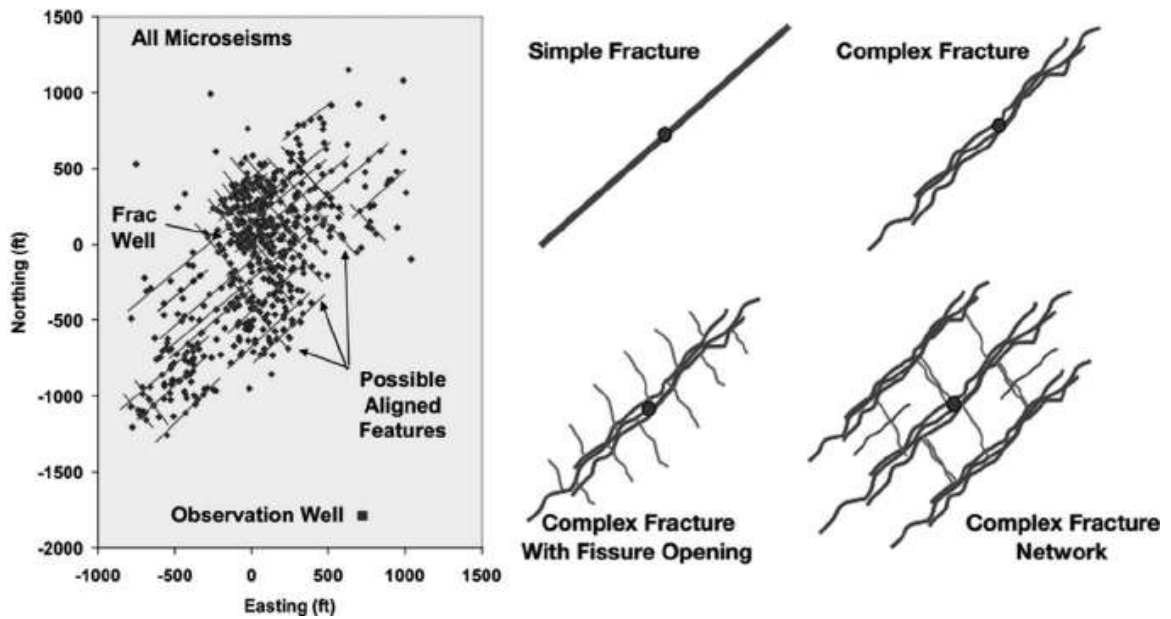


Figure 11: Possible Fracture Geometries (Anderson, Nobakht, Moghadam, & Mattar, 2010)

2.4 Production Analysis

Upon the completion of the stimulation treatments, the only way to evaluate reservoir and completion parameters and forecast production is through analyzing production history. In the following sections, we will explore key analysis methods used to analyze production data with emphasis on rate transient analysis for reasons that are explained in **Section 2.3.3**.

2.4.1 Background

By the end of pumping, well is initially flown back for several days up to couple of weeks for cleanup (**Figure 12**). After that, well is shut-in in preparation for connections to the pipeline network. Wellhead pressure and water production during flowback is considerably high. Gas production starts to pick up several days after the flowback start and increases significantly over few days, and then start declining during the production. The production decline in shale wells is extraordinary steep if compared to conventional wells. For example, first year decline exceeds fifty percent in five examined shale plays in North America (**Figure 13**). A lot of research have been conducted to analyze the reasons behind that severe production decline and how it can be alleviated. Understanding flow behavior in the reservoir and how fractures influences production is critical to improve well performance. Usually, only production period is analyzed for different reasons such as instability of initial gas flow, wellbore storage effect, or supercharged wells after stimulation.

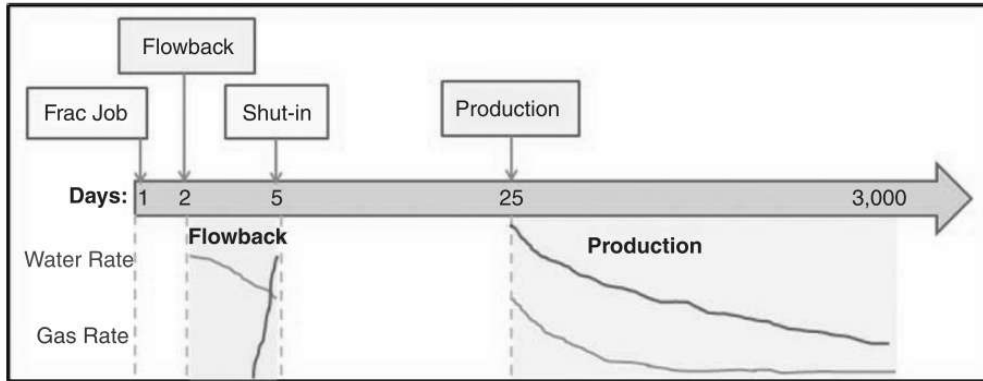


Figure 12: Typical Flow Sequence Adapted Shale Wells Production. Production Period Is Often Extensively Analyzed While Flowback Period Is Often Ignored (Alkough, Wattenbarger, & McKetta, 2014)

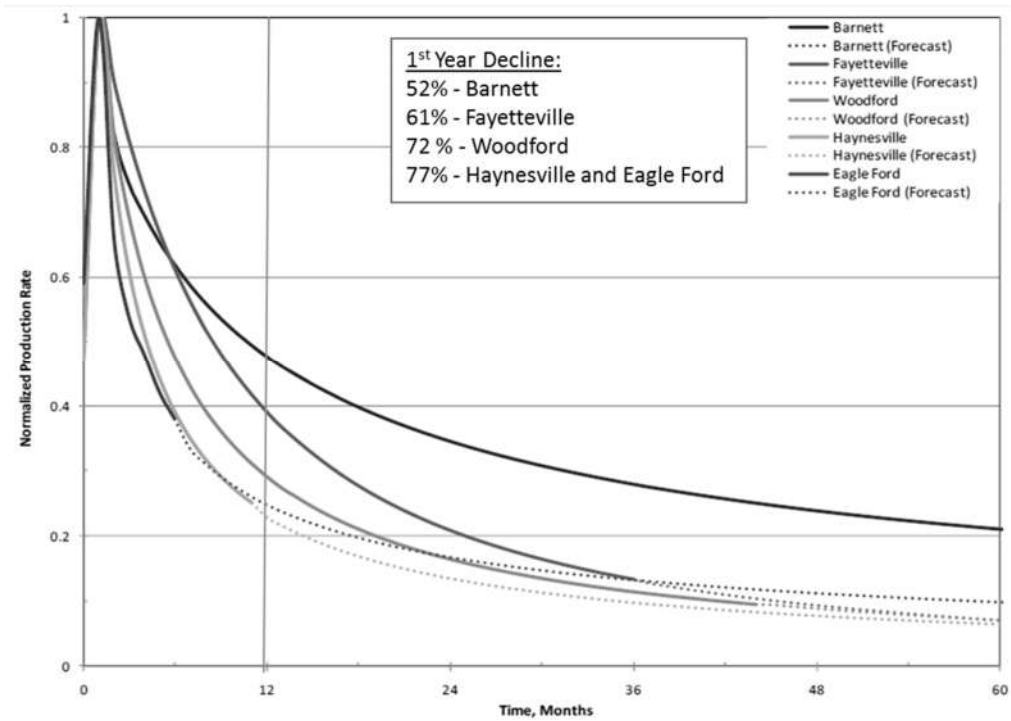


Figure 13: Normalized Rate Over Time in Five Shale Plays in North America (Baihly, Malpani, Altman, Lindsay, & Clayton, 2015)

2.4.2 Flow Regimes

The knowledge of flow regimes in multi-fractured horizontal wells (MFHW) is essential in production analysis. Each flow regime exhibits different decline behavior and reflect different region of fracture and reservoir interaction. Understanding the data that can be extracted from each flow regime is essential in analyzing production data. Flow in vertical wells is simpler; pressure transient radial away from the wellbore through the formation until it reaches a no-flow boundary and then depletes. In MFHW, pressure transient is much more complex and lengthy because of the existence of induced fractures, and change in permeability within SRV. Therefore, many studies have proposed several possible flow regimes sequence that could exist in MFHW. Early publications were conducted to describe flow in less intensive stimulation treatment. (Chen & Rajagopal, 1997; Wan & Aziz, 1999; Clarkson, Jordan, Ilk, & Blasingame, 2009) They describe early pseudoradial flow around the fracture. Later literatures included the effect of intensive stimulation in MFHW. (Song & Ehlig-Economides, 2011) However, all describe flow regimes that include linear flow, radial and compound linear flow. Each flow regime lasts considerable time due to formation low permeability, and it is expected to take years to witness all these flow regimes. Analyzing the historical production data, only three flow regimes have been witnessed: bilinear flow, linear flow, and boundary dominated flow (BDF) as shown in **Figure 15**. (Blasingame T. , 2013; Erdle, et al.; Sharma & Lee, 2016) Flow regimes that precede BDF flow is called “transient flow.” BDF flow starts once the transient flow reached all the reservoir boundary, which is in case of MFHW is the SRV volume (**Figure 14**). Bilinear flow could last form weeks to months and linear flow could last from months to years. When Linear flow & BDF are witnessed, an estimation could be made of effective

permeability, fracture half-length, SRV pore volume, and adsorption index (Song & Ehlig-Economides, 2011). Understanding of the three flow regimes is essential for analyzing MFHWs.

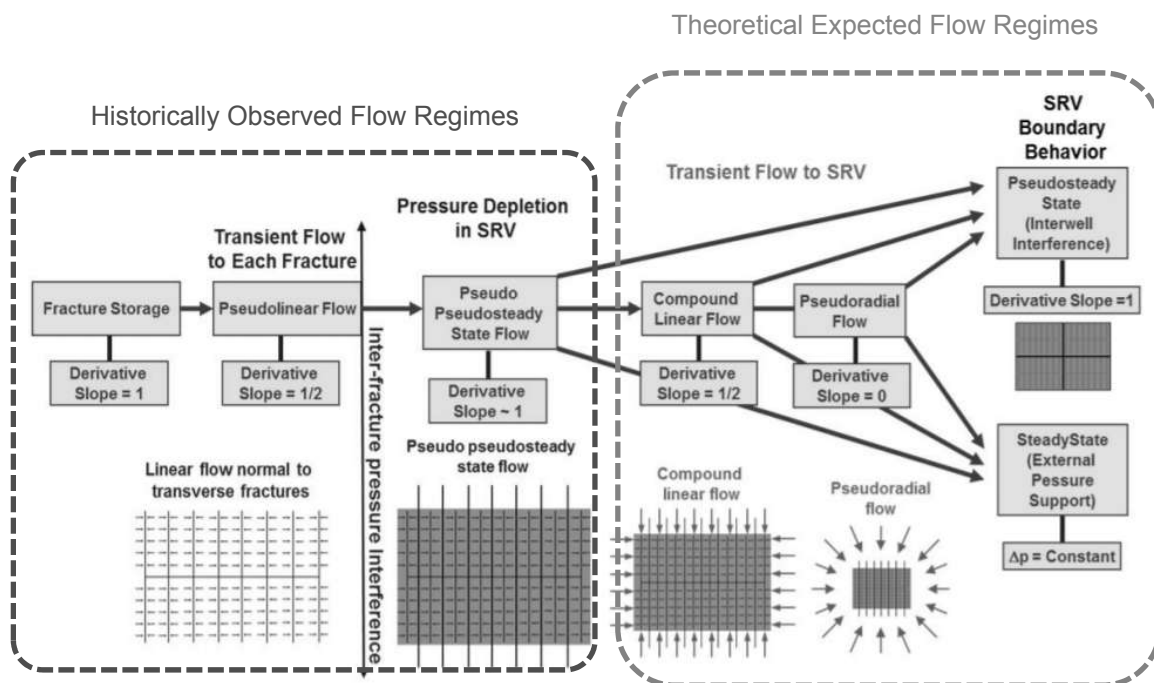


Figure 14: Flow Regime Sequence as Describe by Song & Ehlig-Economides. (2011) Note That Only Three Initial Flow Regimes Have Been Witnessed from Historical Data

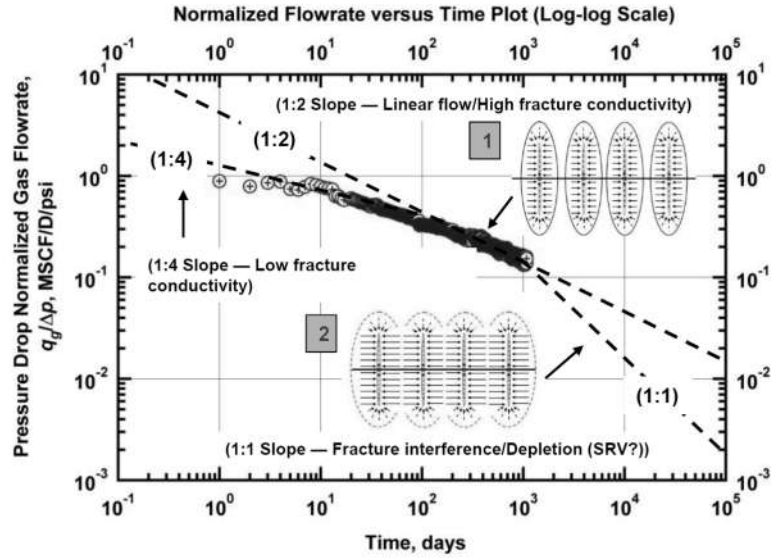


Figure. 15: Flow Regimes Observed in Typical Stimulated Shale Reservoir (Blasingame T. , 2013)

2.4.2.1 Linear Flow

The linear flow behaviors for slightly compressible liquid could be adequately modeled by the following equation (Spivey & Lee, 2013):

$$\left(\frac{P_i - P_{wf}}{q}\right) = 25.54 \frac{B}{4 n_f x_f h} \left(\frac{t\mu}{k\phi c_t}\right)^{1/2} + 141.2 \frac{B\mu}{kh} s_f \quad (1)$$

Equation 1 could be further simplified to Equation 2:

$$\left(\frac{P_i - P_{wf}}{q}\right) = m_L \sqrt{t} + b_L s_f \quad (2)$$

Where a straight line would result from normalized pressure *vs.* \sqrt{t} , or half-slope would have been observed in log-log plot of normalized pressure versus time. The intersection of

the line in square root time plot defines the fracture skin, s_f . The slope of the line is equal to m_L , and if the n_f is known, we can infer $x_f\sqrt{k}$. $x_f\sqrt{k}$ is a non-unique solution, and either fracture half-length or permeability has to be estimated from other methods. Wattenbarger et al. (1998) found that reservoir permeability could be estimated if the time of end linear, t_{elf} , is known using the following equation:

$$k = \frac{1896\phi c_t d_i^2}{t_{elf}} \quad (3)$$

Where d_i is the half distance between fractures in MFHW, and could be calculated by dividing the well effective length by the $2n_f$.

The presence of linear flow might get delayed due to fracture skin change over time. Doung (2011) found that shale wells undergo initial cleanup period after pumping treatment in which s_f is stabilizing over time during; afterward, linear flow could be detected. During fracture skin stabilization, the linear flow might exhibit bilinear flow behavior. Also, if only linear flow is observed, and the BDF is not, only maximum effective permeability, and minimum SRV pore volume could be estimated. (Song & Ehlig-Economides, 2011)

2.4.2.2 Bilinear Flow

The bilinear flow behaviors for slightly compressible liquid could be adequately modeled by the following equation:

$$\left(\frac{P_i - P_{wf}}{q}\right) = 25.54 \frac{49.0 B\mu}{h(w_f k_f)^{0.5} (\mu k \phi c_t)^{0.5}} t^{0.25} + \frac{141.2 q B \mu}{kh} s_f \quad (4)$$

Equation 4 could be further simplified to **Equation 5**:

$$\left(\frac{P_i - P_{wf}}{q}\right) = m_L t^{0.25} + b_L s_f \quad (5)$$

Where a straight line would result from normalized pressure versus $t^{0.25}$, or quarter slope would have been observed in log-log plot. The intersection of the line in normalized pressure plot versus $t^{0.25}$ defines the fracture skin, s_f . The slope of the line is equal to m_L , and if the permeability is known, fracture conductivity, $w_f k_f$, could be estimated.

2.4.2.3 Boundary Dominated Flow

The BDF flow behaviors for slightly compressible liquid could be appropriately modeled by the following equations (Blasingame & Lee, 1986; 1988):

$$\left(\frac{P_i - P_{wf}}{q}\right) = b_{pss} + m t_{mb} \quad (6)$$

Where both b_{pss} and m are constants, and are defined as following:

$$b_{pss} = 70.6 \frac{B\mu}{kh} \ln\left(\frac{4A}{e^\gamma C_a r_w^2}\right) \quad (7)$$

$$m = \frac{1}{24 c_t^i N} \quad (8)$$

And the material balance time, t_{mb} , is defined:

$$t_{mb} = \frac{N}{q} \quad (9)$$

For highly compressible fluid in gas reservoirs, change in viscosity and compressible is accounted by using both pseudo-pressure and material balance pseudo-time. Material balance pseudo-time is defined:

$$t_{mb} = \frac{\mu_i c_{ti}}{q} \int_0^t \frac{q}{\bar{\mu} \bar{c}_t} dt \quad (10)$$

And the pseudo-pressure is defined as:

$$P_p = \frac{\mu_i}{\rho_i} \int_{P_i}^P \frac{\rho}{\mu} dP \quad (11)$$

BDF can be easily defined as a unit slope line on log-log plot of normalized pressure versus material balance time. It usually occurs after transitional period following the linear flow. SRV pore volume (and thus fracture half-length) could be inferred from the slope of the line, m , and minimum permeability could be infer from the line intersection, b_{pss} . (Song & Ehlig-Economides, 2011) It is worthy to notice that well or fracture liquid loading could be mistaken by BDF signature, and thus stable well condition must exist before determining BDF regime.

2.4.3 Analysis Methods

Many empirical, analytical and numerical solution to analyze production date in porous formation have been published. Arps was the first to analyze declining rate in producing wells empirically. His models predict future rate, and expected ultimate recovery, EUR, based on well production history as long as production condition is stable and BDF has prevailed. In shale formation, transient flow lasts typically for years, and application of Arps's equations during this period tends to overestimate future production.

Utilizing Darcy's law and Diffusivity Equation, many numerical and analytical solutions have been proposed to analyze production changing rate and pressure. Numerical solutions demand detailed information about the subject reservoir and require large computing and human resources; therefore, they are considered impractical to be utilized in wide range in economically-marginal shale wells. Analytical solutions are classified into two groups: pressure transient analysis, and rate transient analysis. Pressure transient analysis, or welltest analysis, examine pressure build up during shut-in periods while rate transient analysis, or RTA, examines production decline during flow. Welltest analysis provide detailed reservoir characterization but fail to estimate EUR and forecast future production. Welltest analysis require long shut-in period to analyze shale, and thus is not practical because the unavailability of required shut-in periods. As Result, RTA is more commonly used to analyze shale as summarized in **Figure 16**. (Fekete, 2011; Blasingame T. , 2013; Erdle, et al., 2016)

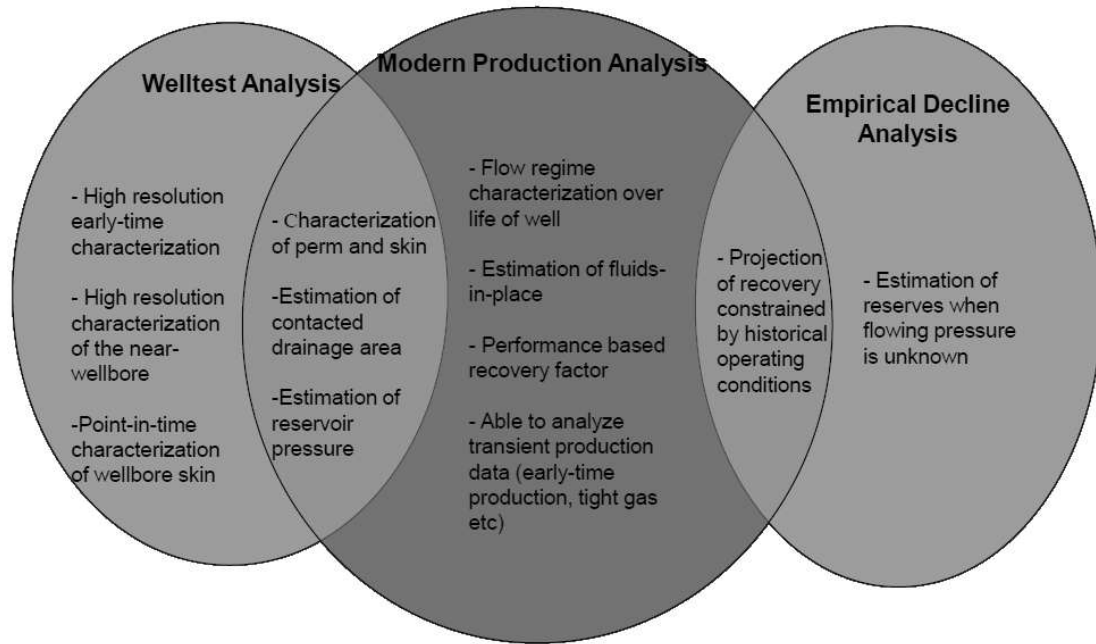


Figure 16: Comparison of Analysis Methods for Gas Shale Production Showing How Rate Transient Analysis Incorporate Key Analysis Parameters (Fekete, 2011)

There are several RTA type curves used to analyze production such as Blasingame, Fetkovich, etc.... However, their solution is not unique if the boundary dominated flow regime has not been reached. Unfortunately, this is the case of many of the emerging shale plays; several weeks to few months of transient flow only are available for analysis. In order to overcome this problem, Straight-line methods mentioned on **Section 2.3.2** or Flowing Material Balance (FMB) ought to be utilized. Due to lack of boundary dominated flow, many assumptions are used to yield reasonable results. (Fekete, 2011)

2.4.3.1 Flowing Material Balance

Flowing Material Balance, FMB, is used to estimate initial gas in place, IGIP, in case where static pressure is not available. Previously, IGIP was estimated by taking several reservoir

static pressure readings over the life of the reservoir in order to perform material balance, and estimate IGIP. Unfortunately, pressure build up in tight reservoirs is not partial due to long transient flow period. In order to overcome this problem, Fekete observed that the well bottom-hole pressure, BHP, decline is proportionate to the decline in average reservoir pressure, \bar{P} . They also noticed that well productivity is proportionate to the pressure drawdown. They formulated both relation and integrated them together to estimate initial hydrocarbon in place. (Fekete, 2011)

2.4.4 Horizontal Multifrac Composite Model

Denney proposed analytical model to simulate the flow of unconventional gas reservoir. The model assumed the inner and outer reservoirs differ in their permeability and dimension. The inner layer is intersected by equally spaced fractures that are similar in their properties (ex. half-length, width, and conductivity) as shown in **Figure 17**. The model assumed three linear flow: (1) along the hydraulic fractures, (2) within the inner reservoir, and (3) within the outer reservoir. The model is preferred to analytically simulate shale gas behaviors because it approximates the different flow regimes observed in shale gas wells, and it takes into account key reservoir and completion parameters. (Denney, 2010)

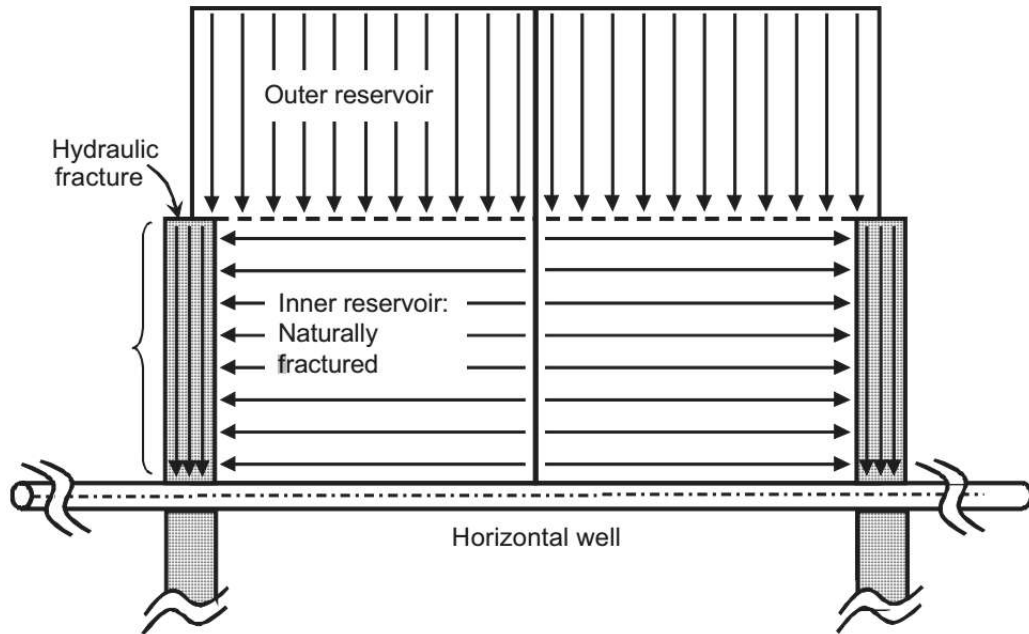


Figure 17: Schematic of Trilinear Flow Within the Composite Model (Denney, 2010)

2.4.5 Proposed Production Analysis Workflow

As mentioned, there are several methods to analyze shale gas production which lead to confusion when dealing with such wells. To resolve the problem, numerous workflows suggested in literatures to analyze unconventional gas reservoirs. Clarkson, Jensen, & Blasingame (2011) a more genreal workflow for filed development optimization in unconetional gas resources. Ilk et al. (2010) suggested a workflow with focus on diagnostic analysis of production data. Anderson et al. (2010) suggested a deterministic workflow mainly based on straight line approach to analyze MFHW production. Clarkson, Jensen, & Blasingame (2011) proposed a more genreal workflow for field development optimization in unconetional gas resources. Clarkson et al. (2013) suggested a workflow to incorporate all transient analysis methods available (**Figure 18**). Most of the workflow revolve about

three main steps: (1) Data Collection & Diagnostic, (2) Data Analysis & Validation, and (3) Data Modeling & Forecast.

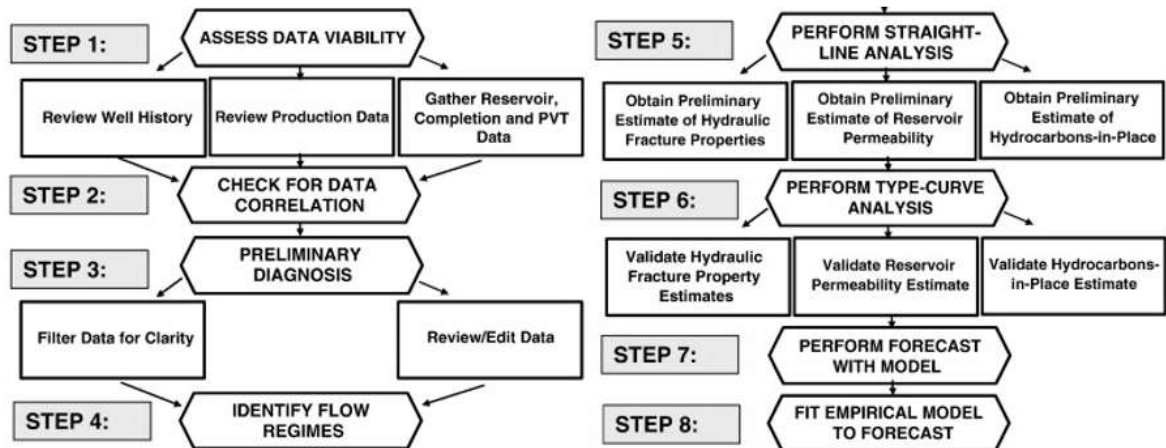


Figure 18: Suggested Production Data Analysis for Unconventional Gas Wells (Clarkson C. R., 2013)

2.4.6 Probabilistic Evaluation

The uncertainty in assisting well performance in shale gas well is high especially when many reservoir and completion variables affecting well production is not well defined. For example, only approximation of average fracture half-length can be estimated in rate transient analysis. The estimation is a function of number of not well-defined parameters fractures cluster number, fracture height, and reservoir permeability. In order to overcome this challenge, a probabilistic approach is recommended to narrow the outcomes. Probabilistic approach has been previous tried to analyze uncertainties in conventional and unconventional resources. (Dong , Holditch , & McVay, 2013; Williams-kovacs & Clarkson, 2013)

CHAPTER 3

RESEARCH OBJECTIVES AND METHODOLOGY

3.1 Problem Statement

Gas shale belongs to reservoirs that are often characterized by low permeability rock formations that produce mainly gas. The quantities of the gas held in shale gas sources exceed that of conventional reservoirs by several folds. Until recently, the commercial production of natural gas from unconventional resources was made difficult due to many technical challenges. The advancements made in commingled well drilling, and hydraulic fracture treatment, all helped in improving recovery by exposing more of the reservoir to the wellbore. However, there is high uncertainty in forecasting shale gas and determining parameters affecting its production. For example, there are uncertainties in estimating key petrophysical data such as porosity and water saturation using log analysis because free and connate water signatures are similar in tight rock with complex pore system, and rich mineralogy. Also, it is challenging to model hydraulic fractures growth and their reaction to natural fracture, and different stress regimes. Furthermore, production analysis results in a nonunique solution to parameters such as the fracture half-length and permeability due

the lengthy transient period that shale reservoir expresses. All of the previous presents uncertainties when analyzing shale gas wells.

3.2 Research Objectives

The objective of this work is to evaluate the reservoir and completion key parameters affecting shale gas production in single, multi-fractured, horizontal wells. The reservoir parameters that will be studied are porosity, permeability, water saturation, and initial pressure. The completion parameters that will be examined are well length, wells spacing and fracture related parameters such as number of cluster, fracture height, fracture half-length, and fracture conductivity. Finally, an attempt will be made to recommend better stimulation treatments based on the sensitivity analysis.

3.3 Research Methodology

In order to achieve Objectives, a workflow composed from three main steps is used: (1) Initial Production Analysis, (2) Probabilistic Evaluation, and (3) Sensitivity Analysis.

Figure 19 illustrates in details the tasks proposed to achieve our objectives.

3.3.1 Initial Production Analysis

In this task, we will first collect available completion and reservoir inputs (**Table 1**). Then, an appropriate rate transient analysis is performed following Clarkson workflow. (Clarkson C. R., 2013).

Table 1: Summary of The Reported Parametes From The Literature

Parameters	Range
Gross Thickness (ft)	80-160
Porosity (%)	2-8
Matrix Permeability (nd)	100-800
Water Saturation (%)	10-40
Depth (ft)	9,000-10,000
Reservoir Pressure (psi)	6,000-9,000

In order to accomplish this task, IHS Harmony and Kappa Sapphire, two software package that specialized in rate and pressure transient analysis, that will be used to analysis the available production and pressure data.

3.3.2 Probabilistic Evaluation

In this task, we first define the probability distribution related to each collected well parameter. Some parameters are more certain while others have some level of uncertainty. For example, well length, and reservoir temperature are more certain than matrix permeability, and fracture half-length (**Table 2**). Therefore, in this step the effort revolves in acquiring inputs and lowering the uncertainty of unknowns.

Table 2: Main Reservoir and Completion Parameters Examined

Parameters	
Reservoir	Initial Pressure Porosity Permeability Reservoir Width
Completion	Fracture Number Fracture Half-length Fracture Height Fracture Conductivity Lateral Length

Once the parameters' probability distributions are defined, Monte Carlo simulation is used to construct parameters stochastic samplings. Monte Carlo picks random samples from each parameter. The samples are then used to run the Composite Model numerous times. Thus, the uncertainties of collected parameters are adequately reflected. The Model is defined in **Table 3**.

Table 3: Reservoir Model for Analysis

Specification	Description
Porosity	Homogenous
Permeability	Isotropic, dual region
Inner region	Near fracs
Outer region	Rectangle
Pressure step	Constant
Lithology	Shale
Well location	Center

There are two main outcomes from the previous steps which are probabilistic production forecast, and final parameters probability distribution. Probabilistic forecast captures the

range of likely production from the study subject well. The final parameters probability distribution would redefine the initial probability in the light of production.

In order to accomplish this task, @Risk (MS Excel add-in) or IHS Harmony is used. @Risk can define the probability distribution related to each collected parameter, and create Monte Carlo samplings. IHS Harmony run the composite model and output the results.

3.3.3 Sensitivity analysis

This is considered the final task in our methodology. During this task a sensitivity analysis is performed to define the impact of completion and completion parameters on the production (**Table 2**). Similar workflow used in the Probabilistic Evaluation is used except the final reservoir parameter probabilistic distribution is used, and the sensitivity completion parameters would be repeatedly verified to output production.

In order to achieve the previous tasks, IHS Harmony is used as main tools.

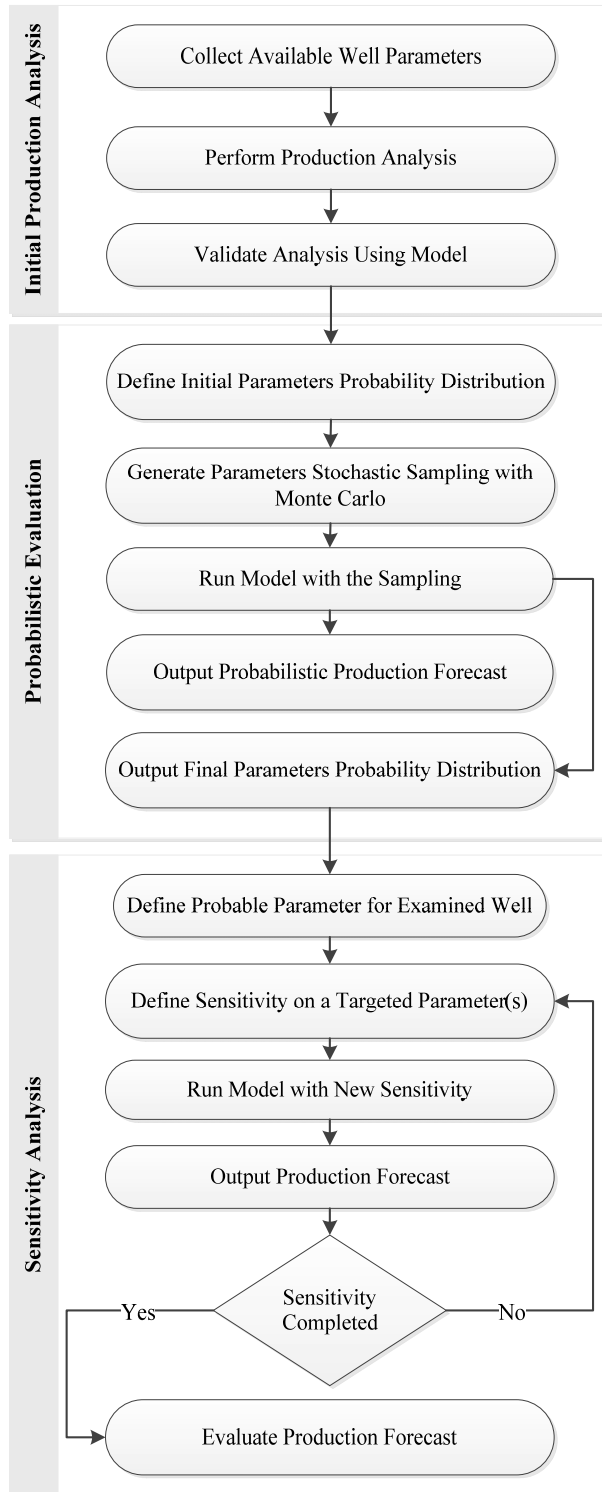


Figure 19: Used Methodology Workflow

CHAPTER 4

RESULTS AND DISCUSSION

In this study, three multi-fractured horizontal wells drilled in a gas window of a shale basin were examined. The wells are in a close proximity to each other and draining similar fluid, but strikingly have different performance. To explore the difference, we will first discuss the uncertainties related to each parameter examined. Then, each case is examined separately. Discussion on the uncertainty effect is presented and then finding is concluded in the result section.

4.1 Uncertainties Constrain

The unknowns are more than the knowns parameters in MFHW with just few weeks or months of production. Therefore, it is important to understand and constrain the limits of each parameter uncertainties. To illustrate, formation temperature, well length, well spacing, fluid properties, and porosity are all parameters that the analysts are almost sure of. Temperature is usually measured during wireline logging. Well length and spacing are accurately measured from the deviation survey. On the other hand, fracture numbers, initial

pressure, and fracture height are all parameters that are dealt with care. For example, in well with 3 cluster per stage, at least one fracture per stage is initiated and at most 3 fractures per stage are initiated. Initial pressure could be estimated with high accuracy using DIFT or mini-fracture analysis. If this is not the case, pressure gradient could be used to estimate initial pressure. In the following sections, parameters with high uncertainty are examined, and how the uncertainty is confined:

4.1.1 Fracture Height

Fracture-height, h_f , is one the least certain parameter during production analysis. There is no direct measurement to determine fracture height in horizontal wells. In vertical wells the problem is simpler, direct measurement of fracture-height could be done by using temperature logging after the treatment, or using GR logs if radioactive tracers were injected during the frac job. In horizontal wells, logging tool has no use, and only indirect estimations of fracture height are available (e.g. hydraulic simulator or microseismic). To resolve this uncertainty, the maximum fracture height is assumed to be the pay thickness. Even if the fracture grows beyond the pay thickness, marginal contribution is expected. The minimum fracture height could be assumed from nearby wells.

4.1.2 Fracture Half-length

Effective fracture half-length could be only estimated by production analysis. Therefore, it is important to constrain our model in order to result in a reasonable estimation. The minimum value for fracture length could be estimated from contacted Flowing Material Balance's GIP. The maximum value for hydraulic fracture length could be estimated by

hydraulic fracture modeling or microseismic, or at most well spacing. If these are not available, public data should be used to constrain the maximum value of effective fracture half length.

4.1.3 Number of Fractures

‘Plug and perf’ was the technique used for stimulation treatment in the three cases in this study. **Section 2.2** is used to relate fracture contribution with cluster number. For example, on average, 80 percent of fractures in 4 clusters per stage contribute to the total production.

4.1.4 Permeability

There are two permeability values to be considered: non-stimulated rock permeability or outer permeability, and stimulated permeability or inner permeability. Maximum inner permeability is estimated using **Equation 2** which relates fracture spacing and time of linear flow to the SRV permeability. Minimum inner permeability is larger than outer permeability. Outer permeability could be estimated from DIFT analysis (preferred) core, and log analysis, or an assumption of 10-100 nd.

4.1.5 Initial Pressure

Accurate pressure estimation could be acquired using post-closure analysis. If pressure direct measurement does not exist, an estimation could be used from nearby wells. The upper limit for initial pressure should not exceed fracture gradient pressure, and lower limit has to be equal to the estimated pressure from pressure build up test.

4.1.6 Fluid Properties

For near critical fluid such as condensate gas, a full PVT study on an early bottom-hole sample is highly recommended. If it is not available, EOS calibrated by recombined wellhead sample should be used. If it is not available, nearby wells, should be considered.

4.2 Case Studies

In this study, three MFHW wells drilled in a gas window of a shale basin were examined. The wells are in a close proximity to each other and draining similar fluid, but strikingly have different performance. In the following sections, the proposed workflow is applied to each case.

4.2.1 Well A

The well was drilled in a gas window. After flowback period of two weeks, the well was suspended for few months for the installation of velocity string (VS) to assist lifting and prevent any liquid loading in the well. The well flowed for several months, with high gas oil ratio (~8000 scf/stb). The only data available was petrophysical logs, completion summary, separator samples and surface pressure, and rate history. Key reservoir parameters are summarized in **Table 4**. Because VS was installed during production, the risk of liquid loading up was lowered and the production is believed to represent reservoir signature.

Table 4: Fixed Well Parameter for Well A

Layer Data	Value
Reservoir temperature (°F)	270
Flowing bottomhole pressure (psia)	100
Reservoir length (ft)	4,812
Reservoir width (ft)	1,300
Number of stages	16
Bulk density (g/cc)	2.5

4.2.1.1 Initial production analysis

The first step in data analysis is to convert surface readings to bottom hole. In order to do so, well configurations, along with fluid properties and production history were uploaded to PROSPER, a well performance simulator. After that, normalized rate versus normalized material balance time was plotted to identify flow regimes. Material balance pseudo-time, $t_{mb} = \frac{\mu_i c_{ti}}{q} \int_0^t \frac{q}{\bar{\mu} \bar{c}_t} dt$, is calculated first and then normalized to the maximum MBT recorded. The rate is divided by pseudo-pressure $P_p = \frac{\mu_i}{\rho_i} \int_{P_i}^P \frac{\rho}{\mu} dP$, and then normalized by highest normalized rate recorded. Two flow regimes were clearly identified: bilinear flow, and linear flow, with no sign of transition to BDF (**Figure 20**). The bilinear period could be attributed to fracture cleanup, and it lasted around 2 months recovering ~13.5 % of fracturing fluid. A stabilization in GWR was noticed afterward to ~ 50 bbl/MMscf which probably indicates well cleanup. Because only linear flow exists, minimum SRV pore volume, and maximum SRV permeability could be possibly estimated.

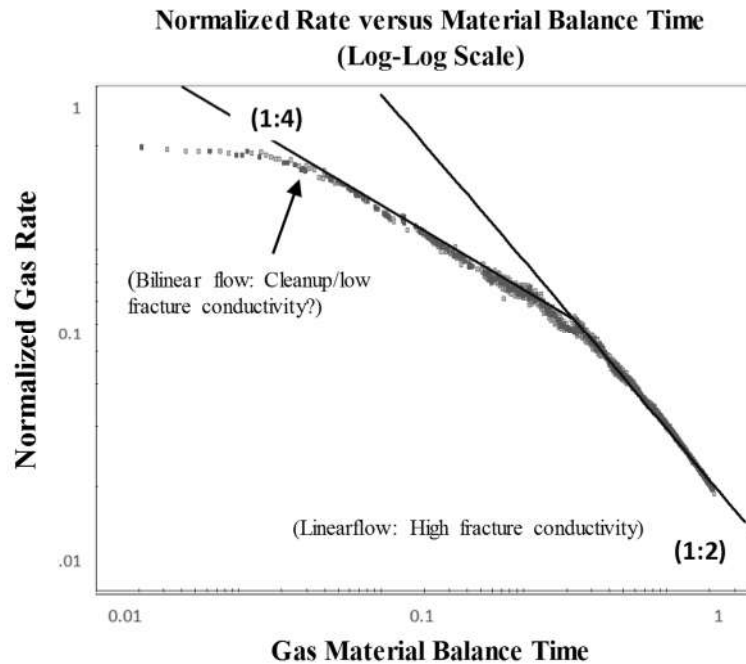


Figure 20: Well A Normalized Rate Versus Material Balance Time (Log-Log Scale)

Next, normalized rate versus square root time was used to estimate $x_f\sqrt{k}$. **Equation 2** defines $x_f\sqrt{k}$ as the slope of the data straight line, which is 30 md^{1/2}.ft. Also, **Equation 3** is used to define the maximum SRV permeability from time of the end of linear flow and fracture spacing. Lastly, minimum SRV volume is estimated by extrapolating using flowing material time plot (**Figure 22**).

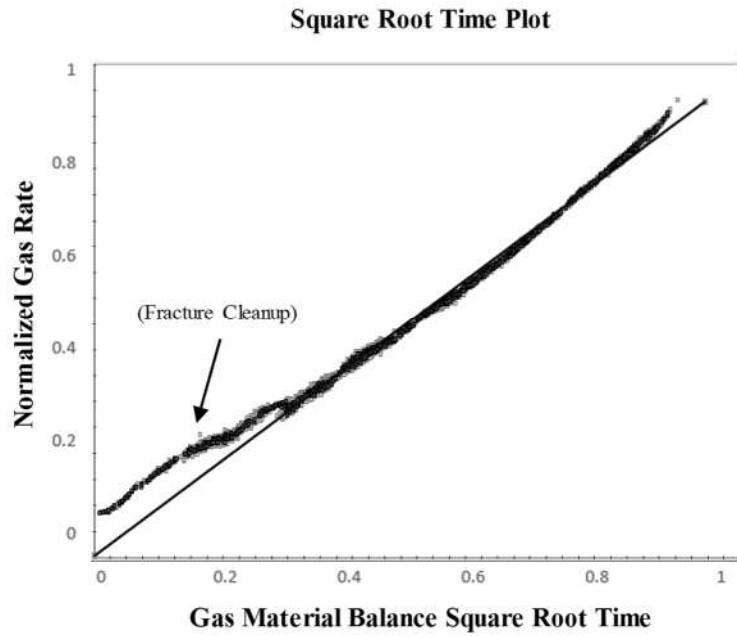


Figure 21: Well A Square Root Time Plot

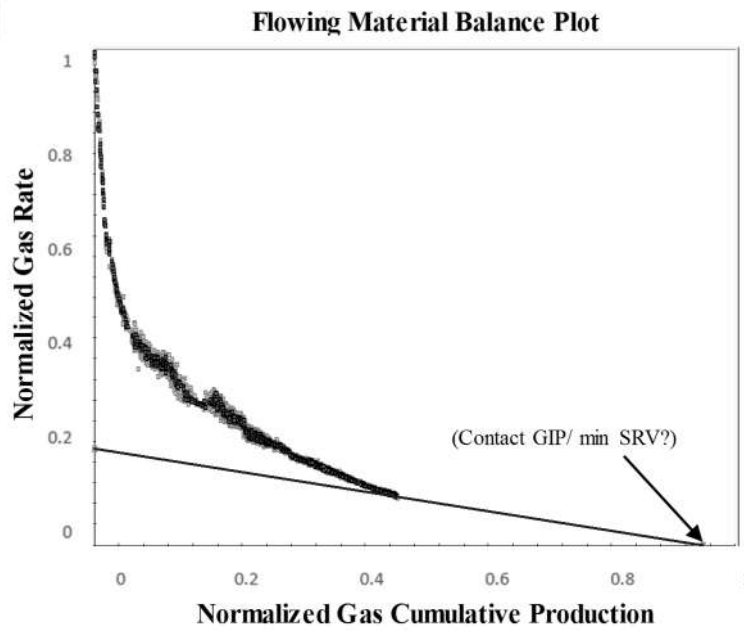


Figure 22: Well A Flowing Material Balance Plot

Utilizing the input data extracted from straight-line analysis, Trilinear composite model was used to model production. Rectangular model, with 45 equally spaced fracture was used to model production. Initial well parameters (

Table 4) and the estimations of straight-line analysis are used as initial input for the model and regression was conducted on inner permeability, fracture half-length, and fracture conductivity. The model succeeded on having an excellent history match of production history as shown in **Figure 23**.

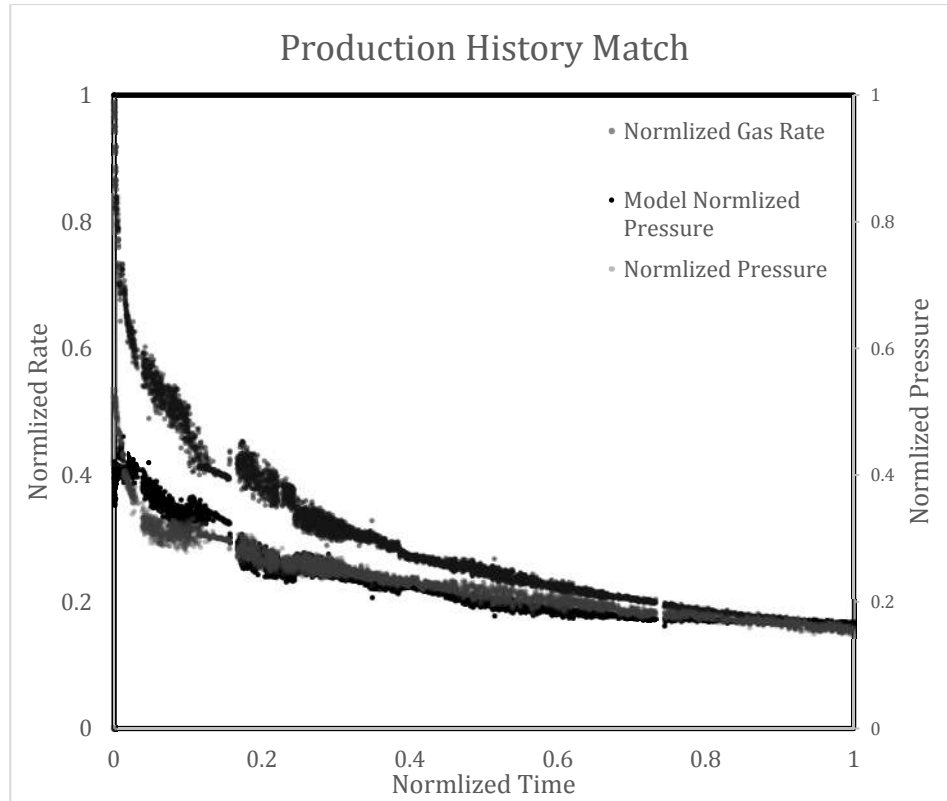


Figure 23: Well A Production History Match

4.2.1.2 Probabilistic Evaluation

In this step, the uncertainty overlooked in Step 1 is considered and evaluated. Each fixed parameter in the previous step is now given an initial distribution (**Table 5**). Positive correlations were considered between porosity and saturation, and negative correlation was given to fracture numbers and fracture half-length. Next, a simulation was conducted to refine the assumed distribution, and to forecast possible production. Initial and final parameter distribution are summarized in **Table 5**. **Figure 24** shows P10, P50, and P90 forecast for Well A.

Table 5: Initial and Final Distribution for Uncertain Well A Parameters

Parameters	Initial Distribution			Final Distruntion				
	Distribution Type	Min	Max	Mean	Distribution Type	Mean	P10	P90
Number of Fractures	Triangular	32	63	48	Normal	47	57	38
Fracture half-length (ft)	Uniform	30	250	-	Log-Normal	118	208	46
Fracture Conductivity (N/A)	Uniform	5	300	-	Normal	21	32	16
Inner permeability (nd)	Uniform	90	400	-	Log-Normal	162	290	117
Outer permeability (nd)	Uniform	20	90	-	Log-Normal	25	34	20

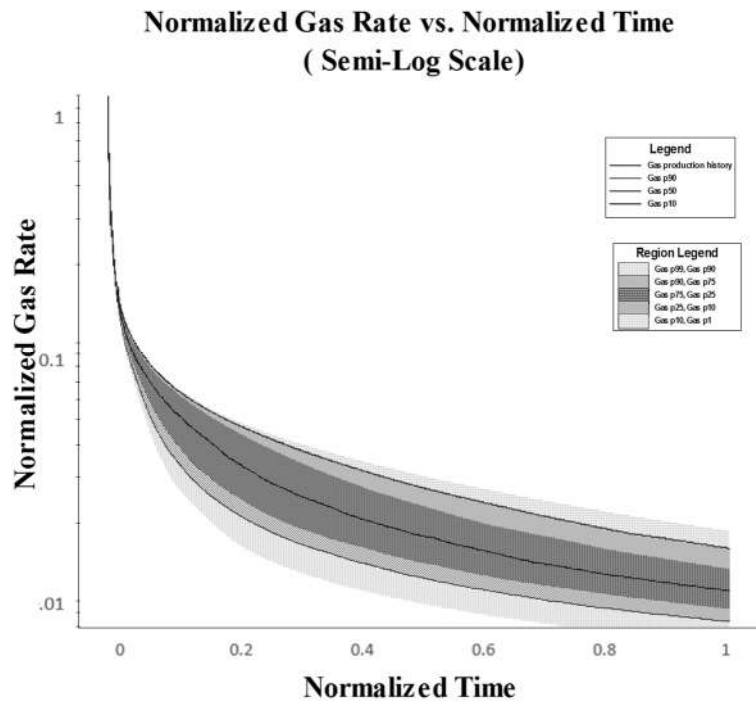


Figure 24: Well A Forecasted Normalized Gas Rate Versus Normalized Time (Semi-Log Scale)

4.2.1.3 Sensitivity Analysis

After the probabilistic analysis, a better understanding of likely completion and reservoir parameters is achieved. A trilinear composite model is now created and fed by the mean value of the final distribution in **Table 5** in order to create a base case scenario. After that,

sensitivities on main reservoir and completion parameters is inputted into the model, and model is run for 60 years in order to see impact of each parameter. Results are presented in both Cartesian and logarithmic scaled figures and normalized to base case maximum value to get different view on the performance. The following results are found as result of sensitivity analysis:

- Production is directly proportional to Fracture half-length. The longer the fracture half-length created, the higher the rate and cumulative production achieved. The ratio in production increase due fracture half-length increase is 1:2 (
- **Figure 25).**
- Flow regimes' durations are not affected by fracture half-length (**Figure 26).**

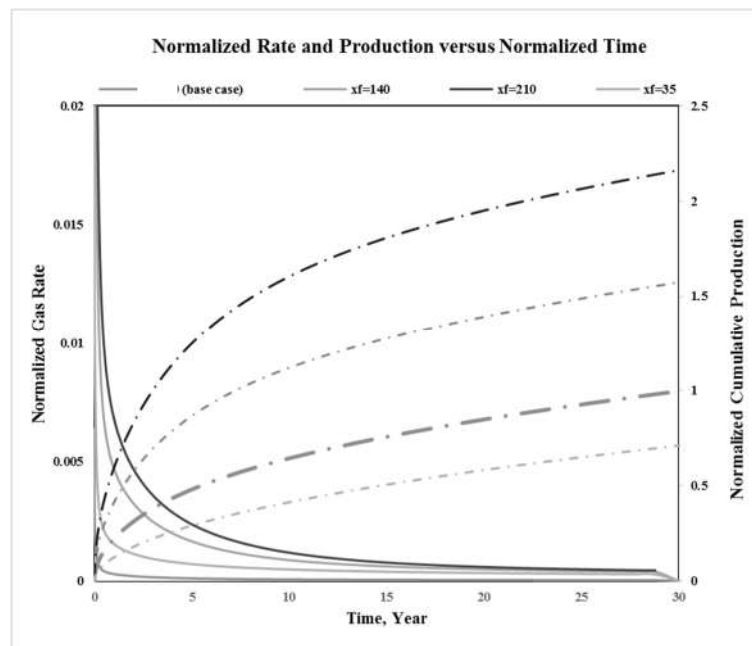


Figure 25: Well A Fracture Half-Length Sensitivity

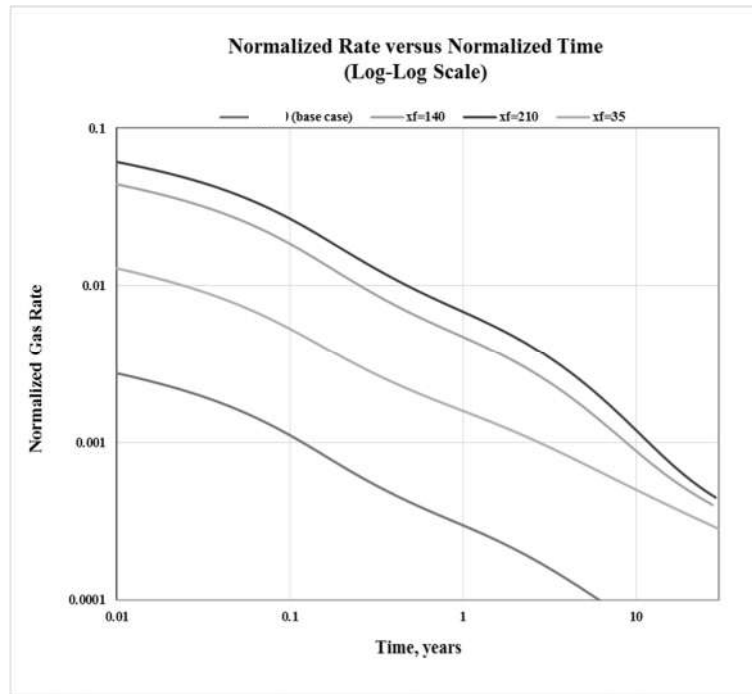


Figure 26: Well A Fracture Half-Length Sensitivity (Log-Log Plot)

- Production is directly proportional to fracture number. The more fractures created, the higher the initial rate and cumulative production are achieved. The initial rate increase only lasts for at most a year. The ratio between production increase after 60 years due fracture number increase is 3:5 (**Figure 27**). The more fractures number, the shorter the transition period between first linear flow and BDF (**Figure 28**).

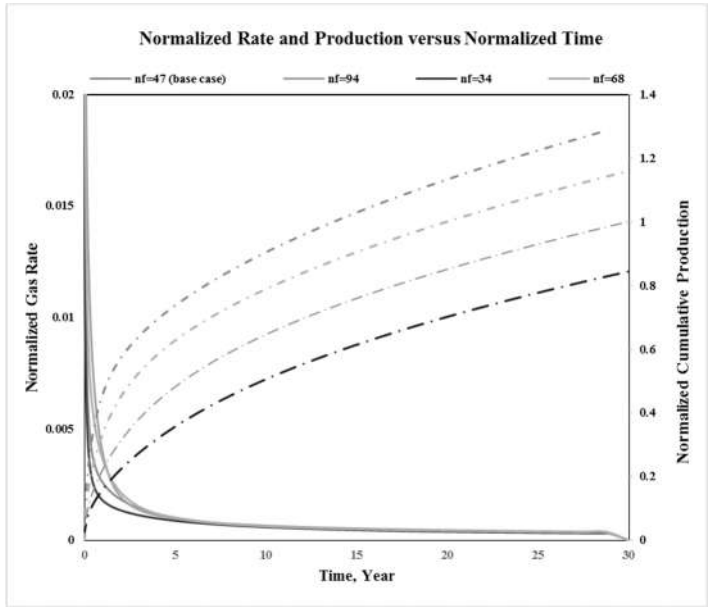


Figure 27: Well A Fracture Number Sensitivity

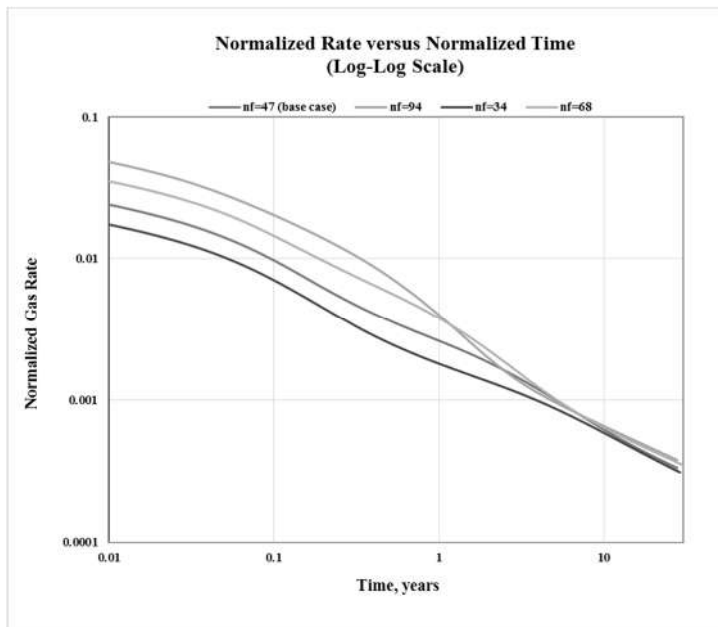


Figure 28: Well A Fracture Number Sensitivity (Log-Log Plot)

- Production is directly proportional to well length; however, the relationship fades away on longer well cases. The effect of longer wells appears after a year of production. The ratio between production increase after 60 years due longer well is 3:5 (**Figure 29**). Longer wells delay BDF regime, and extend the linear flow regime (**Figure 30**).

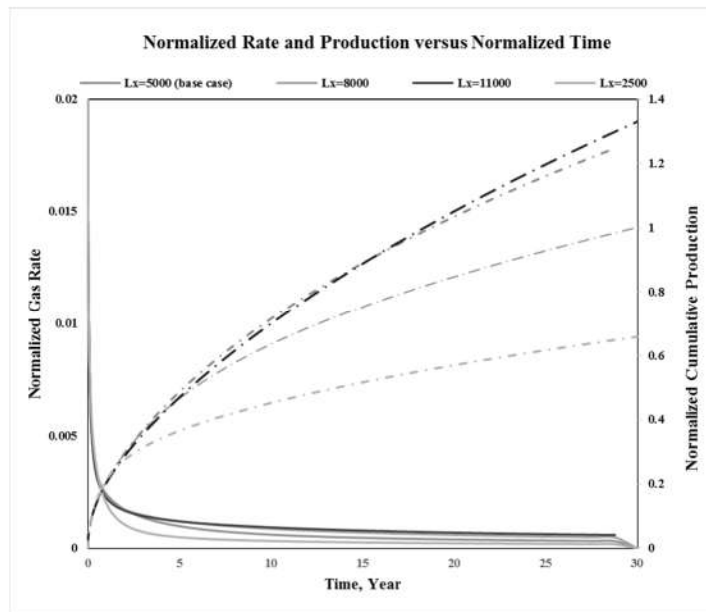


Figure 29: Well A Well Length Sensitivity

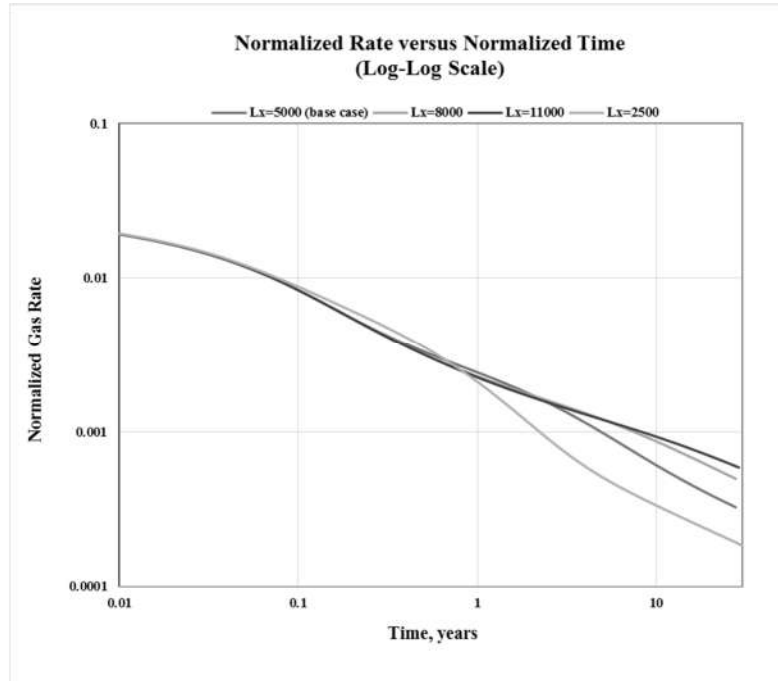


Figure 30: Well A Well Length Sensitivity (Log-Log Plot)

- Production is directly proportional to fracture conductivity. However, the effect of more conductive fractures is negligible and only apparent in the first days and only lasts for up to few months (**Figure 31**). Fracture conductivity does not affect flow regimes duration (**Figure 32**).

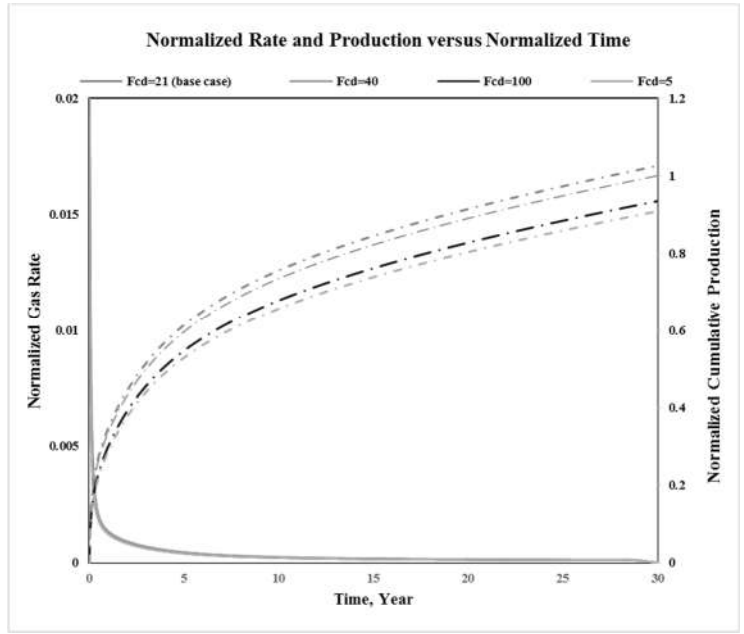


Figure 31: Well A fracture conductivity sensitivity

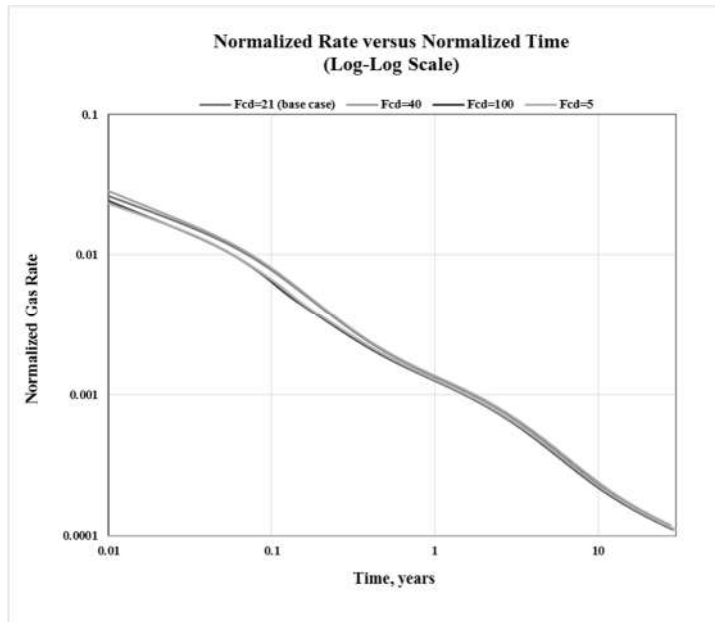


Figure 32: Well A Fracture Conductivity Sensitivity (Log-Log Plot)

- Production is directly proportional to well spacing. The effect of longer spacing is initially negligible and only apparent in the last years of production. However, short spacing that is really close to fracture length shortens well life significantly and thus production (**Figure 33**). Well spacing does not affect flow regimes duration (**Figure 34**).

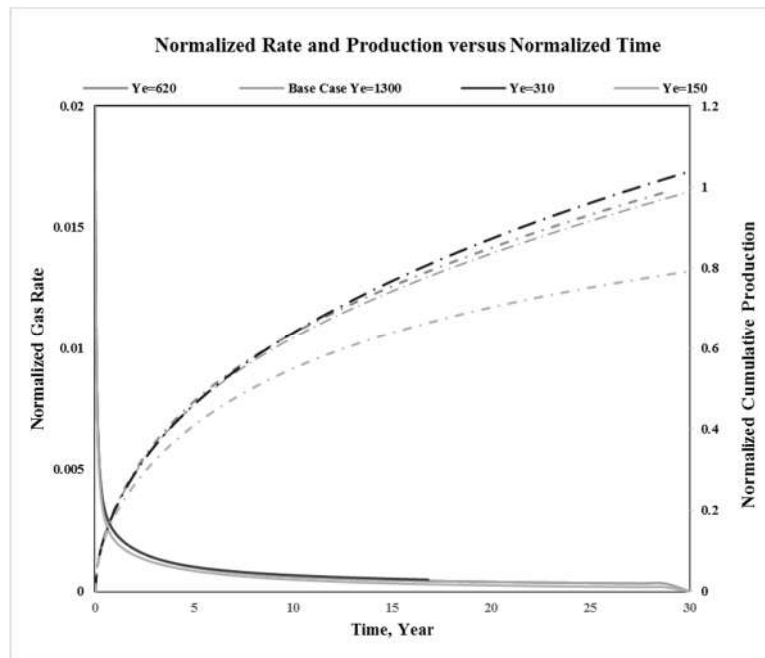


Figure 33: Well A Well Spacing Sensitivity

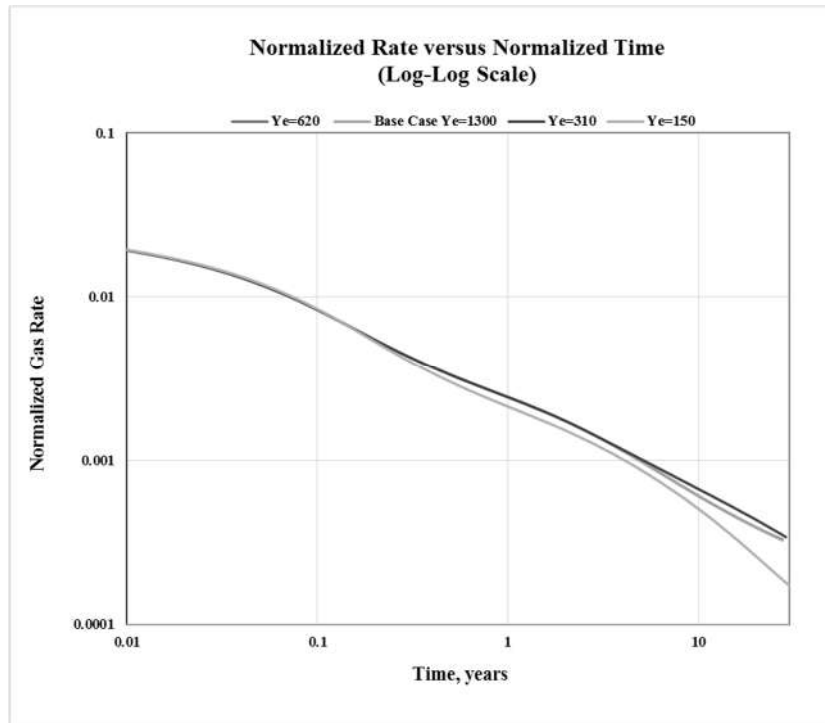


Figure 34: Well A Well Spacing Sensitivity (Log-Log Plot)

- Production is directly proportional to fracture height. The higher created fracture, the higher are the achieved rate and cumulative production. The ratio of production increase due fracture half-length increase is 1:1 (**Figure 35**). Flow regimes' durations are not affected by fracture half-length (**Figure 36**).

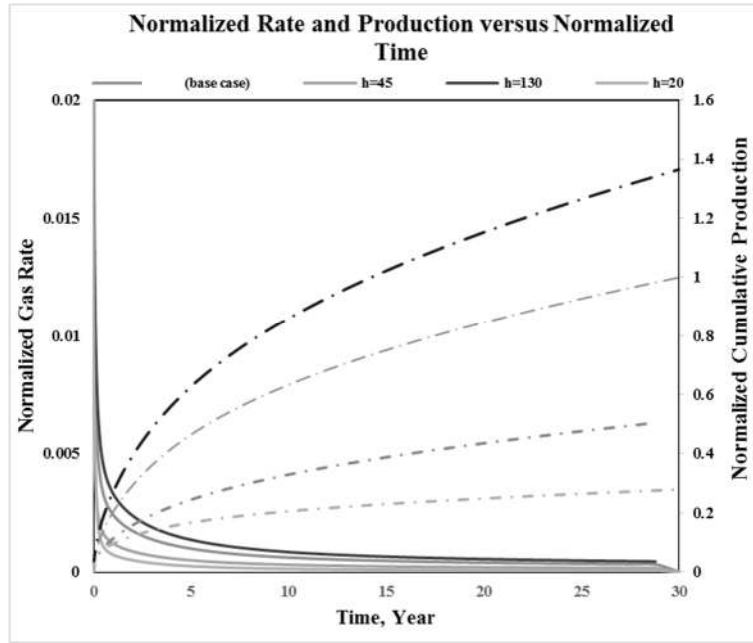


Figure 35: Well A Fracture Height Sensitivity

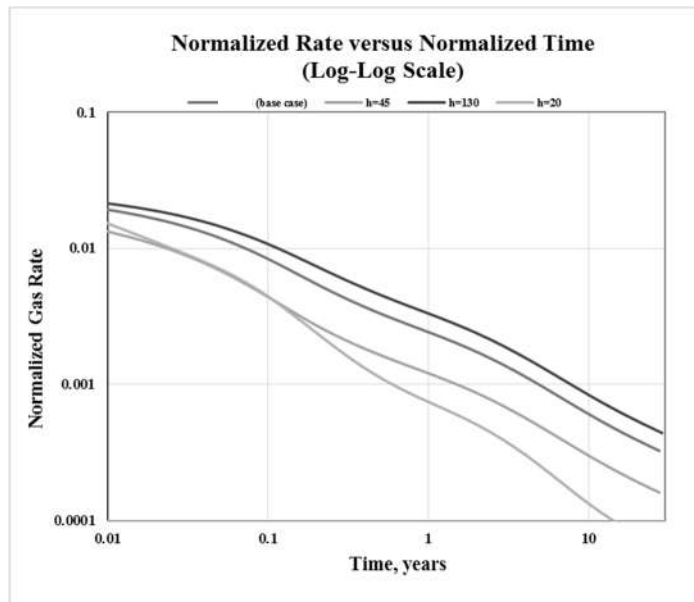


Figure 36: Well A Fracture Height Sensitivity (Log-Log Plot)

- Production is directly proportional to inner permeability. The fold on increase of production due higher permeability is negligible (**Figure 37**). The effect of higher permeability is initially considerable and only apparent in the first few months of production. Higher permeability shortens the initial linear flow regime (**Figure 38**).

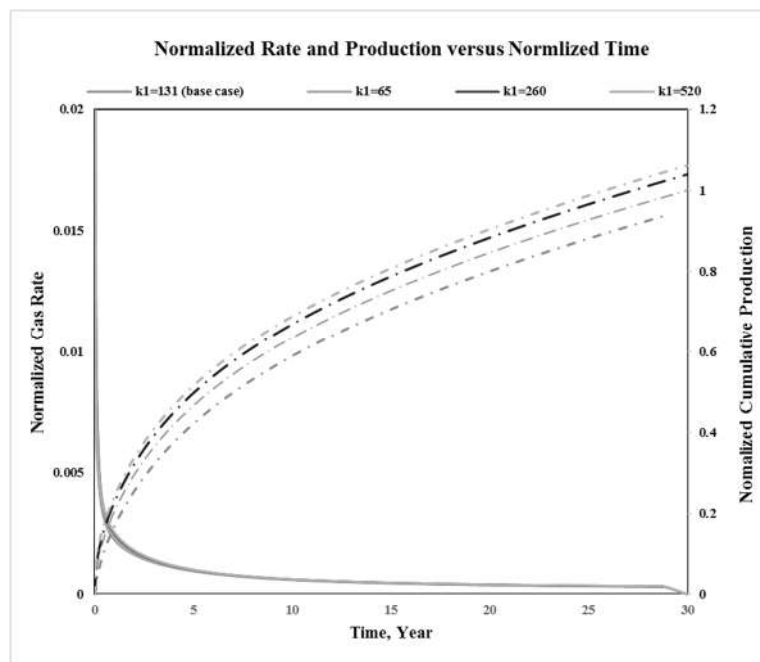


Figure 37: Well A Inner Permeability Sensitivity

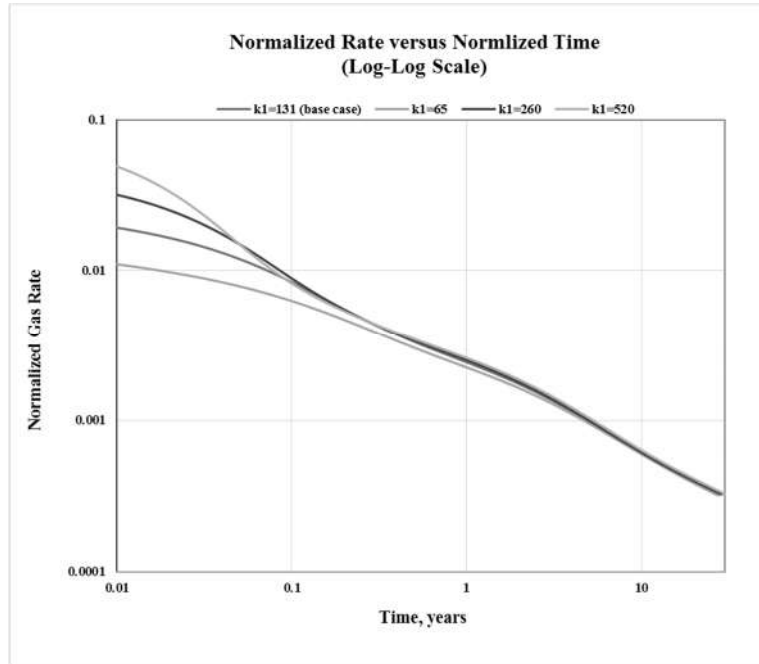


Figure 38: Well A Inner Permeability Sensitivity (Log-Log Plot)

- Production is directly proportional to outer permeability. The ratio of production change due permeability change is 4:5 (**Figure 39**). The effect of higher permeability is initially negligible and only apparent after first linear. Higher permeability shortens the transition between different flow regime (**Figure 40**).

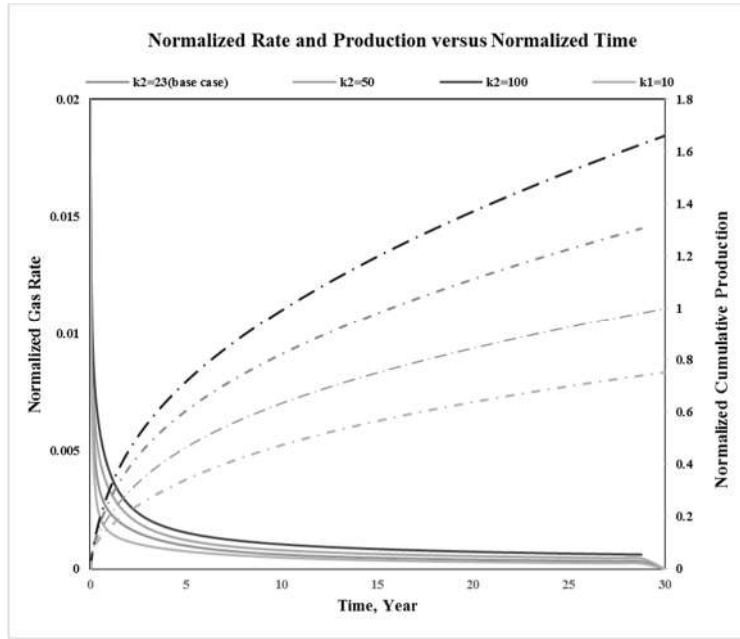


Figure 39: Well A Outer Permeability Sensitivity

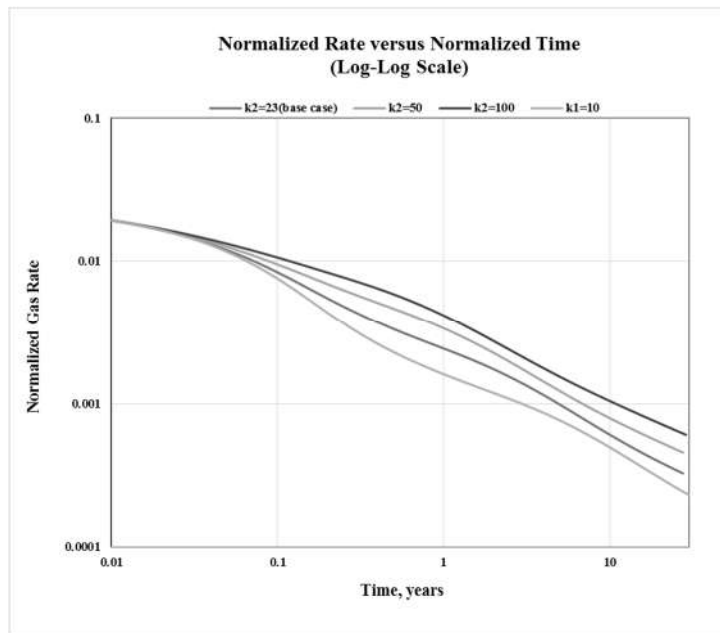


Figure 40: Well A Outer Permeability Sensitivity (Log-Log Plot)

- Production is directly proportional to porosity. The effect of higher porosity is considerable after initial flow. The ratio of production change due porosity change is 1:2 (**Figure 41**). Flow regimes' durations are not affected by porosity change (**Figure 42**).

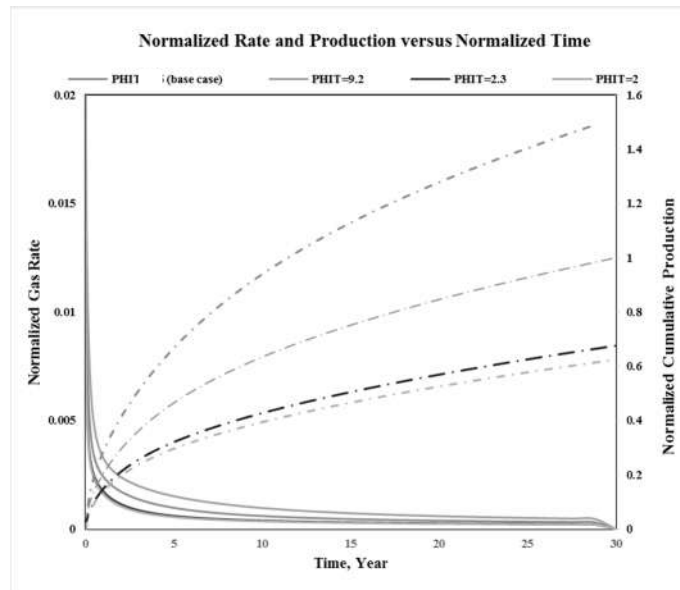


Figure 41: Well A porosity sensitivity

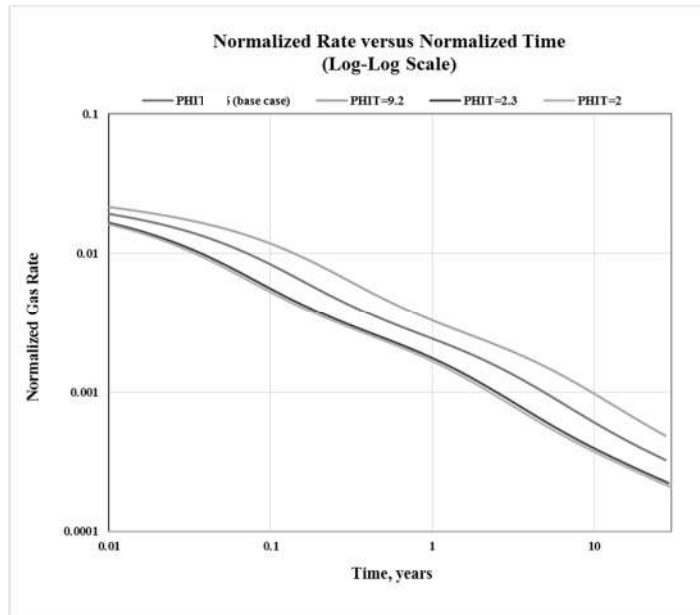


Figure 42: Well A Porosity Sensitivity (Log-Log Plot)

- Production is directly proportional to adsorption. The effect of higher adsorption is considerable after initial flow. The ratio of production change due adsorption change is 2:1 (**Figure 43**). Flow regimes' durations are not affected by adsorption change (**Figure 44**).

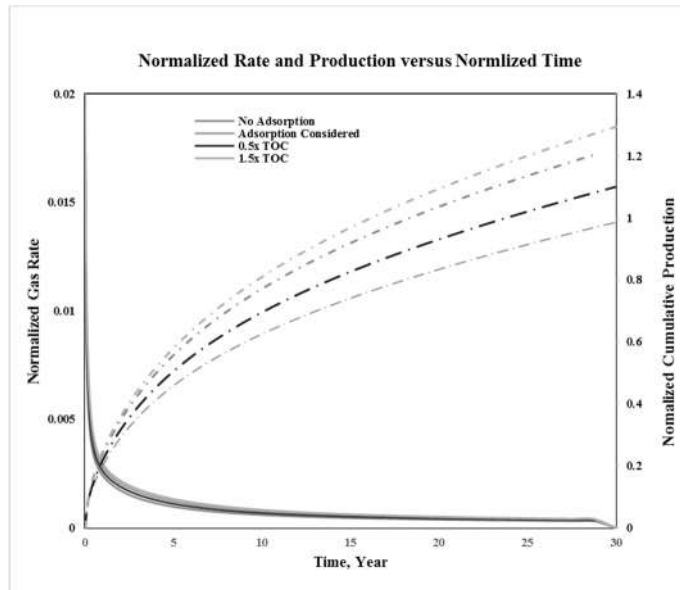


Figure 43: Well A Adsorption Sensitivity

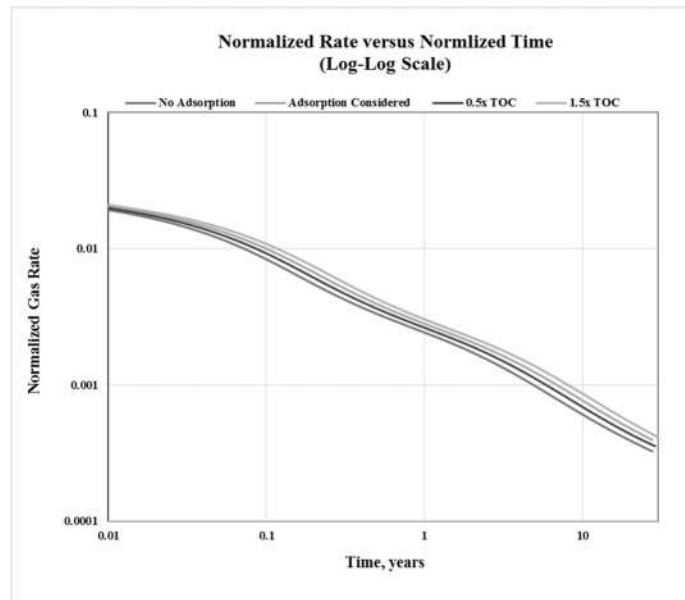


Figure 44: Well A Adsorption Sensitivity (Log-Log Plot)

4.2.1.4 Conclusion

After examining the sensitivity analysis, it seems that completion parameters affect the initial short-term well performance while reservoir parameters impact the final long-term well performance. Therefore, stimulation treatment design defines initial well performance while well placement decision defines well long-term performance. Also, there is minimal cost associated to well placement decision compared to stimulation treatment design. For Well A, production analysis indicates short fractures. Fracture conductivity could be decreased without significant production decrease.

4.2.2 Well B

The well was drilled in close proximity to well A, and has similar completion and production history. After a cleanup period of two weeks, the well was shut down for a month for the installation of velocity string (VS) to assist lifting and prevent probable liquid loading in the well. Before the start of production, downhole gauge was installed and then well put in production for few month, and then had a final shut in period. The production history is shown in **Figure 23**. The data available were petrophysical logs, completion summary, downhole samples, surface rates and pressure. Key reservoir parameters are summarized in **Table 6**. Because VS was installed in the production, the risk of liquid loading up was lowered and the production is believed to represent reservoir signature.

Table 6: Fixed Well Parameter for Well B

Layer Data	Value
Reservoir temperature (°F)	270
Flowing bottomhole pressure (psia)	100
Reservoir length (ft)	4,731
Reservoir width (ft)	450
Number of stages	14
Bulk density (g/cc)	2.5

4.2.2.1 Initial production analysis

Because downhole gauge is available, there was no need to convert surface readings to bottom hole. Normalized rate versus material balance time was plotted to identify flow regimes (**Figure 45**). After that, normalized rate versus normalized material balance time was plotted to identify flow regimes. Material balance pseud-time, $t_{mb} = \frac{\mu_i c_{ti}}{q} \int_0^t \frac{q}{\bar{\mu} \bar{c}_t} dt$, is calculated first and then normalized to the maximum MBT recorded. The rate is normalized by pseud-pressure $P_p = \frac{\mu_i}{\rho_i} \int_{P_i}^P \frac{\rho}{\mu} dP$, and then highest normalized rate recorded. Three flow regimes were identified: bilinear flow, and linear flow, transitional regime toward BDF (**Figure 45**). The bilinear period lasted for few weeks and could be attributed to fracture cleanup, or skin stabilization, and thus has no practical use in the analysis. A transition out of linear flow detected, and the BDF has significantly developed.

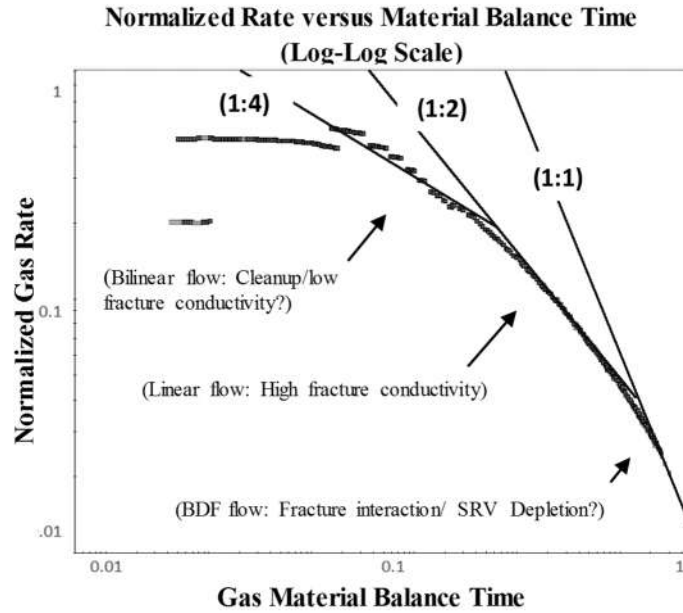


Figure 45: Well B Normalized Rate Versus Material Balance Time (Log-Log Scale)

Next, normalized rate versus square root time was used to estimate $x_f\sqrt{k}$. **Equation 2** defines $x_f\sqrt{k}$ as the slope of the data straight line. Also, **Equation 3** is used to define the maximum SRV permeability from time of the end of linear flow and fracture spacing (**Figure 46**). Lastly, minimum SRV volume is estimated by extrapolating using flowing material time plot (**Figure 47**). It seems that the contacted GIP is small in this well comparing to Well A.

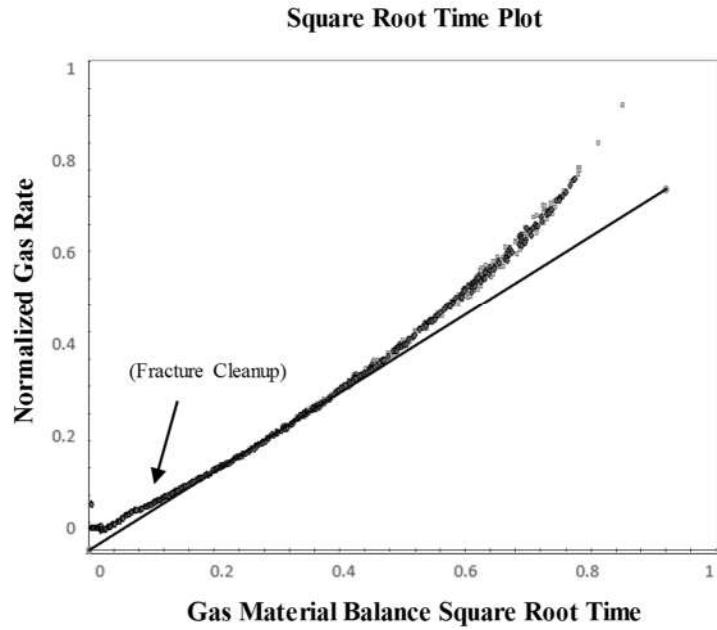


Figure 46: Well B Normalized Rate Versus Square Root Material Balance Time

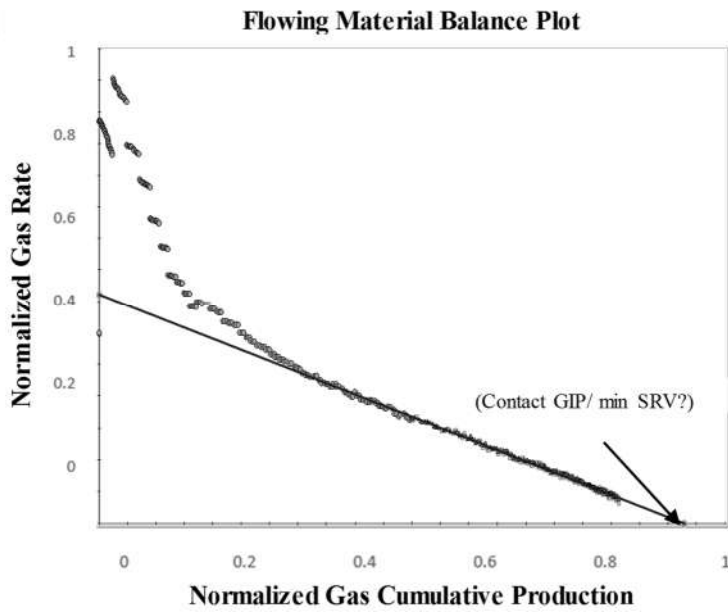


Figure 47: Well B Flowing Material Balance Plot

Utilizing the input data extracted from straight-line analysis, Trilinear composite model was used to model production. Rectangular model, with 45 equally spaced fracture was used to model production. Initial well parameters (**Table 6**) and the estimations of straight-line analysis are used as initial input for the model and regression was conducted on inner permeability, fracture half length, and fracture conductivity. The model successes on having an excellent history match of production history as shown in **Figure 48**.

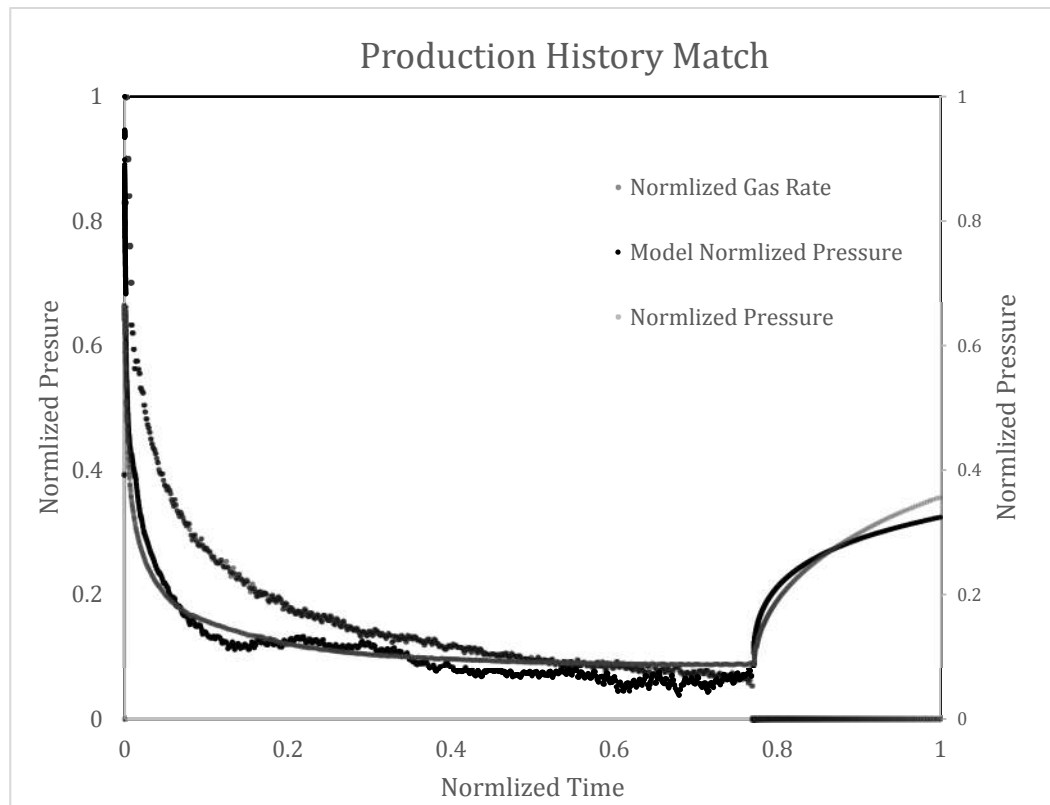


Figure 48: Well B Production History Match

4.2.2.2 Probabilistic Evaluation

In this step, the uncertainty overlooked in Step 1 is considered and evaluated. Each fixed parameter in the previous step is now given an initial distribution (**Table 7**). Positive correlations were considered between porosity and saturation, and negative correlation was given to fracture numbers and fracture half-length. Next, a simulation was conducted to refine the assumed distribution, and to forecast possible production. Initial and final parameter distribution are summarized in **Table 7**. **Figure 49** shows P10, P50, and P90 forecast for Well B.

Table 7: Initial and Final Distribution for Uncertain Well B Parameters

Parameters	Initial Distribution			Final Distribution				
	Distribution Type	Min	Max	Mode	Distribution Type	Mean	P10	P90
Number of Fractures	Triangular	34	56	45	Normal	44	49	37
Fracture half-length (ft)	Uniform	20	150	-	Log-Normal	94	123	67
Fracture Conductivity (N/A)	Uniform	0	500	-	Log Normal	214	296	166
Outer permeability (nd)	Uniform	10	300	-	Log-Normal	11	16	10
Inner permeability (nd)	Uniform	50	300	-	Log-Normal	150	194	133

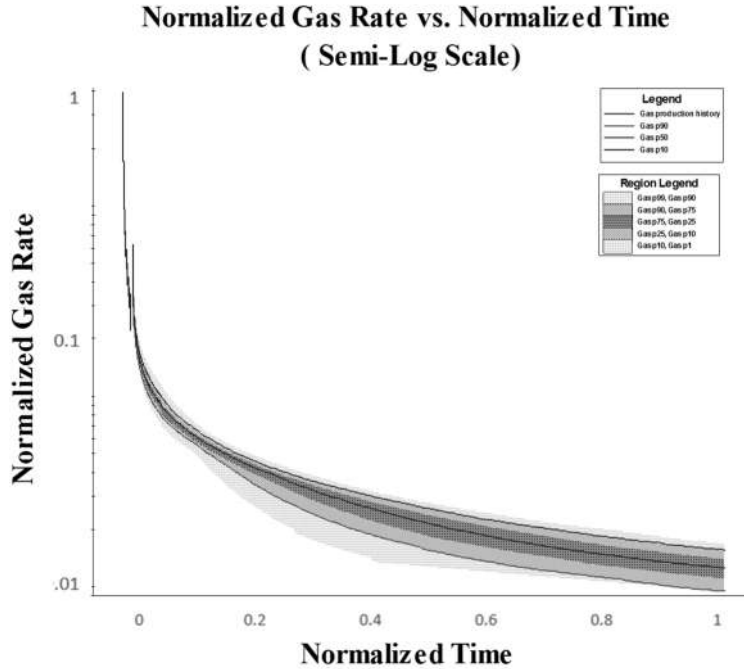


Figure 49: Well B Probabilistic Production Forecast

4.2.2.3 Sensitivity Analysis

After the probabilistic analysis, a better understanding of likely completion and reservoir parameters is achieved. A trilinear composite model is now created and fed by the mean value of the final distribution in **Table 7** in order to create a base case scenario. After that, sensitivities on main reservoir and completion parameters is inputted into the model, and model is run for 60 years in order to see impact of each parameter. Results are presented in **Figures 50 to 71** in both Cartesian and logarithmic scale to get different view on the performance. The following results are found as result of sensitivity analysis:

- Production is directly proportional to fracture half-length. The longer the fracture half-length created, the higher the rate and cumulative production achieved. The ratio production increase due fracture half-length increase is 1:2 (Figure 50). Flow regimes' durations are not affected by fracture half-length (Figure 51).

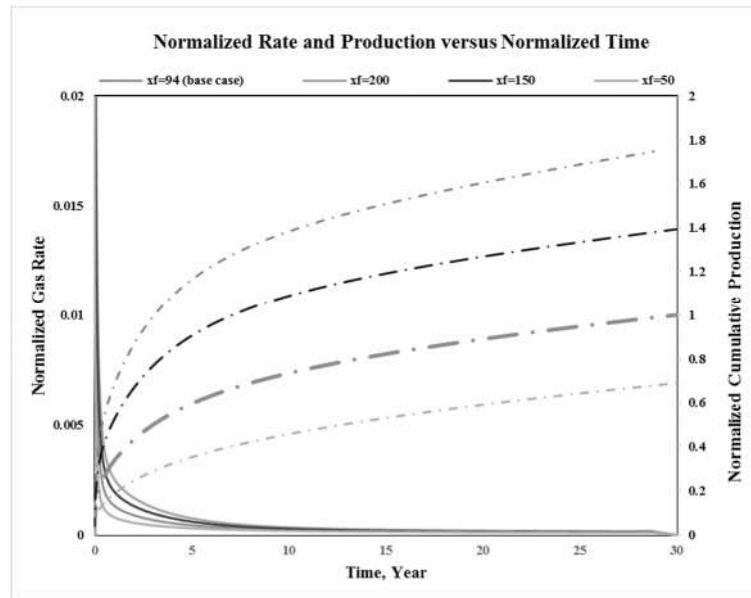


Figure 50: Well B Fracture Half-Length Sensitivity

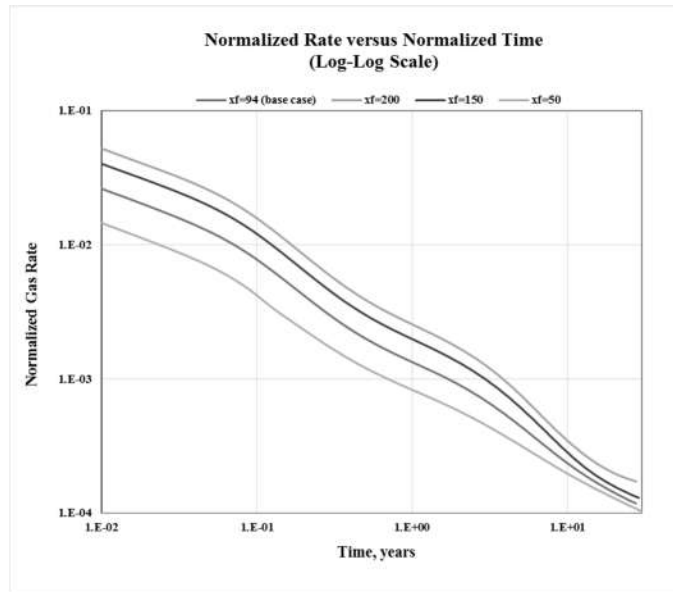


Figure 51: Well B Fracture Half-Length Sensitivity (Log-Log Plot)

- Production is directly proportional to fracture number. The more fractures created, the higher the initial rate and cumulative production achieved. The initial rate increase only lasts for at most a year. The ratio between production increase after 60 years due fracture number increase is 3:5 (**Figure 52**). The more fractures number, the shorter the transition period between first linear flow and BDF is (**Figure 53**).

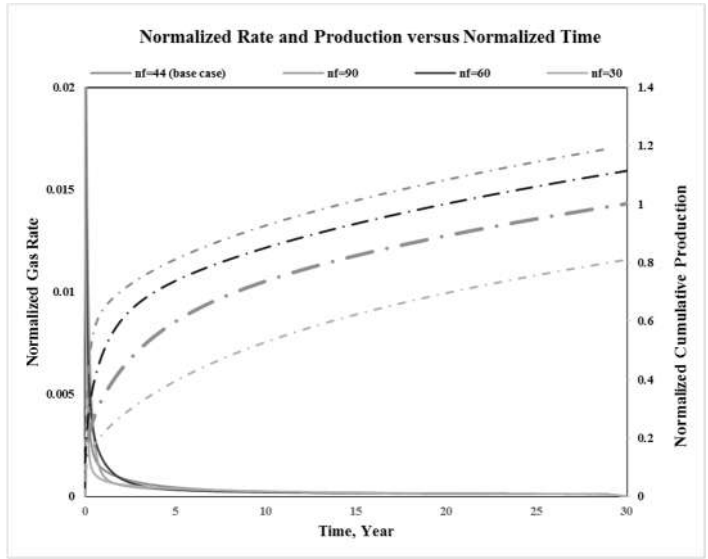


Figure 52: Well B Fracture Number Sensitivity

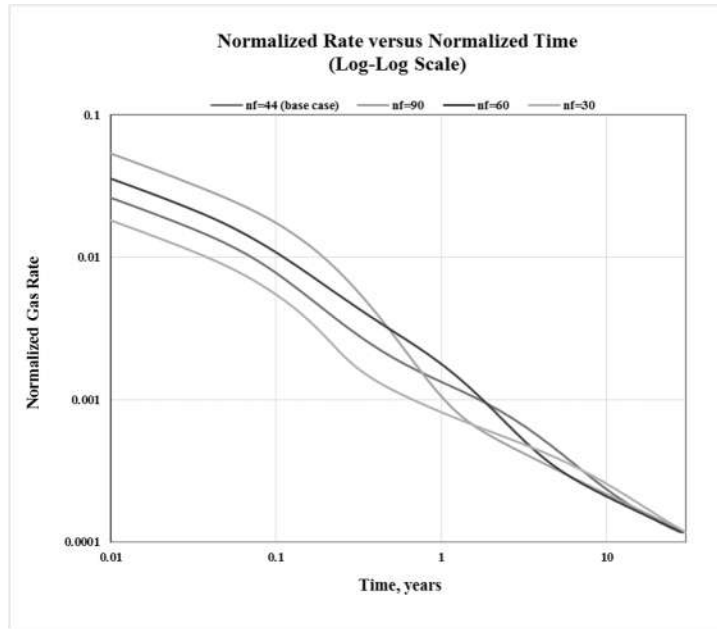


Figure 53: Well B Fracture Number Sensitivity (Log-Log Plot)

- Production is directly proportional to well length; however, the relation fades away on longer well cases. The effect of longer wells appears after a month of production. The ratio between production increase after 60 years due longer well is 3:5 (**Figure 54**). Longer wells delay BDF regime, and extend the linear flow regime (**Figure 55**). It is good notice that there is a model stability issue in extremely longer and short wells. The model does not follow the flow regimes mentioned in the literatures.

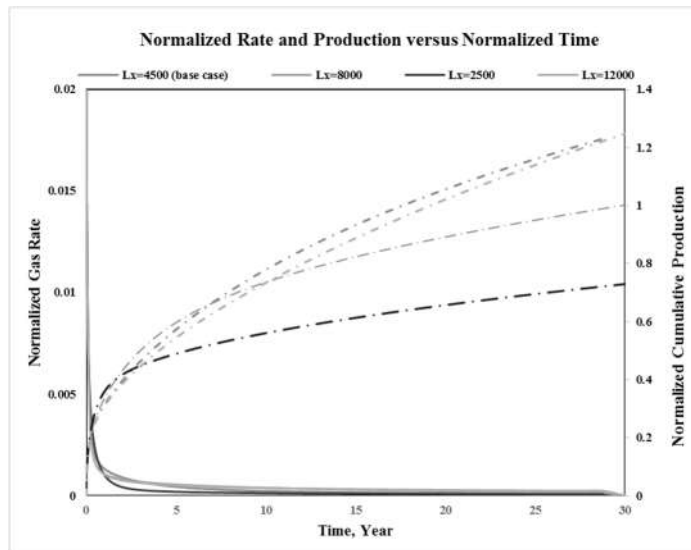


Figure 54: Well B well length sensitivity

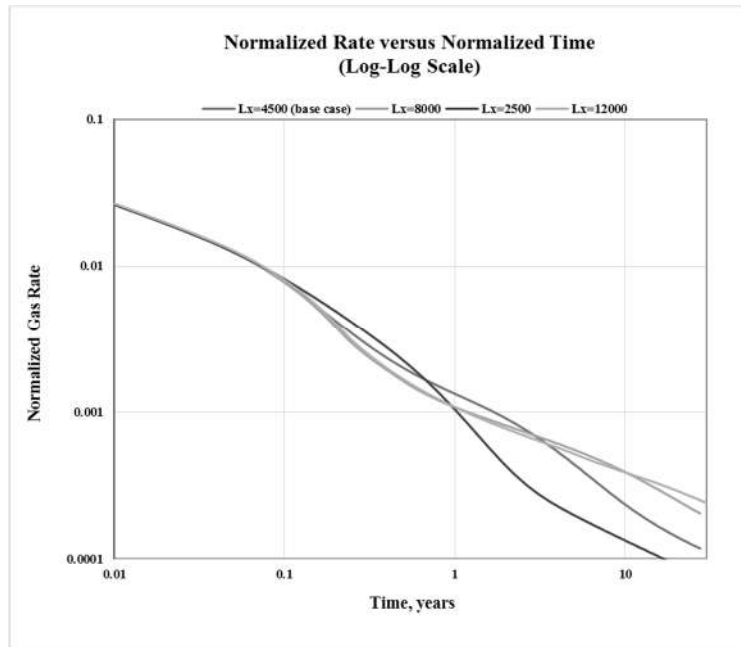


Figure 55: Well B well length sensitivity (log-log plot)

- Production is directly proportional to fracture conductivity. The effect of more conductive fractures is negligible and only apparent in the first days and only last for up to few months (**Figure 56**). Fracture conductivity does not affect flow regimes duration (**Figure 57**).

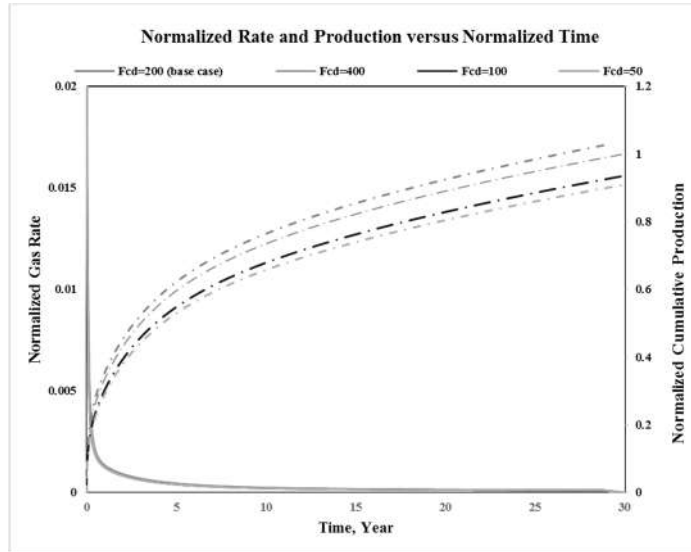


Figure 56: Well B Fracture Conductivity Sensitivity

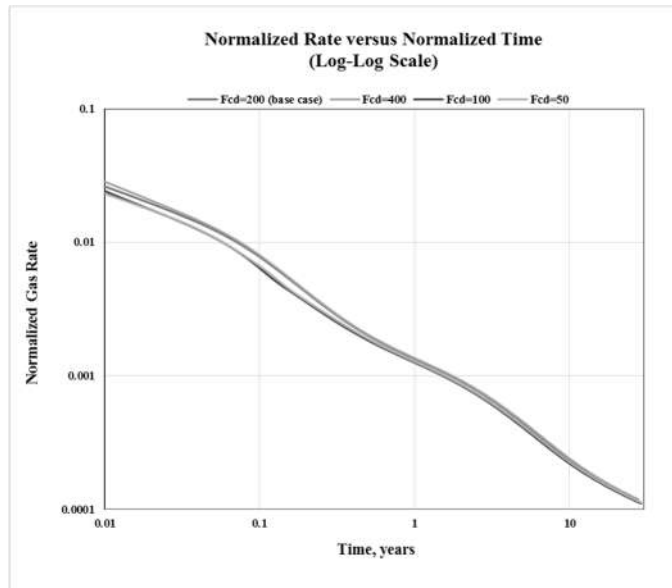


Figure 57: Well B Fracture Conductivity Sensitivity (Log-Log Plot)

- Production is directly proportional to well spacing. The effect of longer spacing is initially negligible and only apparent in the last years of production. However, short spacing seems to shorten well life by about half and thus production (**Figure 58**). Well spacing does not affect flow regimes duration (**Figure 59**).

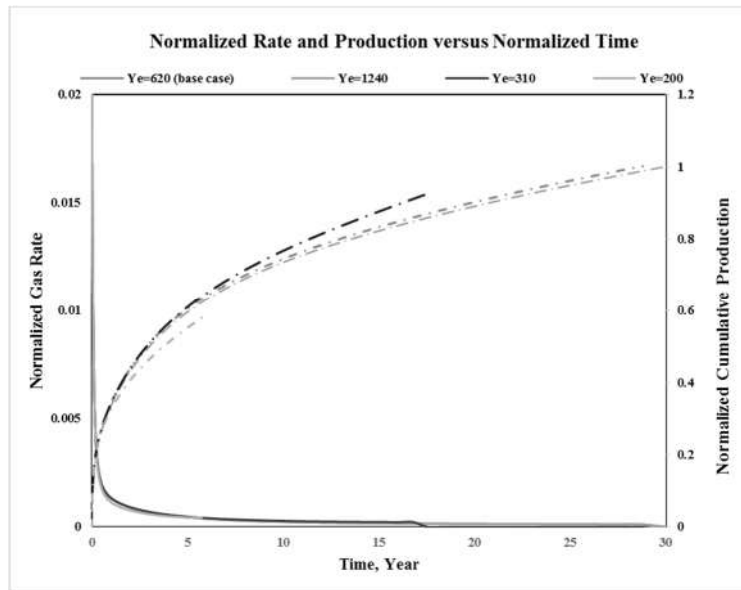


Figure 58: Well B well spacing sensitivity

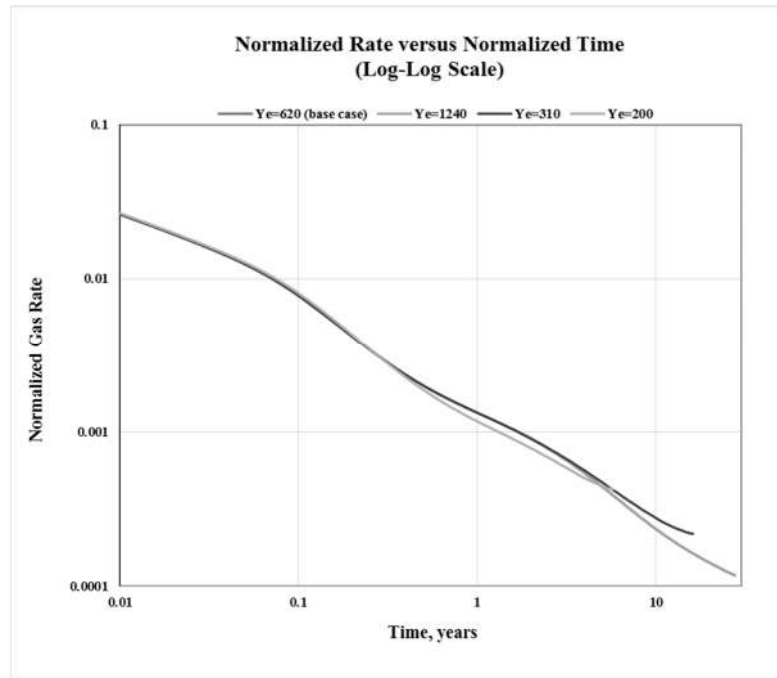


Figure 59: Well B Well Spacing Sensitivity (Log-Log Plot)

- Production is directly proportional to fracture height. The higher created fracture, the higher the rate and cumulative production achieved. The ratio of production increase due fracture half-length increase is 1:1 (**Figure 60**). Flow regimes' durations are not affected by fracture half-length (**Figure 61**).

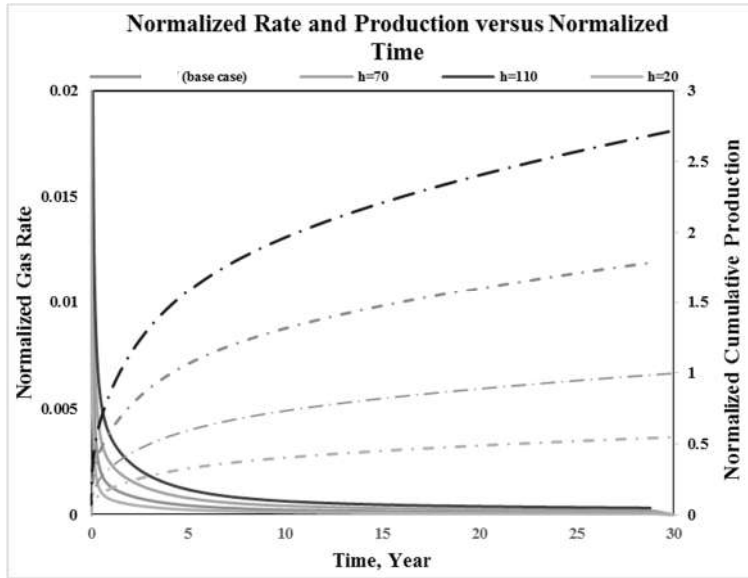


Figure 60: Well B Fracture Height Sensitivity

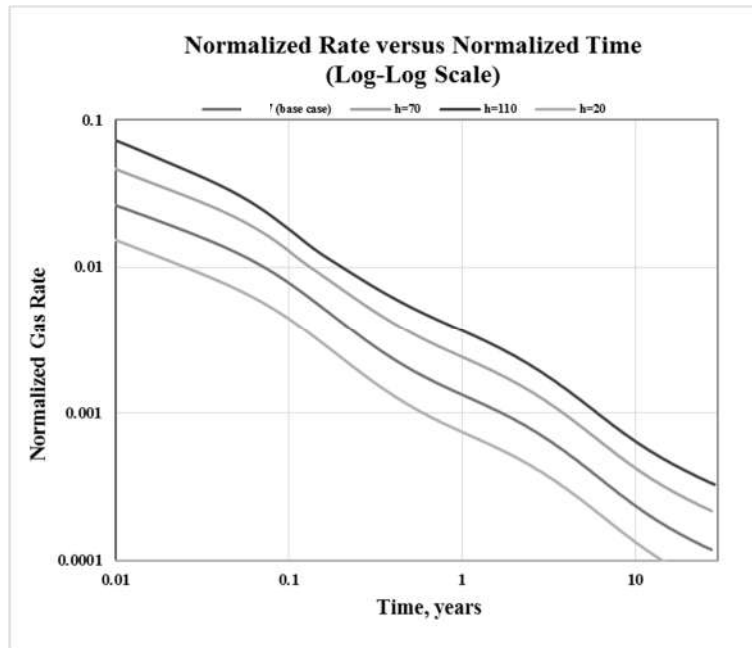


Figure 61: Well B Fracture Height Sensitivity (Log-Log Plot)

- Production is directly proportional to inner permeability. The fold on increase of production due higher permeability is negligible (**Figure 62**). The effect of higher permeability is initially considerable and only apparent in the first few months of production. Higher permeability shortens the initial linear flow regime (**Figure 63**).

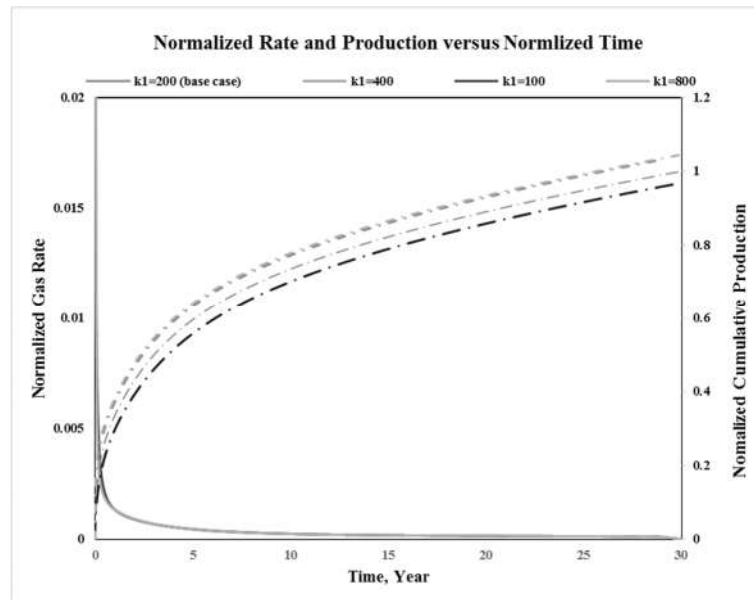


Figure 62: Well B Inner Permeability Sensitivity

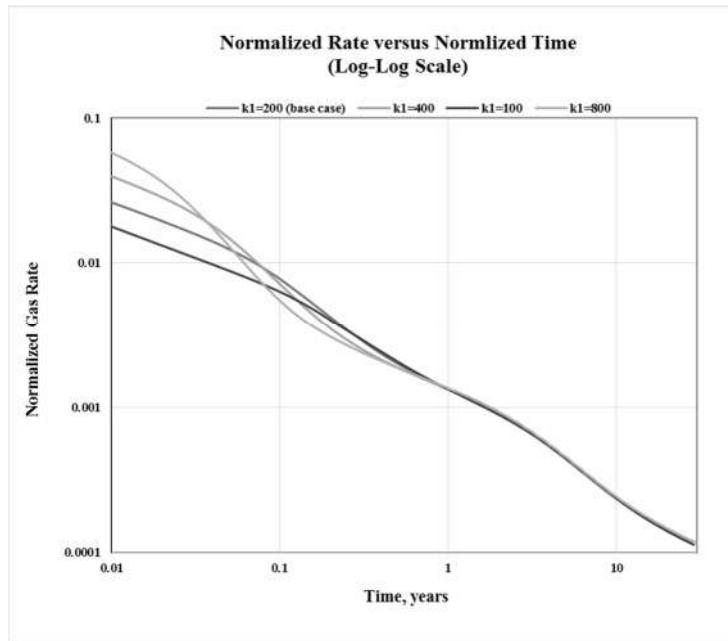


Figure 63: Well B Inner Permeability Sensitivity (Log-Log Plot)

- Production is directly proportional to outer permeability. The ratio of production change due permeability change is 4:5 (**Figure 64**). The effect of higher permeability is initially negligible and only apparent after first linear. Higher permeability shortens the transition between different flow regime (**Figure 65**).

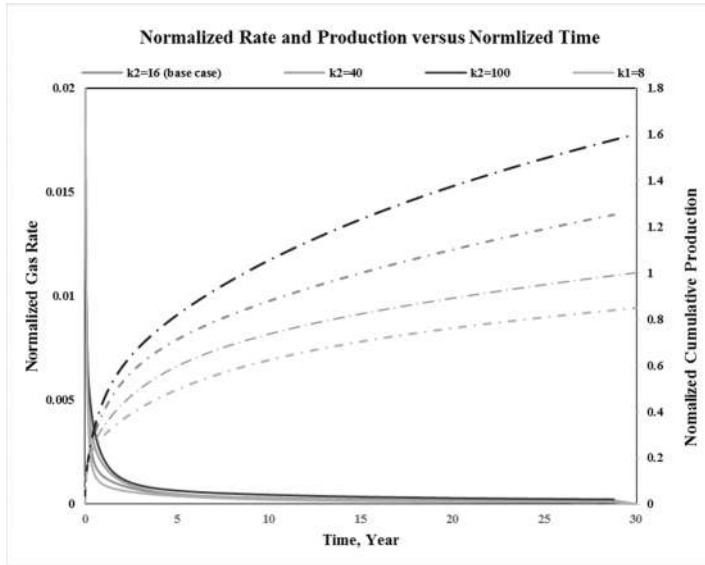


Figure 64: Well B Outer Permeability Sensitivity

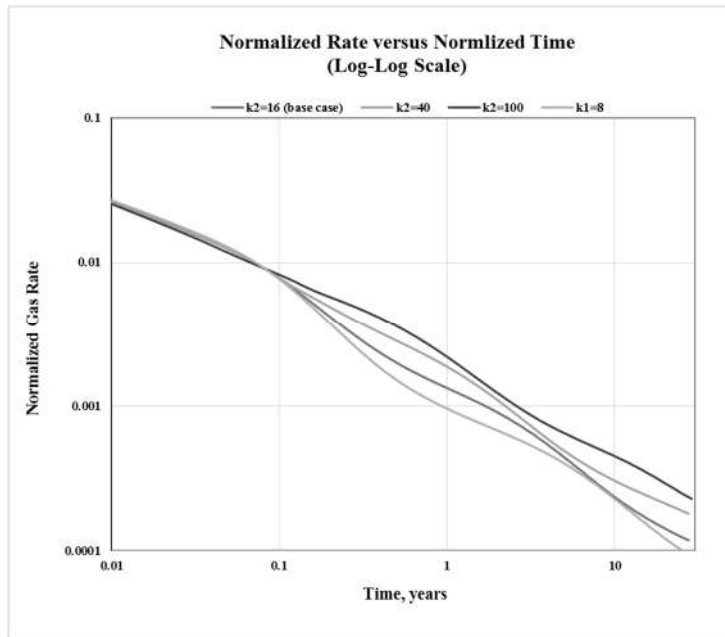


Figure 65: Well B Outer Permeability Sensitivity (Log-Log Plot)

- Production is directly proportional to porosity. The effect of higher porosity is considerable after initial flow. The ratio of production change due porosity change is 1:2 (**Figure 66**). Flow regimes' durations are not affected by porosity change (**Figure 67**).

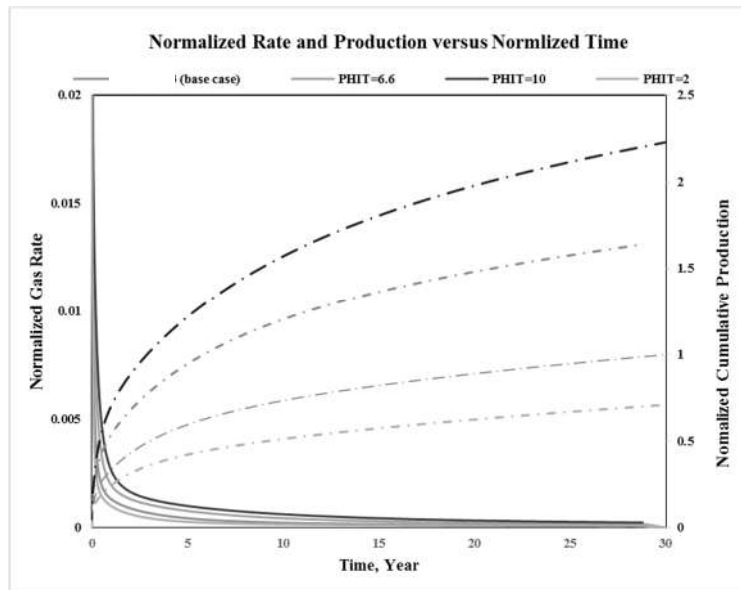


Figure 66: Well B Porosity Sensitivity

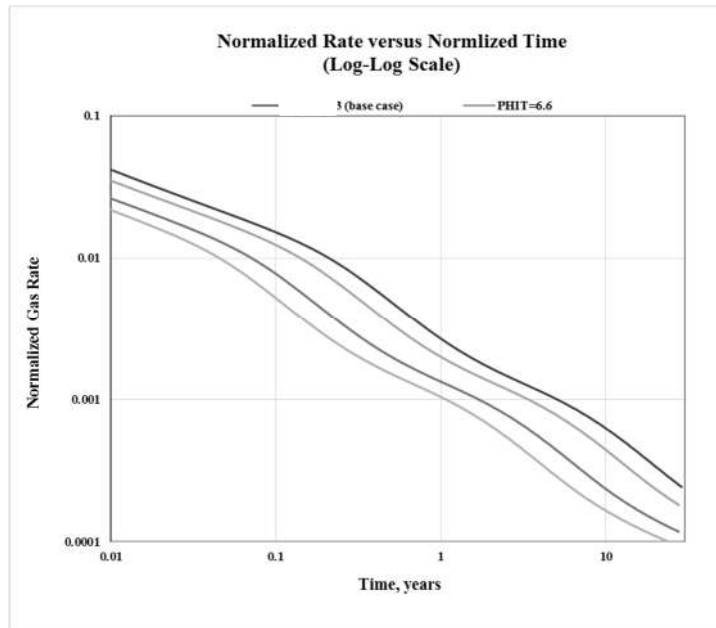


Figure 67: Well B Porosity Sensitivity (Log-Log Plot)

- A positive weak correlation is found between adsorption and production. The effect of higher adsorption is considerable after initial flow. The ratio of production change due to adsorption change is 2:1 (**Figure 68**). Flow regimes' durations are not affected by adsorption change (**Figure 69**).

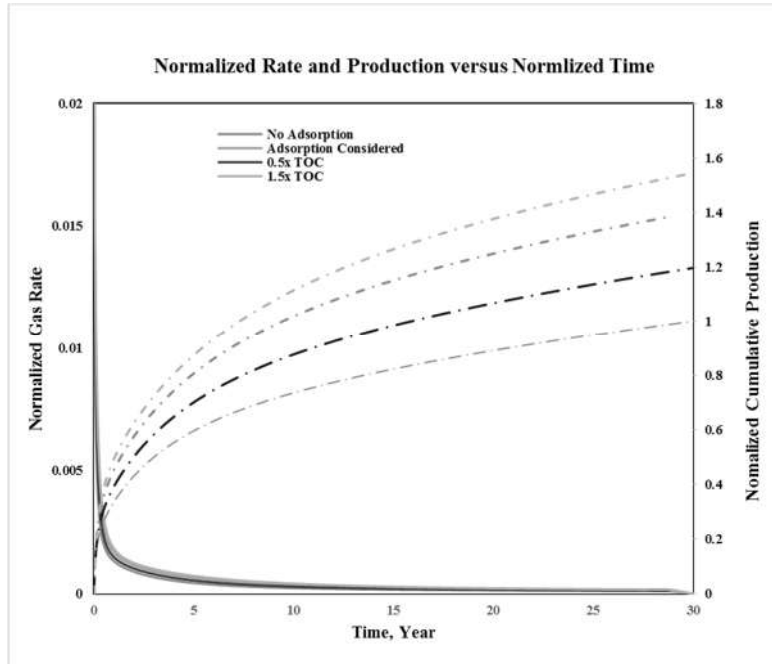


Figure 68: Well B Adsorption Sensitivity

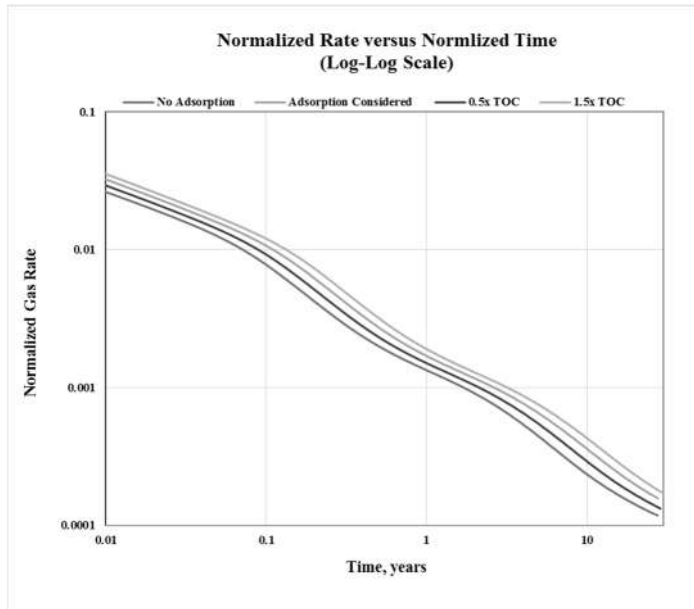


Figure 69: Well B Adsorption Sensitivity (Log-Log Plot)

- Production is directly proportional to initial pressure. However, the correlation weakens at extremely higher pressure (**Figure 70**) which might be attributed to lower gas compressibility at high pressure. Flow regimes' durations are not affected by pressure change (**Figure 71**).

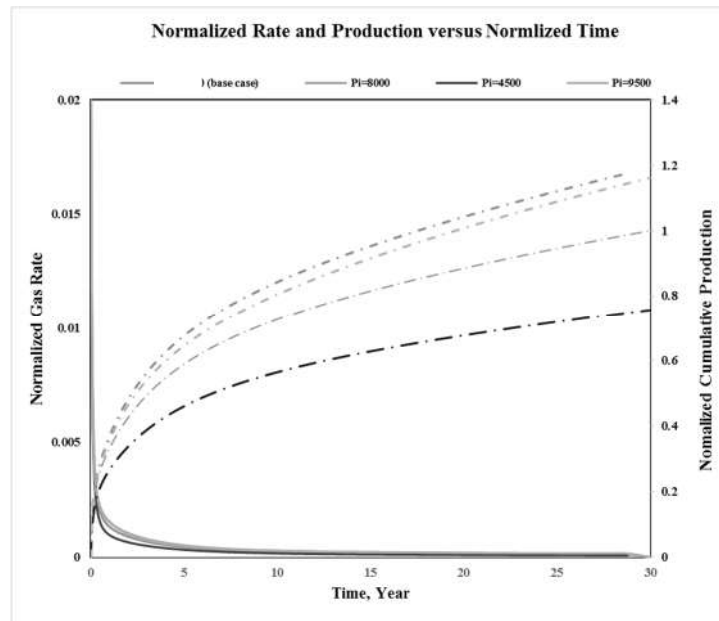


Figure 70: Well B Initial Pressure Sensitivity

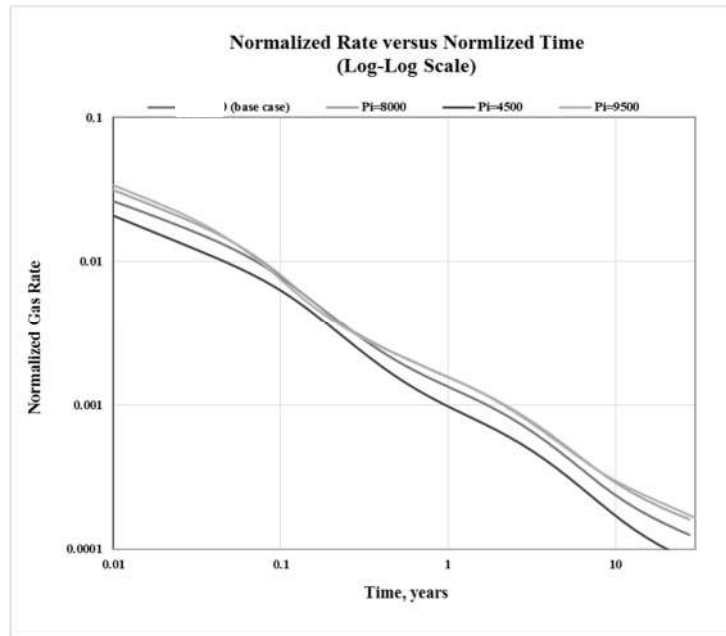


Figure 71: Well B Initial Pressure Sensitivity (Log-Log Plot)

4.2.2.4 Conclusion

After examining the sensitivity analysis, it seems that completion parameters affect the initial short-term well performance while reservoir parameters impact the final long-term well performance. Therefore, stimulation treatment design defines initial well performance while well placement decision defines well long-term performance. Also, there is minimal cost associated to well placement decision compared to stimulation treatment design. For Well B, production analysis indicates small fractures and limited porosity that would be improved by optimizing on fracture half-length and height and avoiding this well location for future wells.

4.2.3 Well C

The well was drilled in gas window. After flowback period of two weeks, the well was suspended for few months for the installation of velocity string (VS) to assist lifting and prevent and prevent any liquid loading in the well. The well flowed for several months, with high gas oil ratio (~20,000 scf/stb). The only data available was petrophysical logs, completion summary, separator samples and surface pressure, and rate history. Key reservoir parameter is summarized on **Table 8**. Because VS was installed in the production, the risk of liquid loading up was lowered and the production is believed to represent reservoir signature.

Table 8: Fixed Well Parameter for Well C

Layer Data	Value
Reservoir temperature (°F)	270
Flowing bottomhole pressure (psia)	100
Reservoir length (ft)	4,812
Reservoir width (ft)	1,300
Number of stages	16
Bulk density (g/cc)	2.5

4.2.3.1 Initial production analysis

The first step in data analysis is to convert surface readings to bottom hole. In order to do so, well configurations, along with fluid properties and production history was uploaded to a PROSPER, a well performance simulator. After that, normalized rate versus material balance time was plotted to identify flow regimes. Material balance pseud-time, $t_{mb} =$

$\frac{\mu_i c_{ti}}{q} \int_0^t \frac{q}{\bar{\mu} \bar{c}_t} dt$, is calculated first and then normalized to the maximum MBT recorded. The

rate is normalized by pseud-pressure $P_p = \frac{\mu_i}{\rho_i} \int_{P_i}^P \frac{\rho}{\mu} dP$, and then highest normalized rate recorded. Two flow regimes were clearly identified: bilinear flow, and linear flow. Transition to BDF, and signs of BDF were witnessed (**Figure 72**). The bilinear period could be attributed to fracture cleanup, and it lasted around several weeks recovering ~13.5 % of frac fluid. A stabilization in GWR was noticed afterward to ~ 100 bbl/MMscf which probably indicates well cleanup. If only linear flow exists, minimum SRV pore volume, and maximum SRV permeability could be estimated.

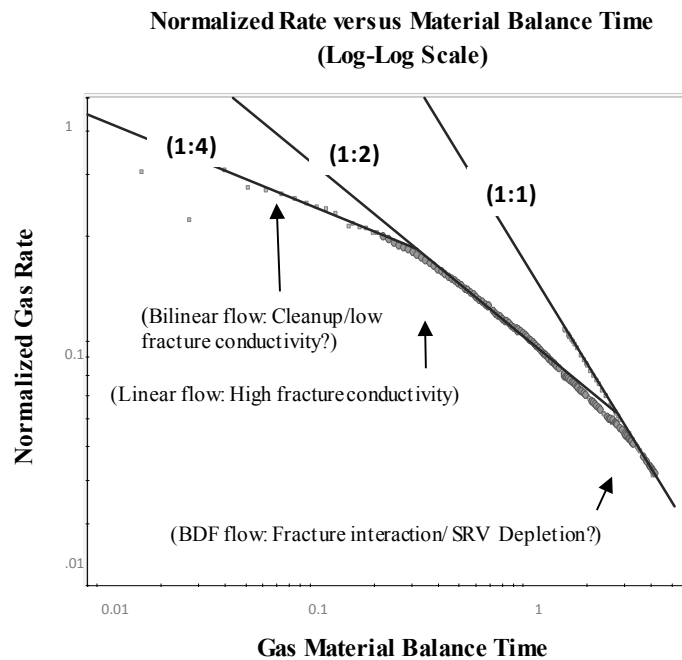


Figure 72: Well C Normalized Rate Versus Material Balance Time (Log-Log Scale)

Next, normalized rate versus square root time was used to estimate $x_f\sqrt{k}$. **Equation 2** defines $x_f\sqrt{k}$ as the slope of the data straight line, which is 27 md^{1/2}.ft (**Figure 73**). Also, **Equation 3** is used to define the maximum SRV permeability from time of the end of linear flow and fracture spacing. Lastly, minimum SRV volume is estimated by extrapolating using flowing material time plot (**Figure 74**).

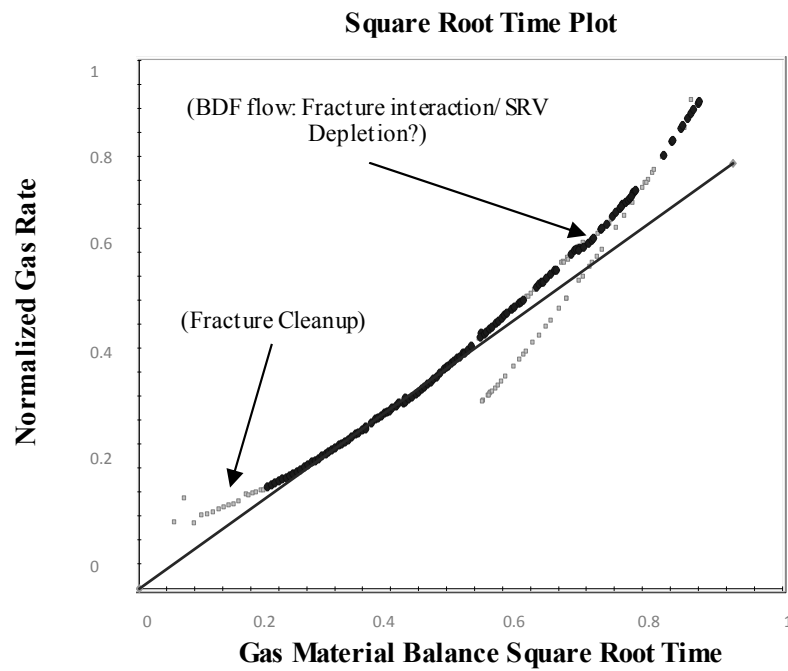


Figure 73: Well C Square Root Time Plot

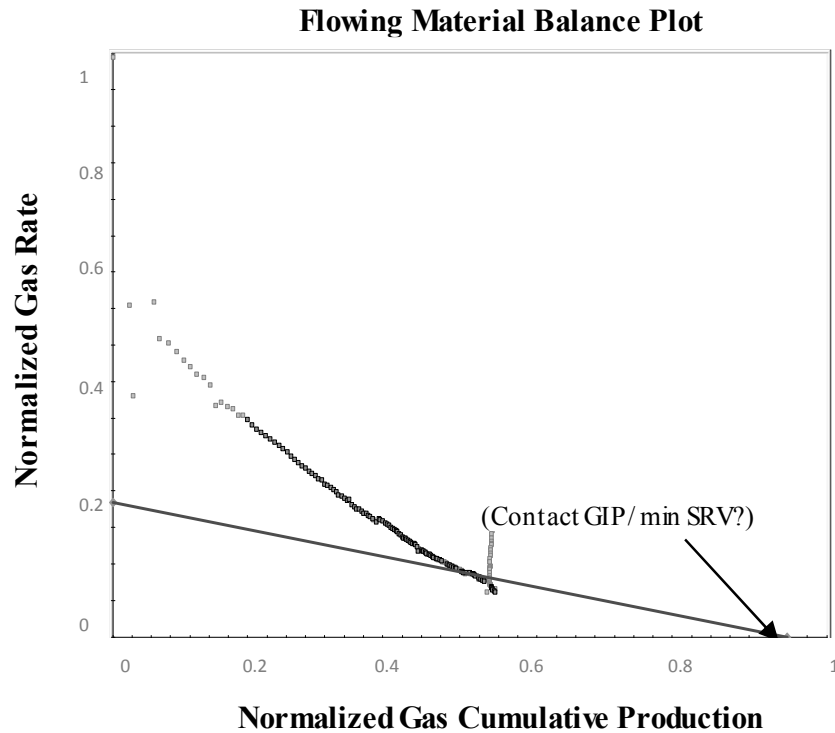


Figure 74: Well C flowing material balance plot

Utilizing the input data extracted from straight-line analysis, Trilinear composite model was used to model production. Rectangular model, with 48 equally spaced fracture was used to model production. **Table 8** were used as initial input for the model and regression was conducted on inner permeability, fracture half length, and fracture conductivity. The model successes on having an excellent history match of production history **Figure 48**.

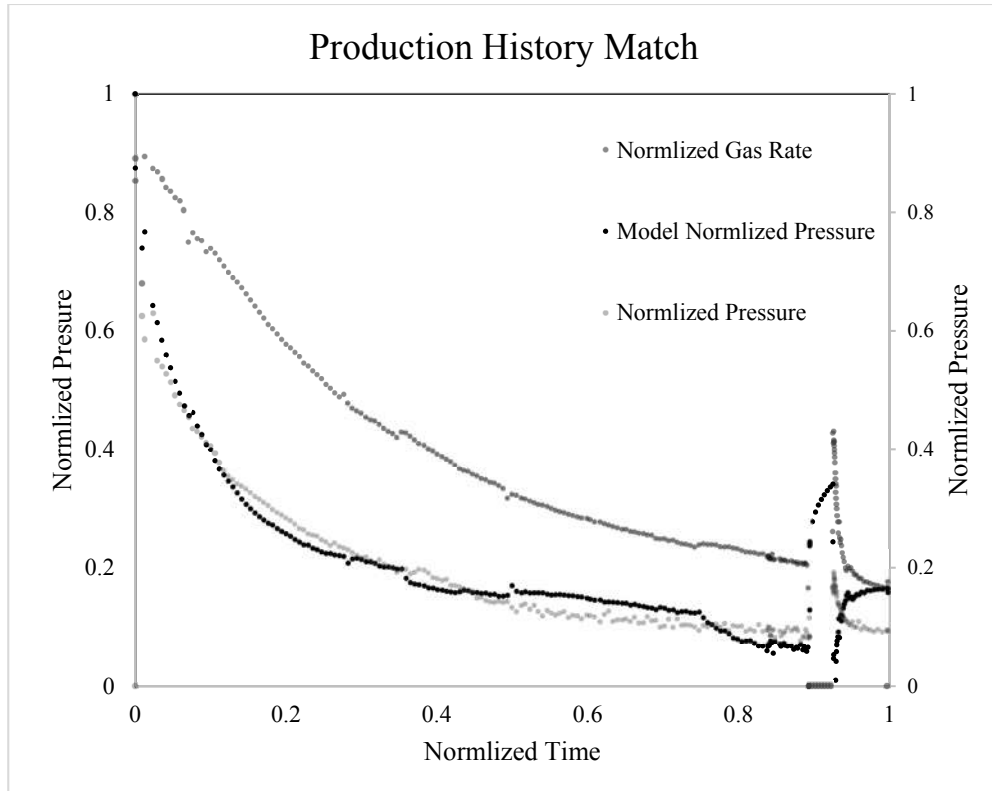


Figure 75: Well C production history match

4.2.3.2 Probabilistic Evaluation

In this step, the uncertainty overlooked in Step 1 is considered and evaluated. Each fixed parameter in the previous step is now given an initial distribution (**Table 7**). Positive correlations were considered between porosity and saturation, and negative correlation was given to fracture numbers and fracture half-length. Next, a simulation was conducted to refine the assumed distribution, and to forecast possible production. Initial and final parameter distribution are summarized in **Table 7**. **Figure 76** shows P10, P50, and P90 forecast for Well C.

Table 9: Initial and Final Distribution for Uncertain Well C Parameters

Parameters	Initial Distribution			Final Distribution						
	Distribution Type	Min	Max	Mean	Distribution Type	Min	Max	Mean	P10	P90
Initial Pressure (psia)	Uniform	6,300	7,500	-	Uniform	6,300	7,500	-	-	-
Number of Fractures	Triangular	18	76	48	Triangular	32	63	47	57	38
Fracture half-length (ft)	Uniform	10	150	-	Log-Normal	-	-	41	56	27
Fracture Conductivity (N/A)	Uniform	5	300	-	Log Normal	-	-	30	170	12.3
Outer permeability (nd)	Uniform	40	1,000	-	Log-Normal	-	-	86	112	53
Inner permeability (nd)	Uniform	20	200	-	Log-Normal	-	-	490	720	300

**Normalized Gas Rate vs. Normalized Time
(Semi-Log Scale)**

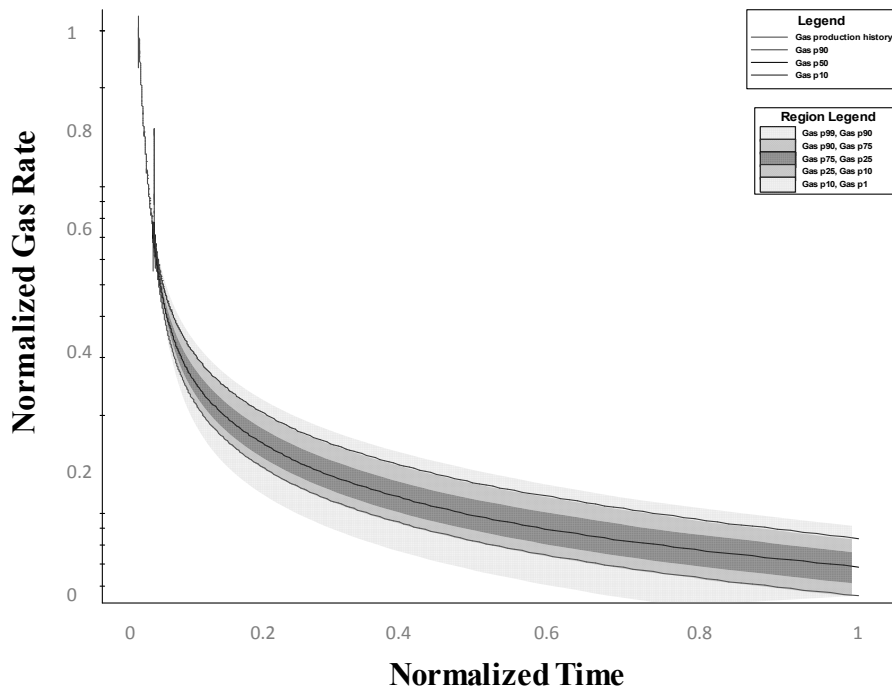


Figure 76: Well C Probabilistic Forecast (Semi-Log Scale)

4.2.3.3 Sensitivity Analysis

After the probabilistic analysis, a better understanding of likely completion and reservoir parameters is achieved. A trilinear composite model is now created and fed by the mean value of the final distribution in **Table 7** in order to create a base case scenario. After that, sensitivities on main reservoir and completion parameters is inputted into the model, and model is run for 60 years in order to see impact of each parameter. Results are presented in below **Figures 77 to 95** in both Cartesian and logarithmic scale to get different view on the performance. The following results are found as result of sensitivity analysis:

- Production is directly proportional to fracture half-length. The longer the fracture half-length created, the higher the rate and cumulative production achieved. The ratio production increase due fracture half-length increase is 1:2 (**Figure 77**). Flow regimes' durations are not affected by fracture half-length (**Figure 78**).

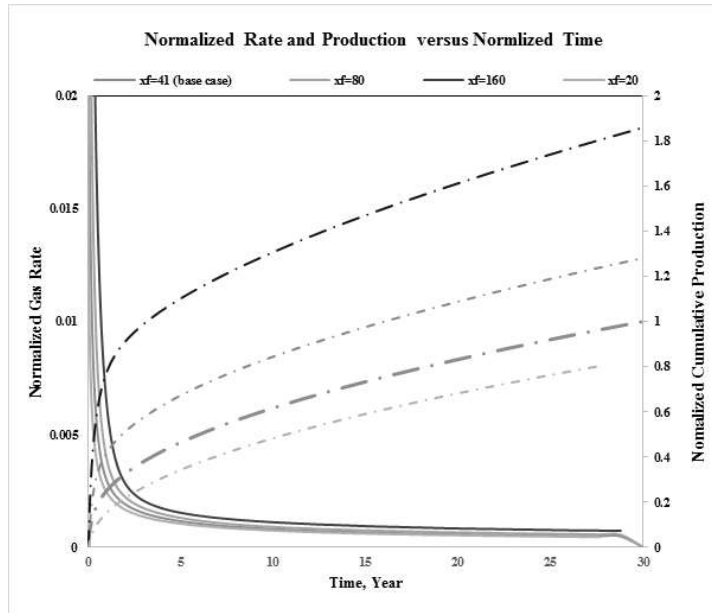


Figure 77: Well C Fracture Half-Length Sensitivity

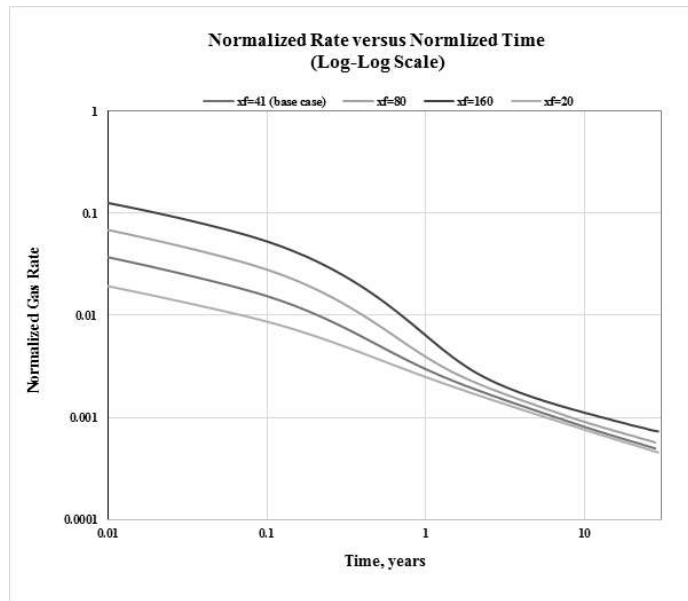


Figure 78: Well C Fracture Half-Length Sensitivity (Log-Log Plot)

- Production is directly proportional to well length. The effect of longer wells appears after a month of production. The ratio between production increase after 60 years due longer well is 3:5 (**Figure 79**). Longer wells delay BDF regime, and extend the linear flow regime (**Figure 80**).

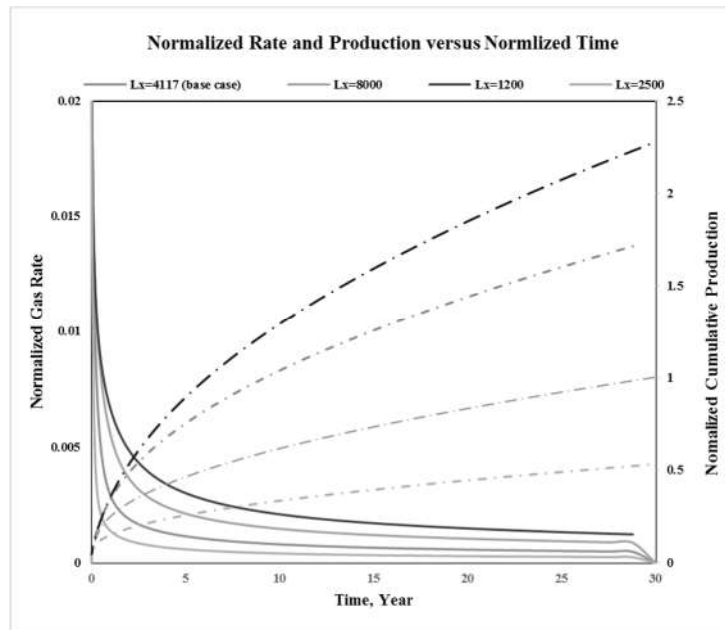


Figure 79: Well C Well Length Sensitivity

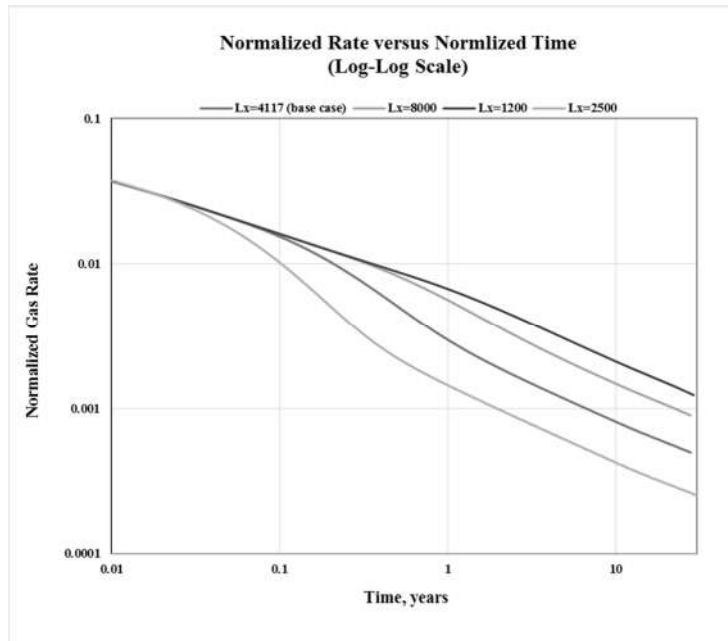


Figure 80: Well C Well Length Sensitivity (Log-Log Plot)

- Production is directly proportional to fracture conductivity. The effect of more conductive fractures is negligible and only apparent in the first days and only last for up to few months (**Figure 81**). Fracture conductivity does not affect flow regimes duration (**Figure 82**).

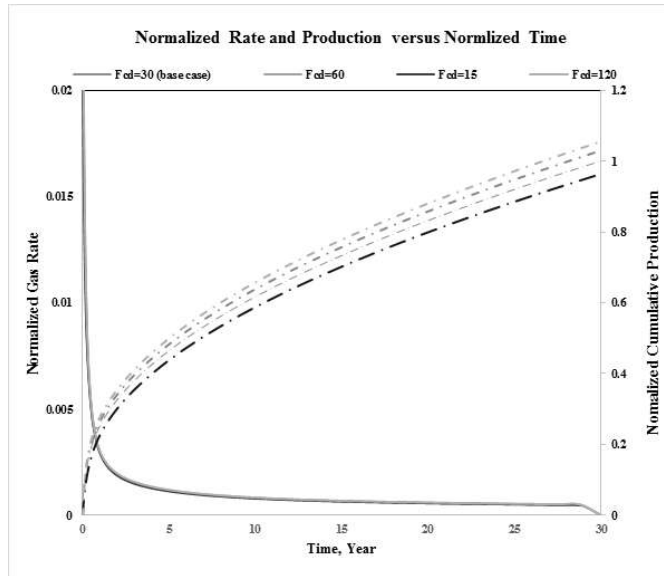


Figure 81: Well C Fracture Conductivity Sensitivity

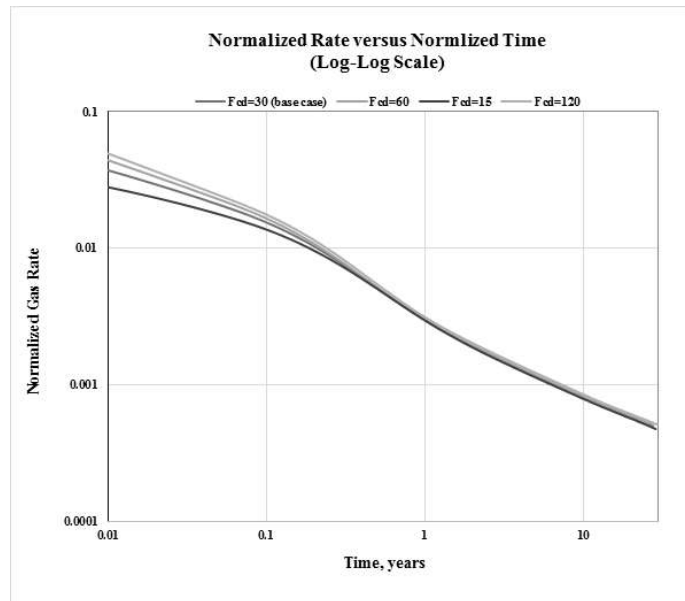


Figure 82: Well C Fracture Conductivity Sensitivity (Log-Log Plot)

- Production is directly proportional to well. The effect of longer spacing is initially negligible and only apparent in the last years of production. However, short spacing seems to shorten well life by about half and thus production (**Figure 83**). Well spacing does not affect flow regimes duration (**Figure 84**).

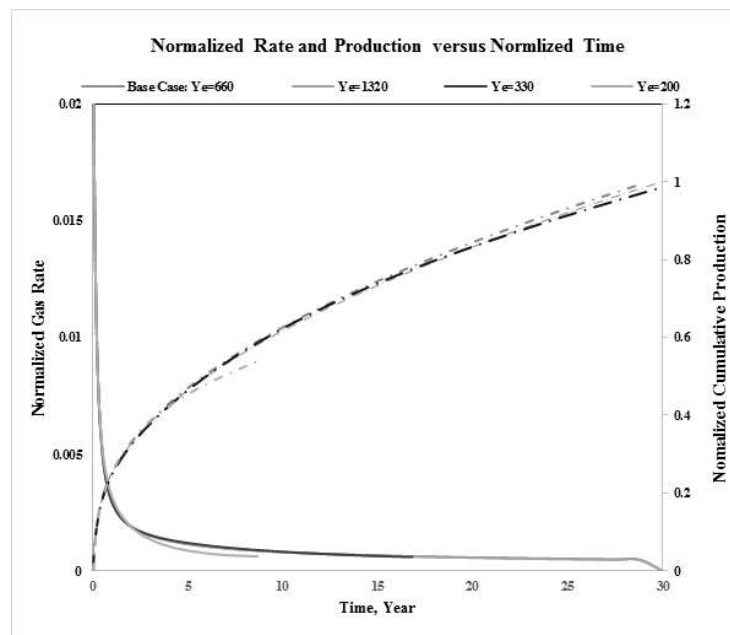


Figure 83: Well C Well Spacing Sensitivity

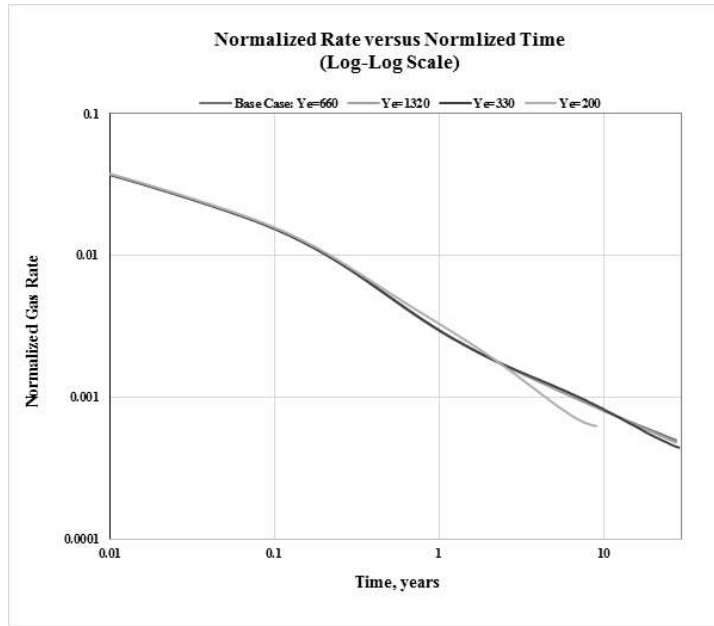


Figure 84: Well C Well Spacing Sensitivity (Log-Log Plot)

- Production is directly proportional to fracture. The higher created fracture, the higher the rate and cumulative production achieved. The ratio of production increase due fracture half-length increase is 1:1 (**Figure 85**). Flow regimes' durations are not affected by fracture half-length (**Figure 86**).

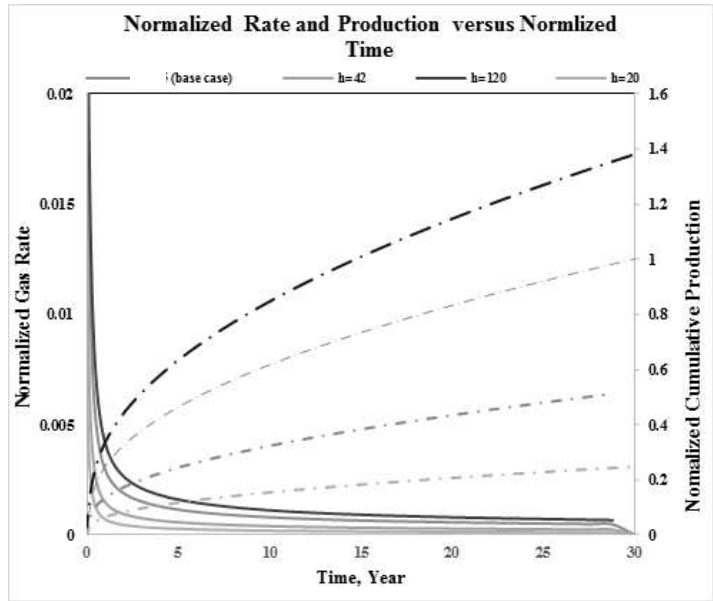


Figure 85: Well C Fracture Height Sensitivity

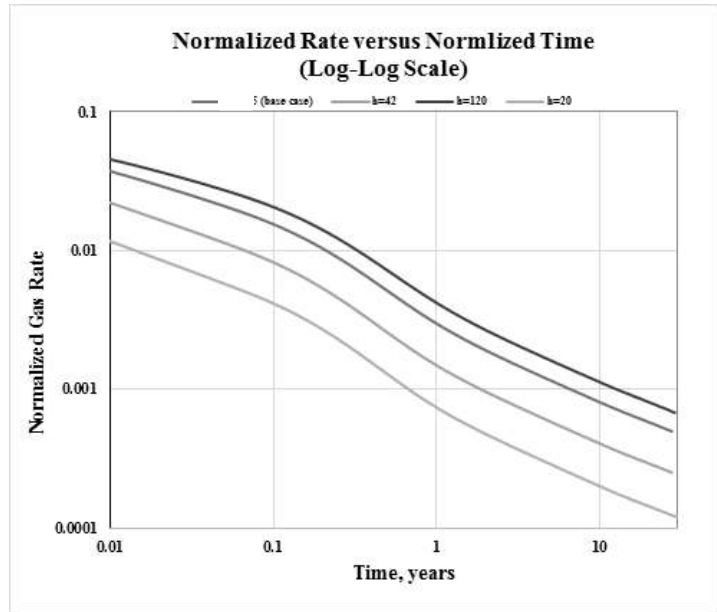


Figure 86: Well C fracture height sensitivity (log-log plot)

- Production is directly proportional to inner permeability. The fold on increase of production due higher permeability is negligible (**Figure 87**). The effect of higher permeability is initially considerable and only apparent in the first few months of production. Higher permeability shortens the initial linear flow regime (**Figure 88**).

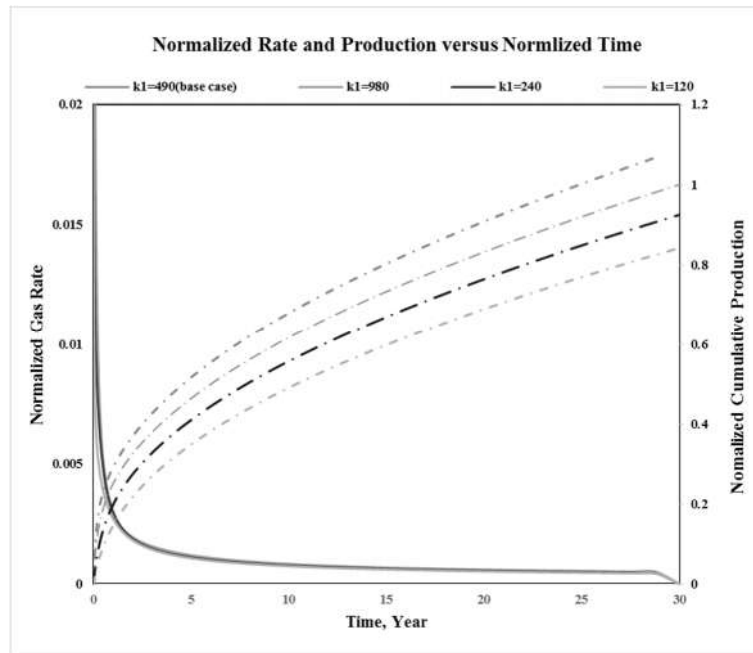


Figure 87: Well C inner permeability sensitivity

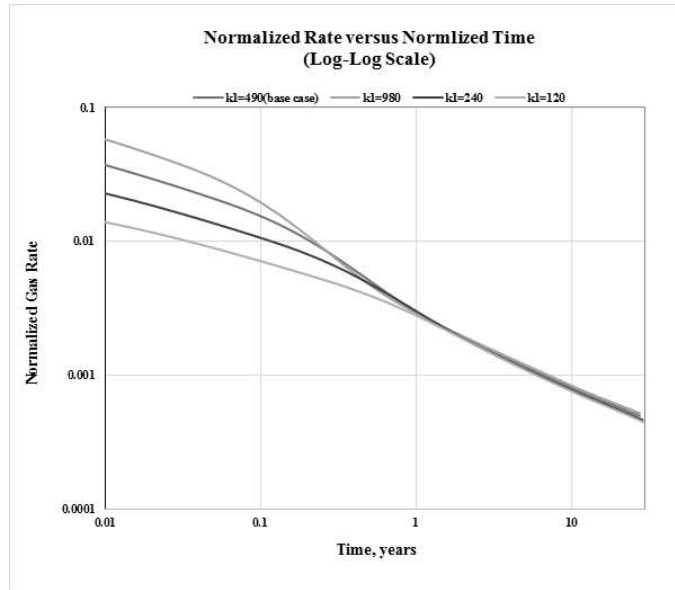


Figure 88: Well C inner permeability sensitivity (log-log plot)

- Production is directly proportional to outer permeability. The ratio of production change due permeability change is 4:5 (**Figure 89**). The effect of higher permeability is initially negligible and only apparent after first linear. Higher permeability shortens the transition between different flow regime (**Figure 90**).

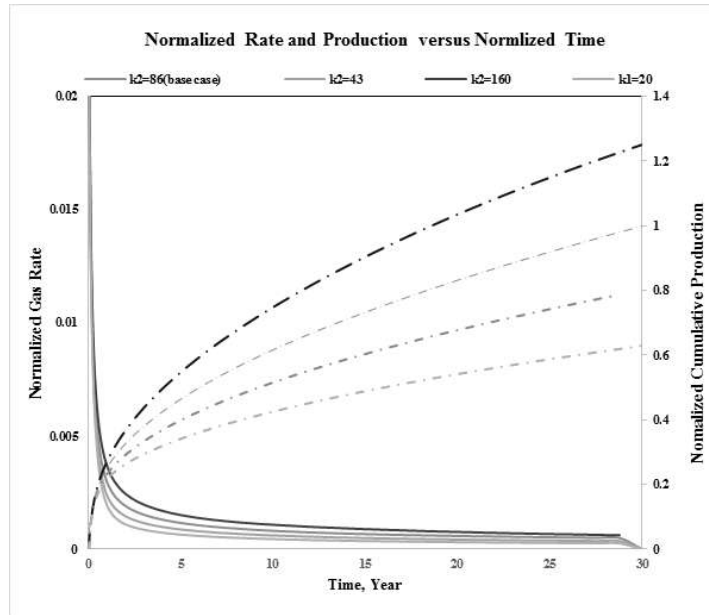


Figure 89: Well C Outer Permeability Sensitivity

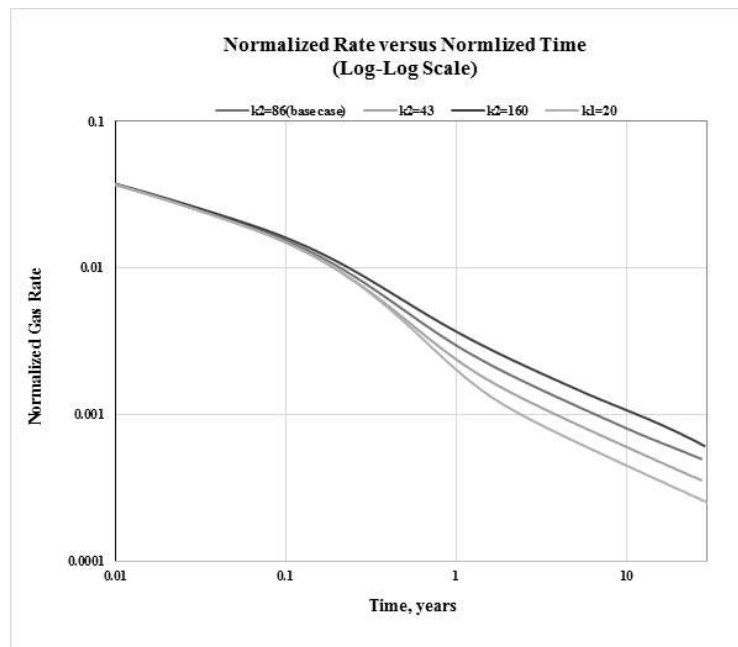


Figure 90: Well C Outer Permeability Sensitivity (Log-Log Plot)

- Production is directly proportional to porosity. The effect of higher porosity is considerable after initial flow. The ratio of production change due porosity change is 1:2 (**Figure 91**). Flow regimes' durations are not affected by porosity change (**Figure 92**).

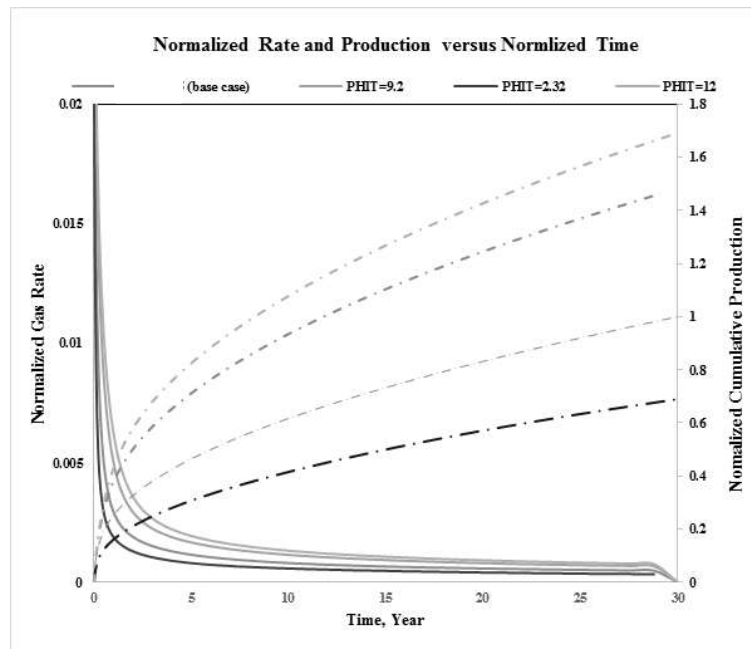


Figure 91: Well C Porosity Sensitivity

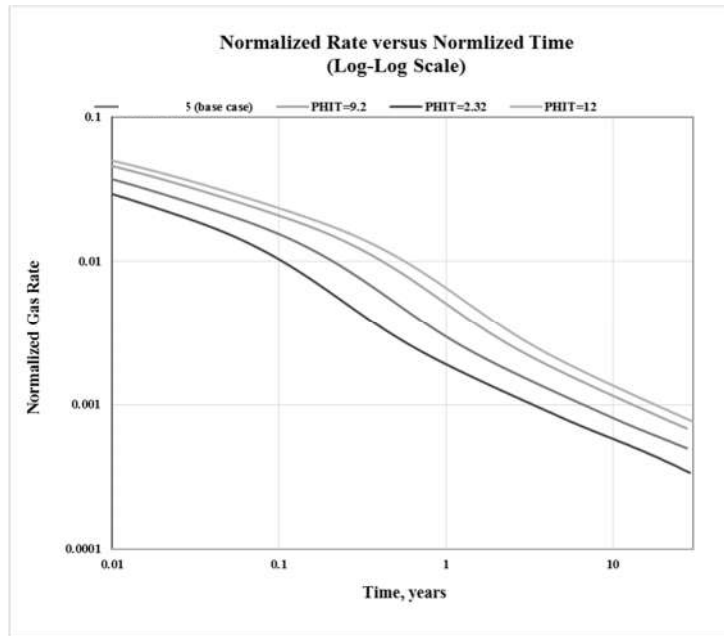


Figure 92: Well C Porosity Sensitivity (Log-Log Plot)

- A positive weak correlation is found between adsorption and production. The effect of higher adsorption is considerable after initial flow. The ratio of production change due to adsorption change is 2:1 (**Figure 93**). Flow regimes' durations are not affected by adsorption change (**Figure 94**).

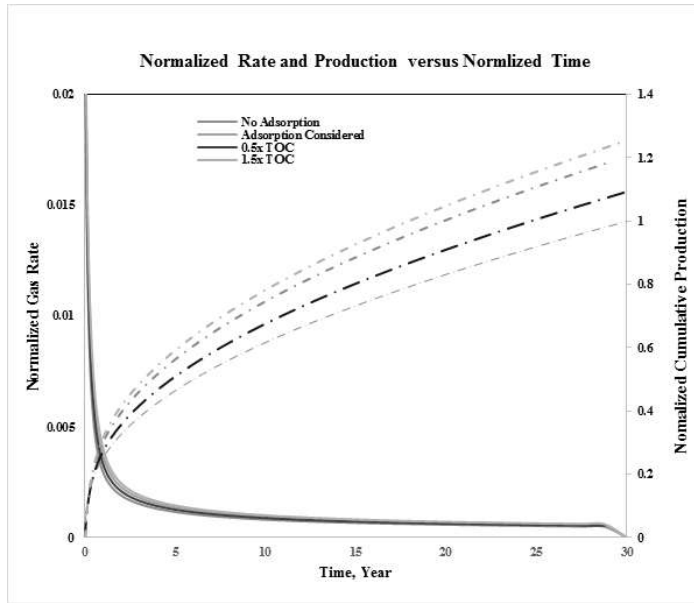


Figure 93: Well C Adsorption Sensitivity

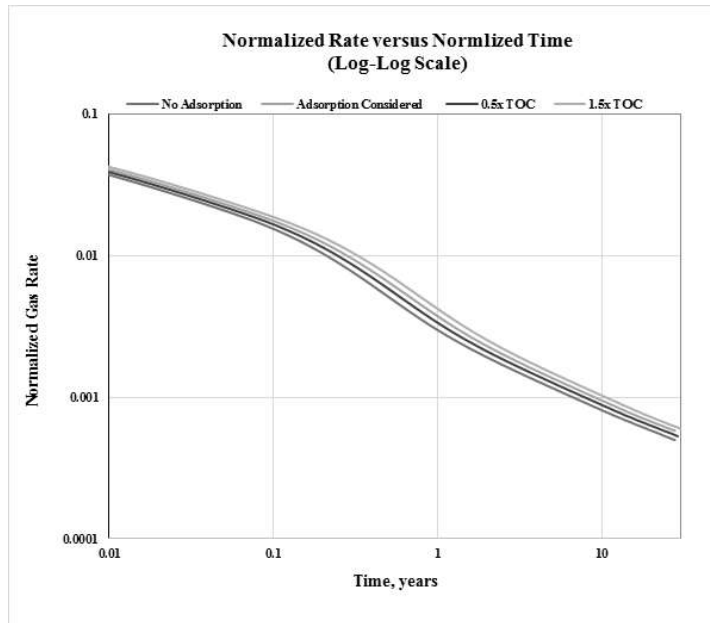


Figure 94: Well C Adsorption Sensitivity (Log-Log Plot)

- Production is directly proportional to initial. However, the correlation weakens at extremely high pressure (**Figure 95**), which might be attributed to lower gas compressibility at high pressure. Flow regimes' durations are not affected by pressure change.

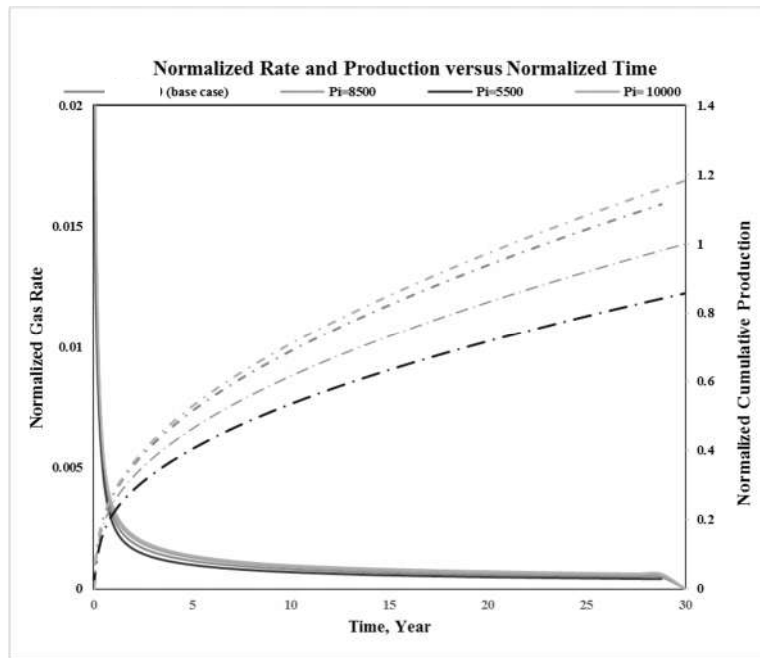


Figure 95: Well C Initial Pressure Sensitivity

4.2.3.4 Conclusion

After examining the sensitivity analysis, it seems that completion parameters affect the initial short-term well performance while reservoir parameters impact the final long-term well performance. Therefore, stimulation treatment design defines initial well performance while well placement decision defines well long-term performance. Also, there is minimal cost associated to well placement decision compared to stimulation treatment design. For Well C, production analysis indicates small fracture size that would be improved by optimizing on fracture half-length as shown in the sensitivity.

CHAPTER 5

CONCLUSIONS

After examine the three case wells, the following conclusions could be derived:

- In all cases, bilinear flow (or cleanup) was confirmed to last for several weeks in oppose to other prominent shale plays where clean up lasts for months. A probable explanation is that the examined wells are highly dehydrated, and most of water is shortly socked to the formation.
- Linear flow seems to last for few months at most indicating high permeability or intensive stimulation treatment.
- BDF could be contributed to liquid loading below the VS. The VS is installed at least 1,000 feet above the landing point and there is still chance of loading below this point in all cases.
- Without clear indication of BDF, outer permeability and exact SRV GIP could not be clearly estimated. Probabilistic approach is the only way to estimate these parameters.
- All cases indicate a limited fracture size (especially Well B), and EUR could be double by doubling fracture half-length.

- All wells show an early, short term, high performance, and sustained, long term, low performance. In all cases, over 50 percent of EUR is produced in the first 5 years of production.
- Different completion and reservoir parameters have dissimilar effects on the flow regime performance and length.
 - In general, completion parameters affect the initial short-term well performance while reservoir parameters impact the long-term well performance.
 - Flow regimes' durations are not affected by fracture conductivity and dimension (height or half-length), wells spacing, reservoir pressure, adsorption, and porosity.
 - Transient flow regime is greatly affected by fracture number, inner permeability, and well length. There is also an inverse relation between the duration of transient flow duration and the performance of the well. The more well is stimulated, the shorter the transient flow regime, and the better early performance of the well.
 - Fracture conductivity affects the performance of the wells only for the first days or weeks of production.
 - Outer permeability and well spacing affect only BDF regime. However, there is a difference in how BDF is affected. The higher the outer permeability, the better the well performance, and the shorter the BDF length while well spacing impact only the length of BDF, but not the well performance.

- Adsorption affects the performance during BDF flow and delays depletion.
- Well spacing affects significantly well life and minimally EUR, but does not impact well performance.
- The parameters that affect well performance the most are fracture half-length, height, and number followed by porosity, permeability, and well length followed then by well spacing, fracture conductivity, adsorption, and initial pressure.

NOMENCLATURE

P_{wf}	bottom hole pressure, psi
t_{elf}	end of liner flow time, day
Q	flow rate, stb/d
B	formation volume factor, stb/day
x_f	fracture half-length, ft
h	fracture height, ft
k_f	fracture permeability, md
s_f	fracture skin, unite less
w_f	fracture width, ft
d_i	half fracture spacing, ft
$MFHW$	multifracture horizontal well
P_i	initial reservoir pressure, psi
t_{mbs}	material balance time, day

n_f	number of fractures
k	permeability, md
k_1	Inner permeability, nd
k_2	Outer permeability, nd
$PHIT$	total porosity, percent
ϕ	porosity, fraction
t	time, day
c_t	total compressibility, psi^{-1}
μ	viscosity, cp

REFERENCES

- Alkough, A., Wattenbarger, R. A., & McKetta, S. (2014). Estimation of Effective-Fracture Volume Using Water-Flowback and Production Data for Shale-Gas Wells. *Journal of Canadian Petroleum Technology*, 290-303.
- Al-Momin, A. K.-S. (2015, September 28). Proving the Concept of Unconventional Gas Reservoirs in Saudi Through Multistage Fractured Horizontal Wells. Houston: Society of Petroleum Engineers.
- Anderson, D. M., Nobakht, M., Moghadam, S., & Mattar, L. F. (2010, February 23-25). Analysis of Production Data from Fractured Shale Gas Wells. doi:10.2118/131787-MS
- Ayers, W. B., Holditch, S. A., & alt, a. (2007). *Facing the Hard Truths about Energy*. National Petroleum Council.
- Baihly, J. D., Malpani, R., Altman, R., Lindsay, G., & Clayton, R. (2015). Shale Gas Production Decline Trend Comparison Over Time and Basins--Revisited . *Unconventional Resources Technology Conference*.
- Blasingame, T. (2013). Reservoir Engineering Aspects of Unconventional Reservoirs. *Schlumberger CONDENFEST Webinar* (p. 14). College Station, TX: Texas A&M University.
- Blasingame, T., & Lee, W. (1986). Variable-Rate Reservoir Limits Testing. Society of Petroleum Engineers.
- Blasingame, T., & Lee, W. (1988). The Variable-Rate Reservoir Limits Testing of Gas Wells. doi:10.2118/17708-MS
- (2016). *BP Energy Outlook*. BP.
- Casey, M. R. (2015). The Opportunity Cost of Exploration for Unconventional Gas in Saudi Arabia. *Society of Petroleum Engineers*, 2-8.
- Chen, C.-C., & Rajagopal, R. (1997). A Multiply-Fractured Horizontal Well in a Rectangular Drainage Region . *Society of Petroleum Engineers* .

- Clarkson, C. R. (2013). Production data analysis of unconventional gas wells: Workflow. *International Journal of Coal Geology*, 147-157.
- Clarkson, C. R., Jensen, J. L., & Blasingame, T. (2011). Reservoir Engineering for Unconventional Reservoirs: What Do We Have to Consider? *SPE NAUGC&E* (p. 2). The Woodland, TX: Society of Petroleum Engineers. doi:10.2118/145080-MS
- Clarkson, C. R., Jordan, C. L., Ilk, D., & Blasingame, T. A. (2009). Production Data Analysis of Fractured and Horizontal CBM Wells. Society of Petroleum Engineers. doi:10.2118/125929-MS
- Daneshy, A. (2011). Uneven Distribution of Proppants in Perf Clusters. *World Oil*, 232(4), 75-76.
- Denney, D. (2010). Practical Solutions for Pressure-Transient Responses of Fractured Horizontal Wells in Unconventional Reservoirs. *Journal of Petroleum Technology*, 62.
- Doung, Z., Holditch, S. A., & McVay, D. A. (2013). Resource Evaluation for Shale Gas Reservoirs. *SPE Economics & Management*, 5-16.
- Duong, A. N. (2011). Rate-Decline Analysis for Fracture-Dominated Shale Reservoirs. *Society of Petroleum Engineers*.
- Ehlig-Economides, C. A., & Economides, M. J. (2011, January 1). Water As Proppant.
- Energy Information Administration. (2012, September). *TODAY IN ENERGY: Pad drilling and rig mobility lead to more efficient drilling*. Retrieved from Energy Information Administration Web site: <https://www.eia.gov>
- Erdle, J., Hale, B., Houze, O., Ilk, D., Jenkins, C., Seidle, J., & Lee, J. (2016). *Mongraph 4: Estimate Ultimate Recovery of Developed Wells in Low Permeability Reservoirs*. (J. Seidle, & D.-J. Weatherford, Eds.) Houston: Society of Petroleum Evaluation Engineers.
- Fekete. (2011). *Modern Production Data Analysis*. Calgary : Fekete . Retrieved April 29, 2016, from Fekete website: <http://fekete.com/>
- Gillis, G., & Varhaug, M. (2010). *Oilfield Glossary*. SLB.
- Gomaa, A. M., Qu, Q., Nelson, S., & Maharidge, R. (2014). New Insights into Shale Fracturing Treatment Design. *Society of Petroleum Engineers*.
- Holditch, S., & Ma, Y. (2016). *Unconventional Oil and Gas Resources Handbook: Evaluation and Development*. Waltham: Elsevier Inc. .
- (2010). *Hydraulic Fracturing*. Oklahoma City: Chesapeake Energy.

- Ilk, D. P. (2008). Integrating multiple production analysis techniques to assess tight gas sand reserves: defining a new paradigm for industry best practices. *CIPC/SPE Gas Technology Symposium Joint Conference*. Calgary, Alberta: SPE.
- Ilk, D., Anderson, D. M., Stotts, G. W., Mattar, L., & Blasingame, T. (2010, Jun 1). Production Data Analysis--Challenges, Pitfalls, Diagnostics. *Society of Petroleum Engineers* . doi:10.2118/102048-PA
- Lee, J. (1987). Pressure-Transient Test Design in Tight Gas Formation . *Journal of Petroleum Technology*(SPE 17088).
- Li, G., Allison, D., & Soliman, M. (2011). Geomechanical Study of the Multistage Fracturing Process For Horizontal Wells. *American Rock Mechanics Association*.
- Lindsay, R. F., Khan, S., Al-Dhubeeb, A. G., Di Simon, S., Davis, R. R., Oyarzabal, F., . . . Peza, E. (2015). Unconventional Jurassic Carbonate Source Rocks, Saudi Arabia. *AAPG 2015 Annual Convention and Exhibition*. Denver: The American Association of Petroleum Geologists.
- Roussel, N. P., & Sharma, M. M. (2011). Optimizing Fracture Spacing and Sequencing in Horizontal-Well Fracturing.
- Sayers, C., & Le Calvez, J. (2011). Characterization of Microseismic Data in Gas Shales Using the Radius of Gyration Tensor. *80th SEG Annual Meeting*, (pp. 2080–2084).
- Smith, M. B., & Montgomery, C. T. (2015). *Hydraulic Fracturing*. Baton Rouge : Taylor & Francis Group, LLC.
- Soliman, M., Daal, J., & East, L. (2012). Fracturing unconventional formations to enhance productivity. *Journal of Natural Gas Science and Engineering*, 8 , 52-67.
- Song, B., & Ehlig-Economides, C. A. (2011). Rate-Normalized Pressure Analysis for Determination of Shale Gas Well Performance . *Society of Petroleum Engineers*.
- Spivey, J. P., & Lee, J. (2013). *Applied Well Test Interpretation*. Society of Petroleum Engineers.
- U.S. Energy Information Administration. (2010). *International Energy Outlook; 2010*. Washington, DC: U.S. Energy Information Administration.
- Wan, J., & Aziz, K. (1999). Multiple Hydraulic Fractures in Horizontal Wells. *Society of Petroleum Engineers*.
- Wattenbarger, R. A.-B. (1998). Production Analysis of Linear Flow Into Fractured Tight Gas Wells. *Society of Petroleum Engineers*, 1-16.

Wigger, E., Viswanathan, A., Fisher, K., Slocombe, R. W., Kaufman, P., & Chadwick, C. (2014). Logging Solutions for Completion Optimization in Unconventional Resource Plays. *Society of Petroleum Engineers*.

VITA

Name: Ahmed Saleh Mohammed Aleid

Nationality: Saudi

Date of Birth: July 1985

Email: ahmdeid@gmail.com

Academic Background: B.Sc. in Petroleum Engineering, (2010) Harold Vance
Department of Petroleum Engineering, Texas A&M
University, College Station, Texas, United States